UC Riverside

UC Riverside Electronic Theses and Dissertations

Title

Development of Methodologies for the Use and Application of Air Quality Sensors to Enable Community Air Monitoring

Permalink

https://escholarship.org/uc/item/0659j8sn

Author

Feenstra, Brandon

Publication Date

2020

Copyright Information

Peer reviewed|Thesis/dissertation

UNIVERSITY OF CALIFORNIA
RIVERSIDE

Development of Methodologies for the Use and Application of Air Quality
Sensors to Enable Community Air Monitoring

A Dissertation submitted in partial satisfaction
of the requirements for the degree of

Doctor of Philosophy

in

Chemical and Environmental Engineering

by

Brandon J. Feenstra

June 2020

Dissertation Committee:
      Dr. David Cocker, Chairperson
      Dr. Don Collins
      Dr. Cesunica Ivey

The Dissertation of Brandon J. Feenstra is approved:

_____

_____

_____
                                      Committee Chairperson

University of California, Riverside

Lastly, I would like to thank my family and friends for their support and encouragement throughout this academic journey. Breanna, my wife, has been a source of joy and encouragement. A special thanks goes to my four energetic kids (Evan, Mason, Ella, and Charlotte) for providing the much-needed smiles and laughs to distract me from research, data analysis, and manuscript preparations. Thank you to my Father and Mother, Steve and Neva, for their guiding care both physically and spiritually along with instilling in me a strong work ethic. In conclusion, I must thank and acknowledge my Heavenly Father who has provided the strength and grace to endure through His constant love and merciful gift of salvation. To Him be the glory for ever and ever.

Chapter 2, part or in full, is a reprint of the material as it appears in *Atmospheric Environment* with contributing authors: Brandon Feenstra, Vasileios Papapostolou, Sina Hasheminassab, Hang Zhang, Berj Der Boghossian, David Cocker, and Andrea Polidori entitled "Performance evaluation of twelve low-cost PM2.5 sensors at an ambient air

monitoring site." Publication information: *Atmospheric Environment* 2019, Volume 216, 116946, https://doi.org/10.1016/j.atmosenv.2019.116946.

Chapter 3, part or in full, is a reprint of the material as it appears in the *Sensors* with contributing authors: Brandon Feenstra, Vasileios Papapostolou, Berj Der Boghossian, David Cocker, and Andrea Polidori entitled "Development of a Network of Accurate Ozone Sensing Nodes for Parallel Monitoring in a Site Relocation Study." Publication information: *Sensors* 2020, 20(1), 16; https://doi.org/10.3390/s20010016.

Chapter 4, part or in full, is a reprint of the material as has been submitted to *Environmental Modelling and Software* with contributing authors: Brandon Feenstra, Ashley Collier-Oxandale, Vasileios Papapostolou, David Cocker, and Andrea Polidori entitled "The AirSensor Open-source R-package and DataViewer Web Application for Interpreting Community Data Collected by Low-cost Sensor Networks." I would like to thank Dr. Jonathan Callahan and Hans Martin at Mazama Science, Inc. (Seattle, WA) for their collaboration and contributions in the development of the AirSensor R-package and the DataViewer application tools along with their valuable feedback on the manuscript submitted to *Environmental Modelling and Software*.

ABSTRACT OF THE DISSERTATION

Development of Methodologies for the Use and Application of Air Quality
Sensors to Enable Community Air Monitoring

by

Brandon J. Feenstra

Doctor of Philosophy, Graduate Program in Chemical and Environmental Engineering
University of California, Riverside, June 2020
Dr. David Cocker, Chairperson

Recent advances in air quality sensor technology have allowed for governments, academia, and communities to use sensors to measure air pollution at unprecedented spatial and temporal scales. While use of low-cost sensors in ambient air monitoring applications has dramatically increased in the past several years, there remain unanswered questions and challenges with designing, implementing, and deploying low-cost sensors. These challenges include quantifying the performance of sensors, developing defensible methods for deploying sensor networks, and communicating sensor data to the public in an understandable and meaningful way. This body of work addresses portions of these challenges by systematically evaluating the performance of sensors, deploying sensors with scientifically defensible methodology for a specific application, and developing methodologies and tools for disseminating and communicating community air monitoring data as information to the public. The main objective of this research is to provide clarity and vision on the appropriate use and applications of low-cost air quality sensors for ambient air monitoring. Systematically evaluating the performance of commercially available low-cost sensors with respect to regulatory grade instrumentation and

understanding the measurement error associated with sensors is critically important when choosing a sensor for a specific monitoring application (i.e. fence-line monitoring, community monitoring, hot spot identification, mobile monitoring) or drawing conclusions from data collected by low-cost sensors. The first part of this research investigates the performance of 12 commercially available low-cost particulate matter (PM) sensors against regulatory-grade instrumentation. The next phase of this research includes the design of an ozone sensor node for a specific ambient air monitoring application - parallel monitoring to select a relocation site for a regulatory ambient air monitoring station. The sensor selection, sensor node development, and network deployment methodologies were designed to collect defensible data for determining a relocation site. In the last phase of this research, data tools are developed to store, process, analyze, and visualize large data sets generated by low-cost sensors to provide communities with information from their community monitoring networks.

Table of Contents

List of Figures

List of Tables

Chapter 1: Introduction

1.1 Background and Significance

Air pollution is associated with adverse human health effects and is a significant contributor to the global disease burden (Cohen et al., 2017). Particulate Matter (PM), an important contributor to air pollution, is a mixture of solid particles and liquid droplets in the air. PM is categorized by the size of particle and is regulated in the United States (U.S.) by mass according to PM size fractions. Fine particulate matter or $PM_{2.5}$ is comprised of particles with an aerodynamic diameter less than 2.5 µm. $PM_{2.5}$ has been linked to respiratory illness, cardiovascular disease, stroke, lung cancer, reproductive issues, and premature death (Pope et al., 2002; Pope et al., 2009; Harris et al., 2014; Apte et al., 2015). In 2015, an estimated 4.2 million people died prematurely due to $PM_{2.5}$ exposure putting it in the top five mortality risk factors worldwide (Cohen et al., 2017). Model predictions estimate that the number of premature deaths attributed to ambient air pollution could double by 2050 (Lelieveld et al., 2015). The World Health Organization (WHO) estimates that 92% of the world's population is exposed to $PM_{2.5}$ concentrations exceeding WHO's recommended annual mean of 10 µg/m^3; indicating the ubiquity of particle pollution across the globe (World Health Organization 2016). In addition to health impacts, PM pollution can impair visibility, damage the environment, and cause material damage to infrastructure (Al-Thani et al., 2018; Wu et al., 2018). Ozone (O_3), another important contributor to air pollution, is a highly reactive gas that is harmful to public health and the environment. The effects of O_3 on human health include reduced lung function and irritation of the respiratory system. Increases in exposure to O_3 have been associated with increases in school absenteeism (Romieu et al., 1992; Gilliland et al., 2001; Park et al., 2002) and increases in

the risk of death from respiratory causes (Jerrett et al., 2009; Turner et al., 2016; Cohen et al., 2017; Song et al., 2019). In a long-term study on children, reductions in air pollutants have been associated with statistically significant decreases in bronchitis symptoms like asthma (Gauderman et al., 2015; Berhane et al., 2016). In 2015, an estimated 254,000 people died prematurely due to O_3 exposure (Cohen et al., 2017). High concentrations of O_3 have been recognized as a phytotoxic threat to forests, crops, and vegetation (Ashmore 2005; Bytnerowicz et al., 2008).

The U.S. Environmental Protection Agency (EPA) regulates air pollution levels under the Clean Air Act (CAA) and establishes the National Ambient Air Quality Standards (NAAQS) for the criteria pollutants: carbon monoxide (CO), lead (Pb), nitrogen dioxide (NO_2), ozone (O_3), particulate matter (PM), and sulfur dioxide (SO_2). The NAAQS are set to protect public health and the environment with the attainment of these standards determined by regional monitoring networks equipped with instrumentation that has been approved by the U.S. EPA as a Federal Reference or Federal Equivalent Method (FRM or FEM). These networks of air monitoring stations (AMS) are typically operated by regulatory air monitoring agencies at the local regional (e.g., South Coast Air Quality Management District in Southern California), state, and/or federal government level. While high quality regulatory air monitoring data is essential for the determination of regional attainment of the established national or international air quality standards, the spatial extent of these measurements may be limited especially for communities impacted by nearby air pollution sources (e.g., freeways) requiring the spatial resolution of measurements to be in the tens of meters (Ahangar et al., 2019). An increasing number of

3

studies have found the spatial and temporal resolution of these regional monitoring networks to be insufficient to characterize air pollutants at a community or neighborhood scale for pollutants that exhibit high spatial variability such as traffic-related PM (Apte et al., 2017; Gu et al., 2018; Ye et al., 2018). Additionally, the spatial distribution of regulatory-grade (FRM or FEM) instrumentation internationally is limited with only 24 of 234 countries have more than 3 monitors per million inhabitants and with nearly 60% of countries having no regular PM monitoring. This lack of monitoring across the globe leads to the statement that "No one knows which city has the highest concentration of fine particulate matter" in 2019 (Martin et al., 2019). In contrast to regulatory-grade instrumentation, low-cost air quality sensors are often more "plug and play" or "plug and sense" than their regulatory counterparts and do not require rigorous maintenance schedules. Additionally, many sensors are coupled with web-based platforms or applications that make it easy to engage with data either in real-time or download for further analysis. Due to their low cost, air quality sensors have the potential to fill in this spatial gap in air quality measurements with the development of large sensor networks allowing researchers to investigate the spatial and temporal gradients of air pollution in areas previously unmeasured or at finer spatial scales than previously monitored.

1.2   Air Quality Sensors

Air quality sensors offer great opportunity, when used properly, to enhance our understanding of physical phenomena around us. While a person can often differentiate between changes in few degrees in temperature, people can often struggle to differentiate between good, moderate, and unhealthy air quality unless that poor air quality is coupled

with visibility impairment, an unpleasant odor, or attributed to a specific point source (Sucker et al., 2008; Stenlund et al., 2009; Claeson et al., 2013; Orru et al., 2018). Due to their lower cost in comparison to regulatory monitoring instrumentation, air pollution sensors offer the ability to be deployed in dense sensor networks that can enhance the spatial and temporal resolution of the current monitoring networks. The emergence of low-cost air quality sensors for measuring both gas and particle pollutants has initiated a paradigm shift in the way air quality data is measured and shared with the public (Snyder et al., 2013). Numerous sensor models with prices ranging from $150 to $3,000 USD are available to the public. These consumer-grade (low-cost) sensors can provide real or near-real time air pollutant information at increased spatial resolutions with the potential to provide meaningful measurements at the local scale and complement and expand the capabilities of existing ambient air monitoring networks equipped with commercial-, research-, and regulatory-grade air monitoring instrumentation (Sadighi et al., 2018). Many potential applications exist for low-cost sensors, including stationary ambient monitoring, mobile ambient monitoring, and personal exposure assessment with wearable sensors. Due to the diversity of these applications, researchers and other stakeholders working on sensor projects often design sensors or select commercially available sensors to be "fit for purpose" based on the desired monitoring application (Morawska et al., 2018).

The utility of these low-cost sensors for specific applications depends on the performance of the sensor in that specific environment and application. As low-cost sensors become increasingly popular for ambient air monitoring for both researchers and the general public, characterizing the performance of these sensors and educating the public

about their appropriate applications and limitations becomes increasingly important. For example, sensors with low intra-model variability could be spatially deployed in a community to supplement existing regulatory-grade measurements and obtain hyper local measurements to better understand pollutant gradients within a community even if that sensor over- or under-estimates actual air pollution levels. Performance characterization of sensors will minimize confusion, particularly when low-cost sensors report information that conflicts with data generated from reference-grade instrumentation operated by the local air pollution control districts (APCD).

The South Coast Air Quality Management District (South Coast AQMD) created the Air Quality Sensor Performance Evaluation Center (AQ-SPEC) in 2014 to provide the public with information on sensor performance. AQ-SPEC evaluates commercially available low-cost air monitoring sensors in both ambient field and controlled laboratory conditions. Evaluation results are communicated to the public through field and laboratory evaluation reports and sensor summary tables for gas and PM sensors, which are available at www.aqmd.gov/aq-spec. In the field, air quality sensors are operated at an air monitoring station (AMS) where FRM or FEM instruments measure the ambient concentration of gaseous or particle pollutants for regulatory purposes. AQ-SPEC examines the performance of low-cost sensors against these regulatory-grade (FRM or FEM) instruments, as well as sensor-specific parameters such as intra-model variability and data recovery. Sensors that demonstrate an acceptable performance in the field are then evaluated under controlled conditions in a chamber. The chamber testing allows for the evaluation of sensor performance across a broader range of pollutant concentration,

temperature, and humidity than may have been experienced during the 2-month field evaluation. The capabilities of the chamber also allow for the evaluation for cross-pollutant sensitivities that could impact sensor performance. While the AQ-SPEC field and laboratory testing results evaluate the performance of sensors, AQ-SPEC does not rank or endorse specific sensors or make recommendations as to which sensor devices should be used for specific applications. Sensor selection is application and project specific with the application defining performance requirements and requirements for connectivity (e.g., Wi-Fi, cellular, Bluetooth), data visualization (e.g., mobile application, screen display on sensor, web-based mapping application), power requirements (e.g., battery-powered, power supply to a wall outlet), and sensor mobility (e.g., stationary, mobile, wearable).

Due to the low hardware and operational cost of these emerging air quality sensors, dense networks of air quality sensors can be deployed. These environmental monitoring networks are increasing in complexity and size with an increasing number of devices reporting data to online data systems. These networks are enabled by technological advances and cost reductions for environmental monitoring sensors along with advances in connectivity with Internet of Things (IoT) devices and cloud-based computing offerings and services. Community scientists are now able to deploy hyper-local community monitoring networks to supplement the established regulatory monitoring networks. As community scientists take an active role in collecting air monitoring data by hosting air quality sensors, they also become increasingly interested in viewing, analyzing, and understanding the collected data to derive hyper local information about their local environment. The increasing complexity and size of today's environmental monitoring

networks have created big data challenges leading to the emergence of a new field: Environmental Data Science (Gibert et al., 2018). Data science combines computer programming skills, math and statistical knowledge, and subject matter expertise (Conway 2013). Environmental data science often uses Free and Open-Source Software (FOSS) like Python and the R environment to develop specific software packages to address these data science challenges (Kadiyala and Kumar 2017a; Kadiyala and Kumar 2017b). Within these FOSS environments, specific packages or modules can be created to assist in processing, analyzing, and displaying data from air monitoring sensors. These FOSS tools allow community scientist to actively participate in the data analysis and visualization to better understand their local air quality conditions.

1.3   Previous Studies and Approaches

To date, there have been a limited number of systematic studies using established protocols to characterize the performance of PM sensors in ambient conditions where end-users are likely to deploy these sensors (Morawska et al., 2018). Additionally, many low-cost sensors are sold to the public with minimal testing, maintenance recommendations, and standard operating procedures. Prior published studies have evaluated the performance of several low-cost PM sensors under ambient conditions. These include the AirBeam (Jiao et al., 2016; Mukherjee et al., 2017; Borghi et al., 2018), Alphasense OPC-N2 (Mukherjee et al., 2017; Crilley et al., 2018), PurpleAir (Kim et al., 2019; Magi et al., 2019), and Foobot for indoor air quality (Moreno-Rangel et al., 2018). These examples represent a small fraction of the PM sensors currently available to consumers. Additionally, many of the performance evaluations in the literature are not performed according to a standard

protocol, but rather performed to determine the performance of a particular sensor or set of sensors as a "fit for purpose" for a specific monitoring project (Morawska et al., 2018). The U.S. EPA has evaluated the performance of low-cost sensors in ambient environments using a standard protocol with evaluation results for the TSI AirAssure, AirBeam, Alphasense OPC-N2, and Shinyei PM Evaluation kit (Williams et al., 2014; Jiao et al., 2016; Feinberg et al., 2018; U.S. Environmental Protection Agency 2019). Rather than evaluating the performance of commercialized sensors, some researchers have evaluated the performance of Original Equipment Manufacturer (OEM) PM sensors that include Plantower, Shinyei, and Nova Fitness OEM sensors (Austin et al., 2015; Kelly et al., 2017; Badura et al., 2018; Johnson et al., 2018; Zheng et al., 2018; Bulot et al., 2019; Liu et al., 2019; Sayahi et al., 2019; Zamora et al., 2019). While the evaluation results on OEM sensors add to the literature and assist sensor manufacturers and/or researchers in selecting OEM sensors for developing sensor solutions or final commercialized products, these evaluation results are not transferable to commercialized end products offerings as the sensor housing, sampling mechanism, and electronics can impact the performance of final commercialized product. A review of air sensor performance metrics and targets indicated that the performance metrics, types and duration of performance evaluations, and types of reference equipment by which sensors are evaluated varied widely in the literature (Williams et al., 2018). This review highlights the diversity of sensor evaluation work currently being published and the need to evaluate sensors according to a documented protocol for consistency across evaluations with regards to performance metrics, reference equipment, duration, and time-resolution used for sensor performance evaluations. Filling

this gap in the literature for sensor performance evaluations performed according to a documented protocol with consistency across evaluations is the goal of the sensor evaluations performed and presented in Chapter 2.

Deploying networks of sensors presents researchers with challenges with regard to maintaining the sensors over time and ensuring that the sensors are producing accurate and reliable data. Developing defensible methods for deploying sensor within a network is important to verify the data produced and quantify the measurement error of the sensor network. The performance of air quality sensors is highly dependent on the methods of deployment chosen and implemented. Calibration methods that are feasible for small networks may not be feasible for large sensor networks. For small networks, researchers often perform a co-location of their sensors with regulatory-grade monitors at ambient air monitoring sites for a pre-deployment calibration and then may verify performance with a post-deployment co-location test (Masson et al., 2015; Sadighi et al., 2018; Badura et al., 2019). Performing a pre-deployment co-location calibration of low-cost air quality sensors with a regulatory-grade instrument, in the same environment as the deployment, can provide more accurate and precise measurements throughout a deployment. Verifying the sensor performance at the conclusion of a deployment or during deployment through co-location with regulatory-grade instrumentation allows for the quantification of the measurement error of the sensor and/or sensor network and identification of potential drift or degradation over time. In contrast to small sensor networks, performing co-location testing for every sensor in a large sensor network at a reference site may not be feasible so researchers often turn to other methods to calibrate or evaluate the performance of large

sensor networks. These network performance evaluations or calibration methods include developing models or machine learning techniques (Bart et al., 2014; Zimmerman et al., 2018; Malings et al., 2019; Vikram et al., 2019) and the use of proxy sites for calibrating the network based on land-use regression within a hierarchical network of low-cost and regulatory-grade instruments (Miskell et al., 2019; Weissert et al., 2020a; Weissert et al., 2020b). Generally, these networks are deployed for the purpose of developing high resolution pollution maps, identifying peak pollution events, and/or linking pollution levels to exposure (Morawska et al., 2018). One of the challenges with the emergence of low-cost air quality sensing is developing specific sensor use applications that go beyond the purpose of increasing the spatial or temporal resolution of current air quality maps. The development of an accurate ozone sensing node for parallel monitoring in a site relocation study provides a sensor use application that all agencies performing regulatory air monitoring may face: the relocation of an ambient air monitoring site. The application and methodology presented in Chapter 3 allows for the quantification of the measurement error of a small sensor network. This quantification of measurement error provides the ability to apply the collected data and subsequent analysis to make decisions with regards to the desired monitoring application: identify which location would be most suitable to replace the current regulatory ozone monitoring site. The work presented in Chapter 3 adds to the literature on how sensor nodes can be designed and how deployment methodology can be utilized for a specific ambient monitoring application to obtain accurate defensible data and make informed decisions.

As sensing networks grow and are often deployed within communities, dissemination and communication of the collected data with that community becomes increasingly important. While large-scale low-cost sensor networks are now recording air pollutant concentrations at finer spatial and temporal scales than previously measured, the large environmental data sets generated by these sensor networks can become overwhelming when considering the scientific skills required to analyze the data and generate interpretable results. Online platforms for viewing regulatory-grade data are available with various features (BreezoMeter 2020; IQAir 2020; OpenAQ 2020; Plume Labs 2020; World Air Quality Index Project 2020). These data viewing sites are useful and provide information to the public at varied granularity spatially and temporally. Online platforms for viewing sensor data are also available but vary in terms of whether they are proprietary or FOSS, what they provide, and whether they are provided by the manufacture, project team, or through a citizen science model. Proprietary platforms are typically available through the manufacturer and offered as a Software as a Service (SaaS) or Platform as a Service (PaaS) requiring accounts with monthly or yearly subscriptions costs. In contrast to this subscription-based model, several sensor resources are available for open-access viewing of data collected from low-cost sensors. These platforms include but are not limited to the HabitatMap AirCasting map, Air Quality Egg Portal, Luft Daten project map, PurpleAir Map, Smart Citizen Kit Map, and the uRADMonitor Network map (Air Quality Egg 2020; HabitatMap 2020; Luftdaten 2020; PurpleAir 2020; Smart Citizen Kit 2020; uRADMonitor 2020). PurpleAir provides open access to the data collected by the PurpleAir network of sensors through an API and provides open viewing and downloading

12

of sensor data through the PurpleAir map. The Luft Daten project is a Citizen Science project with citizen scientist sensors reporting to a map and invites programmers to collaborate in this FOSS development through GitHub (OK Lab Stuttgart 2020). When selecting a sensor in either the PurpleAir or Luftdaten GUI, the user is currently limited to viewing only the last 7-days of data in a time series plot and current data on the map (tested January 2020), which means they do not provide the end-user with historic data to understand the spatial and temporal trends of air pollutants in their community. A project specific site, Breathe London, provides a map displaying sensor monitoring data along with the option to add the regulatory network data to the map (Breathe London 2020). Broadly, these online platforms for both regulatory and sensor data are map centric with point values or interpolated modelled data displayed with options for viewing recent time series data. While these map centric websites work well for viewing real-time data, communities that are monitoring air quality with long term deployments need additional plotting and viewing capabilities to access and understand their local historical air monitoring data. A data dashboard for viewing and analyzing historical data would provide a better understanding of local air quality levels for the community to understand their historical local spatial and temporal air pollutant trends. Chapter 4 of this thesis looks to fill this gap in the currently available data platforms by providing a FOSS R package to deal with community monitoring data sets for a low-cost sensors and providing a DataViewer web application that allows the community to explore historical data and perform trend analysis on the collected data.

1.4   Study Approach and Design: Overall Objective

Designing, developing, implementing, and deploying projects with low-cost sensors for air monitoring applications comes with many challenges. These challenges include quantifying the performance of commercially available low-cost sensors, developing defensible methods for deploying sensor networks, and communicating sensor data to the public in an understandable and meaningful way. This work aims at addressing portions of these three challenges by systematically evaluating the performance of sensors, deploying sensors with scientifically defensible methodology for a specific application, and developing methodologies and tools on how disseminate community air monitoring data as information to the public.

Chapter 2 of this thesis presents the field evaluations results of 12 commercially available "low-cost" PM sensors under ambient conditions as part of the ongoing sensor evaluation work in the AQ-SPEC program that commenced during the summer of 2014. To date, more than 80 consumer-grade air quality sensors measuring particle and/or gas-phase pollutants have been evaluated by the program. The evaluation results in Chapter 2 provide performance metrics for low-cost sensors with calculations for measurement error and investigation into the impact of environmental conditions on the performance of $PM_{2.5}$ sensors in field evaluations. The approach of this work is to evaluate sensors systematically in triplicate according to a documented protocol at one monitoring location with data analysis performed at the 1-hr time interval against a single FEM $PM_{2.5}$ instrument. These performance evaluation results can be used globally to help researchers and community members select sensors to best fit their monitoring needs. This work aims at adding to the

body of literature on sensor performance for PM$_{2.5}$ sensors in field conditions and provides guidance on appropriate performance metrics to evaluate sensor performance against regulatory-grade instrumentation.

Chapter 3 of this thesis presents an application for the development and deployment of air quality sensors as part of an Internet of Things (IoT) network. The ambient air monitoring application was to perform parallel monitoring to determine the appropriateness of three potential relocation sites for an air monitoring station measuring ozone. This application required accurate and defensible data, which in turn guided the sensor selection, deployment methodology, and sensor performance metrics. The deployment methodology included an initial calibration, pre-deployment co-location calibration, and post-deployment co-location verification. Quantifying the measurement error of the sensor network allowed for the creation of defensible data allowing for high confidence in the results and analysis of the data to determine an appropriate relocation monitoring site. The development of the sensor node and the methodology of the field deployment of sensors for parallel monitoring can be duplicated and expanded to other applications, especially when the monitoring application requires quantification of the measurement error of the sensing nodes.

When performing air monitoring studies in a community, communicating the collected data back to the public in an understandable and meaningful format is key to engaging, educating, and empowering the community. Having the right tools to view and understand local air monitoring data allows the community to take appropriate actions and/or make decisions to reduce exposure to harmful air pollutants. With the varied interest and

knowledge in air quality and atmospheric sciences within the community, displaying

community air monitoring content to the public that is both meaningful and understandable

to all or most community members is challenging. Chapter 4 provides an overview of the

AirSensor R package and DataViewer web application that addresses the challenges with

the data management and visualization of low-cost air quality sensors networks. The R

package allows users to download sensor data, add spatial metadata, perform data fusion

with other relevant data sets, and create maps and plots for viewing data collected by air

monitoring sensors. AirSensor was built with useful functions so that minimal coding

would be required to complete tasks within the R software environment. The DataViewer

web application was developed to provide an interactive data experience allowing users to

make selections and explore the community air monitoring data sets by generating pre-

defined data visuals based on their user selected inputs. The data is processed and coupled

with additional data sets to provide useful and informative data visualizations. Informative

plots rendered on the DataViewer application provides the local community member with

interactive plots to better understand their local environment and determine when air

pollution is typically higher within their community by hour of the day, day of the week,

and which direction the pollution may be coming from when entering the community. The

DataViewer application provides an example of how data from low-cost sensors deployed

in a community can be visualized to understand historical air quality trends. The R-package

and DataViewer application provide insights into how to process and display data collected

by sensor networks. This work was performed as FOSS and can therefore be expanded

upon by a community of users or duplicated for other communities that are engaged in community air monitoring.

In each of the main chapters of this thesis (i.e., Chapter 2, 3, and 4), the reader will come across both low-cost sensor data and regulatory-grade instrumentation data sets. The reason for this is that the low-cost sensor data must be analyzed against regulatory-grade instrumentation to determine performance of sensors, measurement error of sensor networks, and trend differences between the nearest regulatory monitor and low-cost sensors located within a community. The data from low-cost sensors can rarely be used in a vacuum and coupling low-cost sensor data to the already established regulatory-grade monitoring networks is recommended as a best practice for implementing sensor networks.

1.5 Dissertation outline

The dissertation is structured into five chapters. Chapter 1 provides an introduction to air pollutants, air monitoring, and the emerging role of air quality sensors in ambient monitoring. Chapters 2, 3, and 4 add to the literature on the emerging use and application of low-cost sensors and includes quantifying the performance of commercially available low-cost sensors, developing defensible methods for deploying sensor networks, and communicating sensor data back to the public. Chapter 2 provides the performance evaluation results of 12 commercially available low-cost $PM_{2.5}$ sensors. Chapter 3 provides the design of an ozone sensing node and the development of a sensor network to perform parallel monitoring in a site relocation study in the San Bernardino mountains in Southern California. Chapter 4 provides a summary of the R package and DataViewer application

for communicating sensor data back to the public in an understandable and meaningful

manner. Chapter 5 provides a summary and conclusions of the work performed.

References

Ahangar, F. E., F. R. Freedman and A. Venkatram (2019). "Using Low-Cost Air Quality Sensor Networks to Improve the Spatial and Temporal Resolution of Concentration Maps." International Journal of Environmental Research and Public Health **16**(7): 17.

Air Quality Egg. (2020). "Air Quality Egg Portal."   Viewed 02/05/2020, from https://airqualityegg.com/portal/.

Al-Thani, H., M. Koc and R. J. Isaifan (2018). "A Review on the Direct Effect of Particulate Atmospheric Pollution on Materials and its Mitigation for Sustainable Cities and Societies." Environmental Science and Pollution Research **25**(28): 27839-27857.

Apte, J. S., J. D. Marshall, A. J. Cohen and M. Brauer (2015). "Addressing Global Mortality from Ambient PM2.5." Environmental Science & Technology **49**(13): 8057-8066.

Apte, J. S., K. P. Messier, S. Gani, M. Brauer, T. W. Kirchstetter, M. M. Lunden, J. D. Marshall, C. J. Portier, R. C. H. Vermeulen and S. P. Hamburg (2017). "High-Resolution Air Pollution Mapping with Google Street View Cars: Exploiting Big Data." Environmental Science & Technology **51**(12): 6999-7008.

Ashmore, M. R. (2005). "Assessing the future global impacts of ozone on vegetation." Plant Cell and Environment **28**(8): 949-964.

Austin, E., I. Novosselov, E. Seto and M. G. Yost (2015). "Laboratory Evaluation of the Shinyei PPD42NS Low-Cost Particulate Matter Sensor." PLoS One **10**(9).

Badura, M., P. Batog, A. Drzeniecka-Osiadacz and P. Modzel (2018). "Evaluation of Low-Cost Sensors for Ambient PM2.5 Monitoring." Journal of Sensors **2018**: 1-16.

Badura, M., P. Batog, A. Drzeniecka-Osiadacz and P. Modzel (2019). "Regression methods in the calibration of low-cost sensors for ambient particulate matter measurements." Sn Applied Sciences **1**(6): 11.

Bart, M., D. E. Williams, B. Ainslie, I. McKendry, J. Salmond, S. K. Grange, M. Alavi-Shoshtari, D. Steyn and G. S. Henshaw (2014). "High Density Ozone Monitoring Using Gas Sensitive Semi-Conductor Sensors in the Lower Fraser Valley, British Columbia." Environmental Science & Technology **48**(7): 3970-3977.

Berhane, K., C. C. Chang, R. McConnell, W. J. Gauderman, E. Avol, E. Rapapport, R. Urman, F. Lurmann and F. Gilliland (2016). "Association of Changes in Air Quality With Bronchitic Symptoms in Children in California, 1993-2012." Journal of the American Medical Association **315**(14): 1491-1501.

Borghi, F., A. Spinazze, D. Campagnolo, S. Rovelli, A. Cattaneo and D. M. Cavallo (2018). "Precision and Accuracy of a Direct-Reading Miniaturized Monitor in PM2.5 Exposure Assessment." Sensors **18**(9).

Breathe London. (2020). "Breathe London Map."   Viewed 02/05/2020, from https://www.breathelondon.org/.

BreezoMeter. (2020). "Air Quality Map."   Viewed 02/04/2020, from https://breezometer.com/air-quality-map.

Bulot, F. M. J., S. J. Johnston, P. J. Basford, N. H. C. Easton, M. Apetroaie-Cristea, G. L. Foster, A. K. R. Morris, S. J. Cox and M. Loxham (2019). "Long-term field comparison of multiple low-cost particulate matter sensors in an outdoor urban environment." Scientific Reports **9**: 13.

Bytnerowicz, A., M. Arbaugh, S. Schilling, W. Fraczek and D. Alexander (2008). "Ozone distribution and phytotoxic potential in mixed conifer forests of the San Bernardino Mountains, Southern California." Environmental Pollution **155**(3): 398-408.

Claeson, A. S., E. Liden, M. Nordin and S. Nordin (2013). "The role of perceived pollution and health risk perception in annoyance and health symptoms: a population-based study of odorous air pollution." International Archives of Occupational and Environmental Health **86**(3): 367-374.

Cohen, A. J., M. Brauer, R. Burnett, H. R. Anderson, J. Frostad, K. Estep, K. Balakrishnan, B. Brunekreef, L. Dandona, R. Dandona, V. Feigin, G. Freedman, B. Hubbell, A. Jobling, H. Kan, L. Knibbs, Y. Liu, R. Martin, L. Morawska, C. A. Pope, H. Shin, K. Straif, G. Shaddick, M. Thomas, R. van Dingenen, A. van Donkelaar, T. Vos, C. J. L. Murray and M. H. Forouzanfar (2017). "Estimates and 25-year trends of the global burden of disease attributable to ambient air pollution: an analysis of data from the Global Burden of Diseases Study 2015." Lancet **389**(10082): 1907-1918.

Conway, D. (2013). "The Data Science Venn Diagram." Viewed 05/31/19, from http://drewconway.com/zia/2013/3/26/the-data-science-venn-diagram.

Crilley, L. R., M. Shaw, R. Pound, L. J. Kramer, R. Price, S. Young, A. C. Lewis and F. D. Pope (2018). "Evaluation of a low-cost optical particle counter (Alphasense OPC-N2) for ambient air monitoring." Atmospheric Measurement Techniques **11**(2): 709-720.

Feinberg, S., R. Williams, G. S. W. Hagler, J. Rickard, R. Brown, D. Garver, G. Harshfield, P. Stauffer, E. Mattson, R. Judge and S. Garvey (2018). "Long-term evaluation of air sensor technology under ambient conditions in Denver, Colorado." Atmospheric Measurement Techniques **11**(8): 4605-4615.

Gauderman, W. J., R. Urman, E. Avol, K. Berhane, R. McConnell, E. Rappaport, R. Chang, F. Lurmann and F. Gilliland (2015). "Association of Improved Air Quality with Lung Development in Children." New England Journal of Medicine **372**(10): 905-913.

Gibert, K., J. S. Horsburgh, I. N. Athanasiadis and G. Holmes (2018). "Environmental Data Science." Environmental Modelling & Software **106**: 4-12.

Gilliland, F. D., K. Berhane, E. B. Rapaport, D. C. Thomas, E. Avol, W. J. Gauderman, S. J. London, H. G. Margolis, R. McConnell, K. T. Islam and J. M. Peters (2001). "The effects of ambient air pollution on school absenteeism due to respiratory illnesses." Epidemiology **12**(1): 43-54.

Gu, P. S., H. Li, Q. Ye, E. S. Robinson, J. S. Apte, A. L. Robinson and A. A. Presto (2018). "Intracity Variability of Particulate Matter Exposure Is Driven by Carbonaceous Sources and Correlated with Land-Use Variables." Environmental Science & Technology **52**(20): 11545-11554.

HabitatMap. (2020). "AirCasting Map."   Viewed 02/05/2020, from http://aircasting.habitatmap.org/mobile_map.

Harris, G., W. D. Thompson, E. Fitzgerald and D. Wartenberg (2014). "The association of PM2.5 with full term low birth weight at different spatial scales." Environmental Research **134**: 427-434.

IQAir. (2020). "AirVisual Map." from https://www.airvisual.com/air-quality-map.
Jerrett, M., R. T. Burnett, C. A. Pope, K. Ito, G. Thurston, D. Krewski, Y. L. Shi, E. Calle and M. Thun (2009). "Long-Term Ozone Exposure and Mortality." New England Journal of Medicine **360**(11): 1085-1095.

Jiao, W., G. Hagler, R. Williams, R. Sharpe, R. Brown, D. Garver, R. Judge, M. Caudill, J. Rickard, M. Davis, L. Weinstock, S. Zimmer-Dauphinee and K. Buckley (2016). "Community Air Sensor Network (CAIRSENSE) project: evaluation of low-cost sensor performance in a suburban environment in the southeastern United States." Atmospheric Measurement Techniques **9**(11): 5281-5292.

Johnson, K. K., M. H. Bergin, A. G. Russell and G. S. W. Hagler (2018). "Field Test of Several Low-Cost Particulate Matter Sensors in High and Low Concentration Urban Environments." Aerosol and Air Quality Research **18**(3): 565-578.

Kadiyala, A. and A. Kumar (2017a). "Applications of Python to evaluate environmental data science problems." Environmental Progress & Sustainable Energy **36**(6): 1580-1586.

Kadiyala, A. and A. Kumar (2017b). "Applications of R to Evaluate Environmental Data Science Problems." Environmental Progress & Sustainable Energy **36**(5): 1358-1364.

Kelly, K. E., J. Whitaker, A. Petty, C. Widmer, A. Dybwad, D. Sleeth, R. Martin and A. Butterfield (2017). "Ambient and laboratory evaluation of a low-cost particulate matter sensor." Environmental Pollution **221**: 491-500.

Kim, S., S. Park and J. Lee (2019). "Evaluation of Performance of Inexpensive Laser Based PM2.5 Sensor Monitors for Typical Indoor and Outdoor Hotspots of South Korea." Applied Sciences **9**(9): 14.

Lelieveld, J., J. S. Evans, M. Fnais, D. Giannadaki and A. Pozzer (2015). "The contribution of outdoor air pollution sources to premature mortality on a global scale." Nature **525**(7569): 367-371.

Liu, H. Y., P. Schneider, R. Haugen and M. Vogt (2019). "Performance Assessment of a Low-Cost PM2.5 Sensor for a near Four-Month Period in Oslo, Norway." Atmosphere **10**(2): 18.

Luftdaten. (2020). "Measuring Air Data with Citizen Science."   Viewed 02/05/2020, from https://luftdaten.info/en/home-en/.

Magi, B. I., C. Cupini, J. Francis, M. Green and C. Hauser (2019). "Evaluation of PM2.5 measured in an urban setting using a low-cost optical particle counter and a Federal Equivalent Method Beta Attenuation Monitor." Aerosol Science and Technology: 13.

Malings, C., R. Tanzer, A. Hauryliuk, S. P. N. Kumar, N. Zimmerman, L. B. Kara, A. A. Presto and R. Subramanian (2019). "Development of a general calibration model and long-term performance evaluation of low-cost sensors for air pollutant gas monitoring." Atmospheric Measurement Techniques **12**(2): 903-920.

Martin, R. V., M. Brauer, A. van Donkelaar, G. Shaddick, U. Narain and S. Dey (2019). "No one knows which city has the highest concentration of fine particulate matter." Atmospheric Environment: X **3**: 100040.

Masson, N., R. Piedrahita and M. Hannigan (2015). "Approach for quantification of metal oxide type semiconductor gas sensors used for ambient air quality monitoring." Sensors and Actuators B-Chemical **208**: 339-345.

Miskell, G., K. Alberti, B. Feenstra, G. S. Henshaw, V. Papapostolou, H. Patel, A. Polidori, J. A. Salmond, L. Weissert and D. E. Williams (2019). "Reliable data from low cost ozone sensors in a hierarchical network." Atmospheric Environment **214**: 116870.

Morawska, L., P. K. Thai, X. T. Liu, A. Asumadu-Sakyi, G. Ayoko, A. Bartonova, A. Bedini, F. H. Chai, B. Christensen, M. Dunbabin, J. Gao, G. S. W. Hagler, R. Jayaratne, P. Kumar, A. K. H. Lau, P. K. K. Louie, M. Mazaheri, Z. Ning, N. Motta, B. Mullins, M. M. Rahman, Z. Ristovski, M. Shafiei, D. Tjondronegoro, D. Westerdahl and R. Williams

(2018). "Applications of low-cost sensing technologies for air quality monitoring and exposure assessment: How far have they gone?" Environment International **116**: 286-299.

Moreno-Rangel, A., T. Sharpe, F. Musau and G. McGill (2018). "Field evaluation of a low-cost indoor air quality monitor to quantify exposure to pollutants in residential environments." Journal of Sensors and Sensor Systems **7**(1): 373-388.

Mukherjee, A., L. G. Stanton, A. R. Graham and P. T. Roberts (2017). "Assessing the Utility of Low-Cost Particulate Matter Sensors over a 12-Week Period in the Cuyama Valley of California." Sensors **17**(8).

OK Lab Stuttgart. (2020). "Open Data Stuttgart."   Viewed 02/05/2020, from www.github.com/opendata-stuttgart.

OpenAQ. (2020). "Open Data: Countries."   Viewed 01/24/2020, from https://openaq.org/#/countries.

Orru, K., S. Nordin, H. Harzia and H. Orru (2018). "The role of perceived air pollution and health risk perception in health symptoms and disease: a population-based study combined with modelled levels of PM10." International Archives of Occupational and Environmental Health **91**(5): 581-589.

Park, H., B. Lee, E. H. Ha, J. T. Lee, H. Kim and Y. C. Hong (2002). "Association of air pollution with school absenteeism due to illness." Archives of Pediatrics & Adolescent Medicine **156**(12): 1235-1239.

Plume Labs. (2020). "Air Quality Map."   Viewed 02/04/2020, from https://air.plumelabs.com/air-quality-map.

Pope, C. A., R. T. Burnett, M. J. Thun, E. E. Calle, D. Krewski, K. Ito and G. D. Thurston (2002). "Lung cancer, cardiopulmonary mortality, and long-term exposure to fine particulate air pollution." Journal of the American Medical Association **287**(9): 1132-1141.

Pope, C. A., III, M. Ezzati and D. W. Dockery (2009). "Fine-Particulate Air Pollution and Life Expectancy in the United States." New England Journal of Medicine **360**(4): 376-386.

PurpleAir. (2020). "PurpleAir Map."   Viewed 02/05/2020, from https://www.purpleair.com/map.

Romieu, I., M. C. Lugo, S. R. Velasco, S. Sanchez, F. Meneses and M. Hernandez (1992). "Air-Pollution and School Absenteeism Among Children in Mexico City." American Journal of Epidemiology **136**(12): 1524-1531.

Sadighi, K., E. Coffey, A. Polidori, B. Feenstra, Q. Lv, D. K. Henze and M. Hannigan (2018). "Intra-Urban Spatial Variability of Surface Ozone in Riverside, CA: Viability and Validation of Low-cost Sensors." Atmospheric Measurement Techniques **11**(3): 1777-1792.

Sayahi, T., A. Butterfield and K. E. Kelly (2019). "Long-term field evaluation of the Plantower PMS low-cost particulate matter sensors." Environmental Pollution **245**: 932-940.

Smart Citizen Kit. (2020). "Smart Citizen Kit Map." 02/05/2020, from https://smartcitizen.me/kits/.

Snyder, E. G., T. H. Watkins, P. A. Solomon, E. D. Thoma, R. W. Williams, G. S. W. Hagler, D. Shelow, D. A. Hindin, V. J. Kilaru and P. W. Preuss (2013). "The Changing Paradigm of Air Pollution Monitoring." Environmental Science & Technology **47**(20): 11369-11377.

Song, W. M., Y. Liu, J. Y. Liu, N. N. Tao, Y. F. Li, Y. Liu, L. X. Wang and H. C. Li (2019). "The burden of air pollution and weather condition on daily respiratory deaths among older adults in China, Jinan from 2011 to 2017." Medicine **98**(10): 9.

Stenlund, T., E. Liden, K. Andersson, J. Garvill and S. Nordin (2009). "Annoyance and health symptoms and their influencing factors: A population-based air pollution intervention study." Public Health **123**(4): 339-345.

Sucker, K., R. Both, M. Bischoff, R. Guski and G. Winneke (2008). "Odor frequency and odor annoyance. Part I: assessment of frequency, intensity and hedonic tone of environmental odors in the field." International Archives of Occupational and Environmental Health **81**(6): 671-682.

Turner, M. C., M. Jerrett, C. A. Pope, D. Krewski, S. M. Gapstur, W. R. Diver, B. S. Beckerman, J. D. Marshall, J. Su, D. L. Crouse and R. T. Burnett (2016). "Long-Term Ozone Exposure and Mortality in a Large Prospective Study." American Journal of Respiratory and Critical Care Medicine **193**(10): 1134-1142.

U.S. Environmental Protection Agency. (2019). "Air Sensor Toolbox."   Viewed 02/02/2019, from https://www.epa.gov/air-sensor-toolbox.

uRADMonitor. (2020). "Global Environmental Monitoring Network."   Viewed 02/05/2020, from https://www.uradmonitor.com/.

Vikram, S., A. Collier-Oxandale, M. H. Ostertag, M. Menarini, C. Chermak, S. Dasgupta, T. Rosing, M. Hannigan and W. G. Griswold (2019). "Evaluating and improving the reliability of gas-phase sensor system calibrations across new locations for ambient

measurements and personal exposure monitoring." <u>Atmospheric Measurement Techniques</u> **12**(8): 4211-4239.

Weissert, L., K. Alberti, E. Miles, G. Miskell, B. Feenstra, G. S. Henshaw, V. Papapostolou, H. Patel, A. Polidori, J. A. Salmond and D. E. Williams (2020a). "Low-cost sensor networks and land-use regression: Interpolating nitrogen dioxide concentration at high temporal and spatial resolution in Southern California." <u>Atmospheric Environment</u> **223**: 10.

Weissert, L., E. Miles, G. Miskell, K. Alberti, B. Feenstra, G. S. Henshaw, V. Papapostolou, H. Patel, A. Polidori, J. A. Salmond and D. E. Williams (2020b). "Hierarchical network design for nitrogen dioxide measurement in urban environments." <u>Atmospheric Environment</u> **228**: 117428.

Williams, R., A. Kaufman, T. Hanley, J. Rice and S. Garvey (2014). Evaluation of Field-deployed Low Cost PM Sensors. Washington, DC, U.S. Environmental Protection Agency.

Williams, R., D. Nash, G. Hagler, K. Benedict, I. MacGregor, B. Seay, M. Lawrence and T. Dye (2018). Peer Review and Supporting Literature Review of Air Sensor Technology Performance Targets. Washington, DC, U.S. Environmental Protection Agency.

World Air Quality Index Project. (2020). "World's Air Pollution: Real-time Air Quality Index." Viewed 01/24/2020, 2020, from https://waqi.info/.

World Health Organization (2016). Ambient Air Pollution: a Global Assessment of Exposure and Burdent of Disease. W. H. Organization. Geneva, Switzerland.

Wu, J., W. Cheng, H. J. Lu, Y. Shi and Y. He (2018). "The Effect of Particulate Matter on Visibility in Hangzhou, China." <u>Journal of Environmental Science and Management</u> **21**(1): 100-109.

Ye, Q., P. Gu, H. Z. Li, E. S. Robinson, E. Lipsky, C. Kaltsonoudis, A. K. Y. Lee, J. S. Apte, A. L. Robinson, R. C. Sullivan, A. A. Presto and N. M. Donahue (2018). "Spatial Variability of Sources and Mixing State of Atmospheric Particles in a Metropolitan Area." <u>Environmental Science & Technology</u> **52**(12): 6807-6815.

Zamora, M., F. Xiong, D. Gentner, B. Kerkez, J. Kohrman-Glaser and K. Koehler (2019). "Field and Laboratory Evaluations of the Low-Cost Plantower Particulate Matter Sensor." <u>Environmental Science & Technology</u> **53**(2): 838-849.

Zheng, T. S., M. H. Bergin, K. K. Johnson, S. N. Tripathi, S. Shirodkar, M. S. Landis, R. Sutaria and D. E. Carlson (2018). "Field evaluation of low-cost particulate matter sensors

in high-and low-concentration environments." <u>Atmospheric Measurement Techniques</u> **11**(8): 4823-4846.

Zimmerman, N., A. A. Presto, S. P. N. Kumar, J. Gu, A. Hauryliuk, E. S. Robinson, A. L. Robinson and R. Subramanian (2018). "A machine learning calibration model using random forests to improve sensor performance for lower-cost air quality monitoring." <u>Atmospheric Measurement Techniques</u> **11**(1): 291-313.

Chapter 2: Performance evaluation of twelve low-cost PM$_{2.5}$ sensors at an ambient air monitoring site

Contributing Authors: Brandon Feenstra, Vasileios Papapostolou, Sina Hasheminassab, Hang Zhang, Berj Der Boghossian, David Cocker, and Andrea Polidori

Abstract

A variety of low-cost sensors are now available on the consumer market for measuring air pollutants. The use of these low-cost sensors for ambient air monitoring applications is increasing and includes fence-line or near-source monitoring, community monitoring, emergency response, hot-spot identification, mobile monitoring, epidemiological studies, and supplemental monitoring to improve the spatial-temporal resolution of current monitoring networks. Evaluating and understanding the performance of these devices is necessary to properly interpret the results and reduce confusion when low-cost sensor measurements are not in agreement with measurements from regulatory-grade instrumentation. Systematic and comprehensive field and laboratory studies comparing low-cost sensors with regulatory-grade instrumentation are necessary to characterize sensor performance. This paper presents the results of 12 particulate matter (PM) sensors measurement of $PM_{2.5}$ (particles with aerodynamic diameter less than 2.5 μm) tested under ambient conditions against a federally equivalent method (FEM) instrument at an ambient air monitoring station in Riverside, CA spanning over a 3-year period from 02/05/15 to 03/27/18. Sensors were evaluated in triplicate with a typical time duration of 8-week. Performance evaluation results found 6 of the 12 sensor triplicates with average R2 values ≥ 0.70 for $PM_{2.5}$ concentrations less than 50 μg/m^3. Within this subset, the Mean Absolute Error (MAE) ranged from 4.4 to 7.0 μg/m^3 indicating the need for caution when interpreting data from these sensors. Additional analysis revealed that the impact of relative humidity on sensor performance varied between models with several models exhibiting increased bias error with increasing humidity. Results indicate that a number of these

sensors have potential as useful tools for characterizing PM$_{2.5}$ levels in ambient environments when data is interpreted and understood correctly with regard to existing ambient air quality networks. The performance evaluation results are specific for Riverside, CA under non-repeatable ambient weather conditions and particle properties with the expectation that performance evaluation testing at other locations with different particle properties and weather conditions would yield similar but non-identical results.

2.1 Introduction

2.1.1 Particle Pollution

Particulate matter (PM) is a ubiquitous environmental pollutant that has been linked to a host of health issues. Fine Particulate matter (PM$_{2.5}$; particles with aerodynamic diameter less than 2.5 µm) have been linked to respiratory illness, cardiovascular disease, stroke, lung cancer, reproductive issues, and premature death (Pope et al., 2002; Pope et al., 2009; Harris et al., 2014; Apte et al., 2015) In 2015, an estimated 4.2 million people died prematurely due to PM$_{2.5}$ exposure putting it in the top five mortality risk factors worldwide (Cohen et al., 2017). Based on modelled data, the World Health Organization (WHO) estimates 92% of people are exposed to PM$_{2.5}$ concentrations exceeding WHO's recommended annual mean of 10 µg/m^3(World Health Organization 2016). In addition to health impacts, PM pollution can impair visibility, damage the environment, and cause material damage. (Al-Thani et al., 2018; Wu et al., 2018)

PM is regulated by the United States Environmental Protection Agency (EPA) under the Clean Air Act .(U.S. Environmental Protection Agency) The National Ambient

Air Quality Standards (NAAQS) are set to protect public health and the environment. For PM$_{2.5}$ concentrations, the NAAQS is set at 12.0 μg/m^3 (annual mean) and 35 μg/m^3 (24-hr daily). Compliance with the NAAQS is determined by stationary ambient air monitoring sites (AMS) utilizing instrumentation operated as United States Environmental Protection Agency (U.S. EPA) Federal Reference Method (FRM) or Federal Equivalent Method (FEM). Networks of monitoring stations are typically designed to monitor air pollutants at a regional level to determine attainment of the NAAQS at a regional scale. An increasing number of studies have found the spatial and temporal resolution of these regional sites to be insufficient to characterize air pollutants at a community or neighborhood scale for pollutants that exhibit high spatial variability such as traffic-related PM (Apte et al., 2017; Gu et al., 2018; Ye et al., 2018).

2.1.2   Low-cost Sensors

Technological advancements have initiated a paradigm shift in the way air quality data is measured and shared to the public. This shift has been driven by the emergence of "low-cost" sensors for measuring both gas and particle pollutants. Numerous sensor models with prices ranging from $150 to $3,000 USD are available to the public with some vendors offering open data access and visualization (Snyder et al., 2013). These low-cost sensors can provide real or near-real time pollutant information at increased spatial resolutions with the potential to complement and expand the capabilities of existing ambient air monitoring networks and provide meaningful measurements at the local scale (Sadighi et al., 2018). While the utility of these measurements depends on the performance of the sensor in a specific environment, sensors with low intra-model variability could be spatially deployed

in a community to supplement existing regulatory-grade measurements and obtain hyper local measurements that could support emission reduction strategies such as those that will be designed for the California Assembly Bill (AB) 617. AB 617 was authored, passed, and signed to address the impacts of air pollution in disadvantaged neighborhoods by providing funding for emission reduction strategies and for air pollution monitoring at the local community scale.

Many low-cost sensors are sold to the public with minimal testing, maintenance recommendations, and standard operating procedures. (Snyder et al., 2013; Lewis and Edwards 2016) To date, there have been a limited number of systematic studies using an established protocol to characterize the performance of PM sensors in ambient conditions where end-users are likely to deploy these sensors (Morawska et al., 2018). Without systematic evaluation of the performance of these devices and dissemination of results in an easy-to-understand manner, the consumers are left to making purchasing decisions based on manufacturer marketing strategies, compatibility with cellular devices, exterior appearance of the sensor, and online product reviews. Some examples of marketing quotes for sensors evaluated in this paper include "Most Advanced Air Quality Sensor," "Professional grade, highly accurate indoor/outdoor air quality monitoring system," "Buy the Best Air Pollution Monitor, and "Tested by AQ-SPEC."

Prior published studies have evaluated the performance of several low-cost PM sensors under ambient conditions that are also evaluated in this paper. To the best of our knowledge, these include the AirBeam (Jiao et al., 2016; Mukherjee et al., 2017; Borghi et al., 2018), Alphasense OPC-N2 (Mukherjee et al., 2017; Crilley et al., 2018), PurpleAir

(Kim et al., 2019; Magi et al., 2019), and Foobot for indoor air quality (Moreno-Rangel et al., 2018). This represents a small fraction of the PM sensors currently available to consumers and with many of the evaluations performed to evaluate the fit for purpose of a sensor for a specific project or deployment. The U.S. EPA has also evaluated the performance of low-cost sensors in ambient environments using a standard protocol with evaluation results for the TSI AirAssure, AirBeam, Alphasense OPC-N2, and Shinyei PM Evaluation kit which are also evaluated in this work (Williams et al., 2014; Jiao et al., 2016; Feinberg et al., 2018; U.S. Environmental Protection Agency 2019). While this paper focuses on commercially available end user products, other researchers have evaluated the performance of the Original Equipment Manufacturer (OEM) PM sensors that include Plantower, Shinyei, and Nova Fitness OEM sensors (Austin et al., 2015; Kelly et al., 2017; Badura et al., 2018; Johnson et al., 2018; Zheng et al., 2018; Bulot et al., 2019; Liu et al., 2019; Sayahi et al., 2019; Zamora et al., 2019). A comprehensive review of low-cost sensors technology, applications, and outcomes is available in the literature (Morawska et al., 2018) and a comprehensive review of air sensor performance metrics and targets has been published (Williams et al., 2018). These reviews point out the diversity of work currently being published with differences in performance metrics used, types and duration of performance evaluations, and types of reference equipment by which sensors are evaluated against. This work differs from prior studies in that it presents the results of a large number of PM sensors evaluated in triplicate under a systematic protocol at one location. Many of these sensors have not been previously evaluated for performance and published in the literature.

As "low-cost" sensors become increasingly popular for both researchers and the general public, characterizing the performance of these sensors and educating the public about their appropriate applications, limitations, and data interpretation has become extremely important. Performance characterization will minimize confusion particularly when low-cost sensors report information that conflicts with data generated from reference-grade instrumentation operated by the local air pollution control districts (APCD). The South Coast Air Quality Management District (South Coast AQMD) established the Air Quality Sensor Performance Evaluation Center (AQ-SPEC; www.aqmd.gov/aq-spec) in mid-2014 to provide the public with unbiased information about the performance of commercially available "low-cost" sensors. AQ-SPEC performs a systematic and thorough performance evaluation of commercially available sensors in both field- and laboratory-based testing. In the field, air quality sensors are evaluated in triplicate for a period of two months to provide adequate statistical information to evaluate overall sensor performance against reference-grade instrumentation (Polidori et al., 2017). In the laboratory, a state-of-the-art characterization chamber is used to challenge the sensors with known concentrations of particle and gaseous pollutants under controlled environmental conditions (Papapostolou et al., 2017). AQ-SPEC has succeeded in providing potential end users (consumers and scientific researchers) with the necessary information to make informed product selections from a wide variety of commercially available products. This paper presents the field evaluations results of 12 commercially available "low-cost" PM sensors under ambient conditions as part of the ongoing AQ-SPEC sensor evaluation work.

Sensor performance is evaluated systematically according to a documented evaluation protocol.

2.2   Methodology

2.2.1   Field Deployment

The methods used to evaluate "low-cost" sensors in the field are described in detail in the AQ-SPEC Field Testing Protocol (Polidori et al., 2017). Briefly, low-cost air quality sensors are evaluated under ambient conditions for an 8-week field deployment at a fully instrumented AMS. Commercialized sensors are typically tested as off-the-shelf and out-of-the-box products without prior modification or calibration (i.e., zero, span). Sensors are operated according to the sensor manufacturer's user guide or manual if available. The low-cost sensors are deployed in triplicate so that intra-model variability can be examined and to provide the ability to detect potential malfunctions or sensor failures in a single unit. Sensors that are ruggedized for inclement weather (designed for ambient air monitoring) are typically mounted outside on the protective railing of the AMS. Sensors that are not ruggedized (designed for indoor air monitoring) are deployed in a custom-built sensor shelter. During the field evaluations, sensors were checked roughly once per week to confirm normal sensor operation and continuous data collection.

2.2.2   Site Location and Characteristics

The sensors evaluations took place at the South Coast AQMD Riverside-Rubidoux Air Monitoring Station (RIVR AMS) as part of the ongoing AQ-SPEC sensor evaluations. RIVR AMS, shown in the Supplemental Information (SI) Figure S2.1 (a), is a fully equipped regulatory air monitoring station with particulate matter instrumentation

operating as FRMs and FEMs. This monitoring station is an inland location that is downwind of the Los Angeles Air Basin and is heavily impacted by transported PM from upwind sources as well as a nearby highway. The nearest major highway to the site is the California State Route 60 (SR-60) located 0.8 km to the north / northeast of the site. In the general vicinity of the station, land use includes apartment complexes and single-family residences, school grounds, retail outlets, and vacant lots. Figure S2.2 shows the typical seasonal average chemical composition of $PM_{2.5}$ at RIVR AMS. Ambient $PM_{2.5}$ in this area is mainly comprised of secondary inorganic aerosols (i.e., nitrate, sulfate, ammonia) which accounts for 49-68% of the total $PM_{2.5}$ mass depending on the season. Organic matter is the second major contributor to $PM_{2.5}$ mass in this area (19-32%), followed by elemental carbon (4-10%), crustal material (dust, 4-6%), trace ions (e.g., sodium, potassium; 1-3%), and other trace elements (e.g., arsenic, barium; ~1%) (Hasheminassab et al., 2014).

2.2.3   Sensor Selection and Evaluation Timing

The 12 commercially available "low-cost" sensors were tested between February 2015 and March 2018. These sensors vary in cost from approximately $150 to $3000 USD. Table 2.1 provides a description of the 12 sensors with make, model, time resolution, estimated cost, and pollutants measured. Even though several of these sensors are developed for indoor air quality monitoring and not specifically for outdoor ambient monitoring, the evaluation of the technology provides valuable insights into the emerging market of air quality sensors with regards to their use in ambient air monitoring applications.

Manufacturer	Model	Pollutants Measured	Time Resolution	Cost
Shinyei	PM Evaluation Kit	$PM_{2.5}$	1-min	$1,000
Alphasense	OPC-N2	$PM_{2.5}$	< 1-min	$450
TSI	AirAssure	$PM_{2.5}$	5-min	$1,000
Hanvon	N1	$PM_{2.5}$, HCHO	1-min	$200
Airboxlab	Foobot	$PM_{2.5}$, CO_2, VOC	5-min	$200
Kaiterra	LaserEgg	$PM_{2.5}$	< 1-min	$200
PurpleAir	PA-II	$PM_{2.5}$, PM_{10}, $PM_{1.0}$	< 1-min	$230
HabitatMap	Air Beam 1	$PM_{2.5}$	1-min	$200
SainSmart	Pure Morning P3	$PM_{2.5}$, CO_2, HCHO	< 1-min	$170
IQAir	AirVisual Pro	$PM_{2.5}$, CO_2,	< 1-min	$270
Uhoo	uhoo	$PM_{2.5}$, O_3, NO_2, CO, CO_2, TVOC	1-min	$300
Aeroqual	AQY	$PM_{2.5}$, O_3, NO_2	1-min	$3,000

Table 2.1 List of sensors evaluated and sensor specifications.

While more than 12 PM sensors have been evaluated in the AQ-SPEC program, the selection of these 12 sensors was based on whether the sensor is commercially available, measures $PM_{2.5}$ ($\mu g/m^3$), tested within the three-year time span, and exhibited acceptable data recovery during the evaluation time period. The sensors were exposed to ambient air for a period of approximately 30-60 days. The timing of the evaluation was dependent on when the sensors were received and when space was available at RIVR AMS or in the sensor shelter.

2.2.4   Reference Instrumentation

While the RIVR AMS is equipped with both FRM and FEM instrumentation, the performance of the PM sensors selected for this study are evaluated against 1-hour FEM measurements of $PM_{2.5}$. The gravimetric FRM 24-hour integrated filter mass measurements do not capture the high time resolution of low-cost sensors. For the purposes

of this paper, a Met One Beta Attenuation Monitor (BAM), U.S. EPA designated Class III FEM (EQPM-0308-170) for monitoring $PM_{2.5}$, was used to compare against the low-cost sensor measurements. The Met One BAM provides 1-hr average $PM_{2.5}$ concentrations and is shown in Figure S2.1 (b & c).

2.2.5   Principle of Operation of Particulate Matter Sensors

The 12 $PM_{2.5}$ sensors evaluated in this paper are categorized as optical sensors with regards to their principle of operation. Optical methods are based on the light scattering of aerosols which is a function of the wavelength of the light source along with the size, composition, and refractive index of the aerosol. Aerosols flow across a focused beam of light and a photodetector records the intensity of the scattered light. These sensors can be categorized into volume scattering devices and optical particle counters (OPCs). In volume scattering devices, light is scattered by the ensemble of particles and detected by a photodetector which provides a single digital or analog output. This output is converted to particle mass concentrations by a prior calibration with a test aerosol and collocation with some reference or research grade instrumentation. In OPCs, the aerosol particles are counted and categorized into distinct size bins. Particle mass concentrations are then calculated based on number, size, and assumptions with regards to the shape, density, and refractive index of the aerosol (Morawska et al., 2018). The OEM sensor manufacturer and/or end-product integrator often develops software algorithms to provide a corrected value for particle mass concentration and consider these algorithms as proprietary technology.

2.2.6   Sensor Shelter

A louvered aluminum shelter was designed and constructed to house and protect the non-ruggedized air quality sensors from inclement weather conditions, such as rain, wind, and direct sunlight. The shelter is shown in appendix Figure S2.1 (d & e). The main compartment of the shelter is approximately 1 x 1 x 1 meter and designed with louvered vents and a mesh floor to allow for air circulation. The shelter has three aluminum mesh shelves upon which the sensors are placed for the field deployment. The shelter is designed in a manner to provide maximum movement of air through the enclosure and a sensing environment that is near-ambient conditions for pollutants and weather conditions.

2.2.7   Data analysis

Upon completion of the field deployment, the data was collected and joined for analysis. Data from the sensor triplicate was first validated following basic QA/QC procedures in which obvious time-series outliers, negative values, continuing zeros, and invalid data points (text, symbols, and blanks) were removed. Obvious time-series outliers were typically extremely high values that were found to be outside of the measurement range of a sensor or outside the bounds of typical ambient $PM_{2.5}$ concentrations. The remaining data were then averaged over 1-hour time intervals and matched by date and time to the hourly FEM BAM $PM_{2.5}$ data. Data recovery of at least 75% of the sub hourly raw sensor data was required for a 1-hr average data point to be considered valid. The 1-hr average reduces the noise associated with measurements at shorter time resolutions.

Statistical analysis was conducted on the 1-hr time matched data to examine data completeness,   intra-model   variability,   least-squares   linear   regression   statistics,

measurement error, and impact of environmental conditions. Following the data recovery calculations, the 1-hr time matched data sets were subjected to two data reduction filters to improve inter- and cross-model comparability. First, all rows with a missing $PM_{2.5}$ concentration for either the reference instrument or one of the three sensors was dropped from further analysis. Secondly, as regression statistics can be dependent on the range of PM experienced during the evaluation, data rows where the FEM BAM $PM_{2.5}$ concentration exceeded 50 $\mu g/m^3$ were removed from further analysis. The $PM_{2.5}$ concentration of 50 $\mu g/m^3$ was selected to include nearly four average standard deviations (8.9 $\mu g/m^3$) from the mean of means BAM $PM_{2.5}$ concentration (14.2 $\mu g/m^3$, SI Table S2.1) experienced during the 12 evaluations periods. This filter excludes only a small fraction (< 3% filtered per data set) and improves the comparability between the sensor evaluations. The equations for data recovery are provided in the SI with Equation (Eq.) S2.1 and S2.2.

Intra-model variability within a triplicate of sensors is defined as the degree to which the three sensors agree with one another. This is determined by calculating the mean $PM_{2.5}$ concentrations as measured by individual sensors within a triplicate and comparing with the mean of means and standard deviation (SD) for the mean of means. The SD for the mean of means provides a metric for intra-model variability. A high SD for the mean of means indicates high intra-model variability whereas a low SD indicates low intra-model variability.

Accuracy is defined as the degree to which the 1-hr average $PM_{2.5}$ concentrations generated from the low-cost sensors conforms to the $PM_{2.5}$ measurements from the FEM BAM instrument. Accuracy can be examined by looking at the regression statistics and

measurement error between sensor and reference instruments. When reviewing the slope and intercept of the best fit line for determining accuracy, the importance of the R^2 statistic must not be overlooked. The least squares linear regression provides a best fit linear equation that is shown in Eq. S2.3. In an ideal situation where the sensor perfectly matches the reference grade instrumentation, the slope (m) would be 1.0, intercept (b) 0.0, and the coefficient of determination (R^2) would be at or near 1.0. The R^2 statistic measures the scatter of the data points around the fitted linear regression line and provides a measure for how strongly variations in sensor-generated $PM_{2.5}$ concentrations are related to variations in BAM-generated $PM_{2.5}$ concentrations. When the R^2 value is below a certain threshold ($R^2 < 0.70$ for the purposes of this paper), examining the slope and intercept values to determine accuracy is not relevant due to the magnitude of scatter around the best fit line.

Mean Bias Error (MBE) and Mean Absolute Error (MAE) are calculated in similar fashion with the MAE taking the absolute value of the hourly differences between the sensor and BAM measurements. The MBE between the sensor and the reference BAM instrument provides a metric that indicates the tendency of the sensor to either under- or over-estimate the reference $PM_{2.5}$ mass concentrations. The units of both MBE and MAE are calculated in $\mu g/m^3$ which is identical to the units of measurement for both sensor and FEM instrument. This provides a hands-on way to visualize the error especially with regards to identifying the cause of the error when reviewing the linear regression results. Care must be taken with the MBE statistic as over-estimated errors will cancel out under-estimated errors in the calculation of MBE. The MAE provides a better metric for actual measurement error between sensor and reference. The equations for MBE and MAE are

found in Eq. 2.1 and 2.2, respectively. The Root Mean Square Error (RMSE) statistic is an additional metric for looking at the measurement error with the RMSE being disproportionately impacted by large errors with the equation for RMSE provided in Eq. 2.3.

$$\text{Eq. 2.1} \qquad \text{Mean Bias Error (MBE)} = \frac{1}{n} \sum_{i=1}^{n} (X_i - X_t)$$

$$\text{Eq. 2.2} \qquad \text{Mean Absolute Error (MAE)} = \frac{1}{n} \sum_{i=1}^{n} |(X_i - X_t)|$$

$$\text{Eq. 2.3} \qquad \text{Root Mean Square Error (RMSE)} = \sqrt{\frac{\sum_{i=1}^{n}(X_i - X_t)^2}{n}}$$

Where,
X_i is the 1-hr average measurement by the low-cost sensor
X_t is the 1-hr average measurement provided by the FEM $PM_{2.5}$ Met One BAM
n is the number of 1-hr time-matched data pairs

Some of the sensors have unique data recovery situations or unique methods for reporting data that require further attention and analysis. Due to a sensor malfunction, the Uhoo #2 sensor had a low data recovery of 47.2% and was therefore excluded from subsequent data analysis. The Purple Air PA-II has two OEM sensors and reports two similar but non-identical $PM_{2.5}$ concentrations. Data from these two OEM sensors were time matched and then averaged to provide one $PM_{2.5}$ concentration per PA-II sensor to compare with the reference instrumentation. The CF=atm measurement was selected for the Purple Air Sensor based on the OEM sensor manufacturer's, Plantower, recommendation for ambient measurements according to their manual (Yong and Haoxin 2016).

2.3   Results and Discussion

2.3.1   Field Conditions and Data Recovery

Twelve sensors were evaluated during specific and unique time periods taking place over three years: 02/05/15 to 03/27/18. The actual time periods of the evaluations are random and take place as the AQ-SPEC program receives sensors to evaluate and space is available in the sensor shelter. The ambient environment under which each triplicate of sensors is evaluated is characterized by specific, non-repeatable conditions for aerosol particles (size, count, shape, refractive index, speciation, and mass distribution) and climate conditions (temperature, relative humidity, wind, precipitation, etc.). Table S2.1 in the SI provides a summary of the field conditions for temperature, relative humidity, and hourly BAM FEM $PM_{2.5}$ mass concentrations experienced for the 12 distinct evaluation periods. The mean ambient temperature varies between the 12 evaluations and ranges between 12.3 and 25.2 ˚C indicating that seasonality differences in temperature do exist between the individual sensor evaluations. The mean RH between the 12 evaluations ranges from 48.1 to 67.9 % with a mean of means at 54.3 ± 5.3 %. The average SD for RH for the individual evaluations is ± 23.3% RH indicating that while moderate seasonal differences in RH exists between evaluations, the individual evaluations experienced a wide range of RH conditions. The BAM $PM_{2.5}$ mean concentration for the 12 evaluations ranged from 11.1 to 17.2 µg/m³ with a mean of means at 14.2 ± 2.0 µg/m³. The average SD for $PM_{2.5}$ individual evaluation periods is 8.9 µg/m³ indicating that while moderate seasonality differences in $PM_{2.5}$ exist, the individual evaluation periods experienced a range of $PM_{2.5}$ concentrations. The max $PM_{2.5}$ values experienced during the 12 evaluations varied

significantly between evaluations with max hourly concentrations ranging from 38 to 133 $\mu g/m^3$ indicating the need to filter out these higher $PM_{2.5}$ events to maintain a consistent concentration range between the evaluations.

The 1-hr average data recovery for the sensor triplicates is high with recovery > 79% for all sensors with most sensors nearing 99% data recovery as shown in SI Table S2.1. After processing the hourly matched data points for missing values (sensor triplicate or reference) and filtering out values for BAM $PM_{2.5}$ concentrations > 50 $\mu g/m^3$, the number of hourly matched data points (n) varied between the 12 evaluations ranging between 732 and 1917 data points with data recovery ranging from 71 to 98%.

2.3.2 Summary Statistics and Intra-model variability

Table 2.2 provides summary statistics with mean $PM_{2.5}$ concentrations measured for the three sensors, the mean of means, and the ± SD around the mean of means which provides a metric for intra-model variability. Four sensors, namely Aeroqual AQY, Purple Air PA-II, SainSmart P3, and TSI Air Assure, indicate low intra-model variability with the SD less than 0.75 with regards to the mean of means. Three sensors, namely the Laser Egg, Shinyei PM evaluation kit, and IQAir AirVisual Pro, indicate low to moderate intra-model variability with $0.76 \leq SD \leq 1.5$. Four sensors, namely Alphasense OPC-N2, Air Beam 1, Foobot, and Hanvon N1, indicate moderate to high intra-model variability with $1.51 \leq SD \leq 2.75$. The Uhoo indicates high intra-model variability with SD at ± 6.23.

	Sensor			Mean of Means	Reference BAM PM$_{2.5}$
	Mean ± SD (µg/m^3)				
Sensor	**1**	**2**	**3**	Mean ± SD (µg/m^3)	Mean ± SD (µg/m3)
Shinyei PM Evaluation Kit	14.8 ± 13.1	14.6 ± 12.7	13.0 ± 11.5	14.1 ± 0.80	15.2 ± 12.3
Alphasense OPC-N2	14.3 ± 6.2	10.1 ± 6.1	11.4 ± 7.0	11.9 ± 1.74	15.6 ± 6.6
TSI AirAssure	15.6 ± 13.4	17.4 ± 13.0	16.7 ± 12.4	16.6 ± 0.75	13.2 ± 11.3
Hanvon N1	32.0 ± 21.7	30.5 ± 19.7	27.6 ± 17.3	30.0 ± 1.80	15.2 ± 10.3
Airboxlab Foobot	19.7 ± 10.3	17.3 ± 8.6	24.0 ± 10.3	20.3 ± 2.75	14.4 ± 6.4
Kaiterra LaserEgg	15.6 ± 9.2	13.5 ± 8.2	12.9 ± 8.0	14.0 ± 1.16	14.0 ± 6.1
PurpleAir PA-II	16.9 ± 19.1	16.5 ± 18.6	16.7 ± 18.0	16.3 ± 0.13	12.1 ± 11.3
HabitatMap Air Beam 1	14.1 ± 9.3	17.0 ± 12.8	18.0 ± 14.5	16.4 ± 1.64	11.1 ± 6.6
SainSmart Pure Morning P3	14.6 ± 12.2	15.7 ± 12.8	14.7 ± 10.6	15.0 ± 0.51	11.1 ± 6.6
IQAir Air Visual Pro	17.5 ± 10.2	17.6 ± 10.2	20.7 ± 11.4	18.6 ± 1.51	17.2 ± 7.3
Uhoo	32.6 ± 14.9	-	20.1 ± 11.0	26.3 ± 6.23	17.1 ± 7.3
Aeroqual AQY	9.8 ± 11.5	9.7 ± 11.7	9.3 ± 10.8	9.6 ± 0.24	13.8 ± 14.4

Table 2.2 Summary statistics and intra-model variability for sensor triplicates.

2.3.3 Least Squares Linear Regression and Measurement Error

Least squares linear regression was performed for each sensor within a triplicate with the results shown in Table 2.3. Six of the 12 sensors were found to have a triplicate average of $R^2 \geq 0.70$ and will be discussed further with regards to slope/intercept for accuracy. Four sensors, namely Aeroqual AQY, Purple Air PA-II, Sainsmart P3, and the Shinyei PM Evaluation kit indicated high linearity with $R^2 \geq 0.75$ and two sensors, namely TSI Air Assure and Air Visual pro, indicated linearity with $0.70 \geq R^2 \geq 0.74$. With regards

to slope as a measure for accuracy, four of these six sensors, namely Aeroqual AQY, Shinyei PM Evaluation kit, TSI Air Assure, and IQAir Air Visual Pro, were found to have slope values within ± 0.25 of the 1.0 ideal value. The Purple Air PA-II and the SainSmart P3 were found to generally overestimate FEM $PM_{2.5}$ concentrations by roughly 50% with slope values between 1.31 and 1.68. With regards to intercept value as a measure for accuracy, three sensors, namely the Sainsmart P3, Shinyei, and IAQir Air Visual Pro were found to have intercept values $|b| < 2.5$ from the ideal 0.0 value. The remaining three sensors, namely the Aeroqual AQY, Purple Air PA-II, and TSI AirAssure, were found to have higher intercept values ranging from $2.6 < |b| < 4.0$.

The calculated measurement errors (MBE and MAE) between sensors and the BAM $PM_{2.5}$ measurements are shown in Table 2.3. Four sensors, namely the Aeroqual AQY, Kaiterra LaserEgg, Shinyei PM Kit, and IQAir AirVisual Pro, have MAE near or less than 5 $\mu g/m^3$. Five sensors, namely the Alphasense OPC, Air Beam 1, Purple Air PA-II, Sainsmart P3, and the TSI Air Assure, have MAE in the 5 to 7.5 $\mu g/m^3$ range. Three sensors, namely the Foobot, Hanvon N1, and the Uhoo, have MAE greater than 7.5 $\mu g/m^3$. For 8 of the 12 sensors, namely the Aeroqual, Foobot, Alphasense OPC, AirBeam 1, Hanvon N1, Purple Air PA-II, SainSmart P3, and TSI Air Assure, the proportion of MBE to MAE is greater than 0.65 indicating that the predominant error associated with these sensors is systematic in nature rather than random. Accounting for systematic bias errors could significantly reduce the measurement errors associated with sensors.

Sensor	#	R^2	Slope	Slope 95% CI	Intercept	Intercept 95% CI	MBE	MAE	RMSE
							Measurement Error ($\mu g/m^3$)		
Shinyei PM Evaluation Kit	1	0.75	1.18	0.04	-1.48	0.59	0.9	4.5	6.8
	2	0.73	1.13	0.04	-1.07	0.60	0.7	4.5	6.7
	3	0.75	1.03	0.03	-1.29	0.52	-0.9	4.2	5.8
Alphasense OPC-N2	1	0.67	0.78	0.04	2.08	0.67	-1.3	3.3	4.1
	2	0.38	0.57	0.05	1.18	0.90	-5.5	6.5	7.8
	3	0.40	0.67	0.06	1.03	1.01	-4.2	5.9	7.2
TSI AirAssure	1	0.73	1.10	0.04	1.61	0.60	2.9	5.1	7.6
	2	0.74	1.08	0.03	3.66	0.57	4.7	6.0	8.2
	3	0.72	1.01	0.03	3.81	0.56	4.0	5.6	7.6
Hanvon N1	1	0.56	2.13	0.10	0.91	1.71	17.4	18.1	24.1
	2	0.54	1.91	0.10	2.69	1.59	15.9	16.3	21.9
	3	0.58	1.73	0.08	2.39	1.34	13.1	13.5	18.1
Airboxlab Foobot	1	0.57	1.32	0.06	0.28	1.00	5.0	6.4	8.6
	2	0.54	1.08	0.05	1.35	0.86	2.6	4.7	6.4
	3	0.54	1.29	0.07	4.89	1.03	9.2	9.5	11.7
Kaiterra LaserEgg	1	0.57	1.15	0.06	-0.08	0.95	2.0	4.7	6.4
	2	0.56	1.02	0.06	-0.40	0.85	-0.1	4.1	5.4
	3	0.58	1.01	0.06	-0.80	0.82	-0.7	4.0	5.2
PurpleAir PA-II	1	0.95	1.68	0.03	-3.06	0.51	5.0	7.0	10.6
	2	0.95	1.63	0.03	-2.84	0.49	4.7	6.7	10.0
	3	0.95	1.58	0.03	-2.08	0.48	4.8	6.7	9.7
HabitatMap Air Beam 1	1	0.59	1.08	0.05	2.03	0.63	2.9	4.4	6.6
	2	0.57	1.47	0.07	0.46	0.90	5.7	6.5	10.6
	3	0.57	1.66	0.08	-0.62	1.01	6.8	7.5	12.4
SainSmart Pure Morning P3	1	0.76	1.52	0.05	-2.34	0.69	3.5	5.3	7.8
	2	0.77	1.61	0.05	-2.19	0.70	4.6	5.9	8.8
	3	0.74	1.31	0.05	0.06	0.62	3.5	5.0	6.8
IQAir AirVisual Pro	1	0.69	1.15	0.04	-2.38	0.73	0.2	4.4	5.8
	2	0.69	1.16	0.04	-2.42	0.73	0.3	4.4	5.8
	3	0.72	1.31	0.04	-1.97	0.77	3.4	5.3	7.3
Uhoo	1	0.00	0.09	0.11	31.11	2.03	15.4	17.7	22.4
	2	-	-	-	-	-	-	-	-
	3	0.00	0.02	0.08	19.74	1.51	2.9	10.1	13.5
Aeroqual AQY	1	0.78	0.99	0.02	-2.75	0.39	-2.9	4.5	6.1
	2	0.79	1.01	0.02	-3.08	0.38	-3.0	4.7	6.2
	3	0.79	0.94	0.02	-2.63	0.35	-3.4	4.6	6.1

Table 2.3 Linear Regression Statistics and measurement error for sensor triplicates.

Several interesting observations can be made with regards to the regression statistics and measurement errors. The Aeroqual AQY bias error (triplicate average: 3.1 $\mu g/m^3$) is strikingly close to the linear regression intercept values (triplicate average: 2.8 $\mu g/m^3$) indicating that the sensor may suffer from a zero offset and that correcting for this offset may potentially reduce measurement error. For the Hanvon N1, the MBE accounts for over 95% of the MAE indicating a strong positive bias error which is confirmed with slope values > 1.73 with the sensor often overestimating BAM $PM_{2.5}$ concentrations by over 100%. The Kaiterra Laser Eggs regression statistics show near ideal slope and intercept values, but the R^2 was found to be less than 0.60. The MBE/MAE ratio for the Laser Eggs is less than 0.5 indicating that the measurement error is dominated by random error rather that systematic or bias error. This sensor highlights the importance of evaluating accuracy not only on slope/intercept values, but also with the R^2 statistic and measurement error to gain a more comprehensive understanding of sensor performance.

2.3.4   Comparison of Results with Previous Sensor Evaluations

Sensor performance evaluations from prior studies often differ with regards to methodology with differences in geographic locations, length of evaluation, meteorological conditions, particle properties, reference instrumentation, and purpose of evaluation. The most comparable sensor evaluations to this work have been performed by the U.S. EPA according to a standard EPA protocol at a reference air monitoring site with non-ruggedized sensors housed in a sensor shelter. The comparison between the results of the AQ-SPEC and U.S. EPA sensor evaluations for the TSI AirAssure, Habitat Map AirBeam, Alphasense OPC-N2, and the Shinyei PM evaluation kit are provided in Table

2.4. The differences in slope, intercept, and correlation between these distinct geographic locations indicate that sensor performance may vary by geographic regions that experience different concentration ranges and aerosol optical properties (Feinberg et al., 2018).

Location	South Coast AQMD Riverside, California			U.S. EPA Denver, Colorado			U.S. EPA Atlanta, Georgia		
Reference Comparison				Feinberg, et al., 2018			Jiao, et al., 2016		
Instrument	Met One BAM 1020			Grimm 180 EDM			Met One BAM 1020		
Time-period	~ 8 weeks			Long-term			> 30 days		
Time Average	1-HR			1-HR			12-HR		
	Avg Regression Stats			Avg Regression Stats			Avg Regression Stats		
Sensor	Slope	Intercept	R^2	Slope	Intercept	R^2	Slope	Intercept	R^2
TSI AirAssure	1.06	3.03	0.73	1.15	0.41	0.63	-	-	-
Habitat Map AirBeam	1.40	0.62	0.58	-	-	0.69	-	-	0.43
Alphasense OPC-N2	0.67	1.43	0.48	0.47	-1.48	0.16	-	-	-
Shinyei PM Evaluation Kit	1.11	-1.28	0.74	0.56	0.52	0.51	0.72	7.48	0.36

Table 2.4 Comparison between published sensor evaluation results

The AirBeam and Alphasense OPC-N2 were also evaluated in Cuyama Valley, CA against a Grimm 11-R for 12 weeks. Average regression statistics for the AirBeam were slope of 0.38, intercept of 4.1, and R^2 of 0.66 and for the Alphasense OPC-N2 were slope of 0.14, intercept of 2.5, and R^2 of 0.41 for hourly data (Mukherjee et al., 2017). While the correlations are similar to the results presented in this study, the slope/intercepts between evaluations differ with the AirBeam overestimating $PM_{2.5}$ in Riverside and underestimating

it in the Cuyama Valley. While both studies found the Alphasense OPC-N2 to underestimate $PM_{2.5}$ concentrations, the magnitude of the negative bias was larger in the Cuyama Valley than in Riverside. In a long-term performance evaluation of the Purple Air PA-II sensor against a Met One BAM 1020 in Charlotte, North Carolina, regression statistics found slope at 2.2, intercept at 1.3, and R^2 at 0.54 (Magi et al., 2019). These long-term evaluation results differ from the findings in this study with 2-month evaluation average regression statistics finding a slope of 1.63, intercept of -2.66, and R^2 of 0.95. This significant discrepancy between studies indicates that the length of the evaluation may also impact correlation against reference monitors especially if a sensor degrades or malfunctions during the time period of a long-term evaluation.

2.3.5   Impact of Environmental Conditions on Bias Error

A contributing factor for diminishing performance of low-cost sensors when compared against reference instrumentation is due to the impact of RH (Jayaratne et al., 2018). Some low-cost optical methods adjust or calibrate in real-time for the impacts of RH on the conversion from particle count to particle mass concentration (Hojaiji et al., 2017; Di Antonio et al., 2018). While the BAM FEM monitor is equipped with a heater to condition the aerosol to a set temperature and RH prior to sampling, the low-cost sensors measure PM at ambient temperature and RH. To examine the potential impact of RH on sensor response, hourly bias errors were plotted against the hourly RH for all 12 sensors (Figure 2.1).
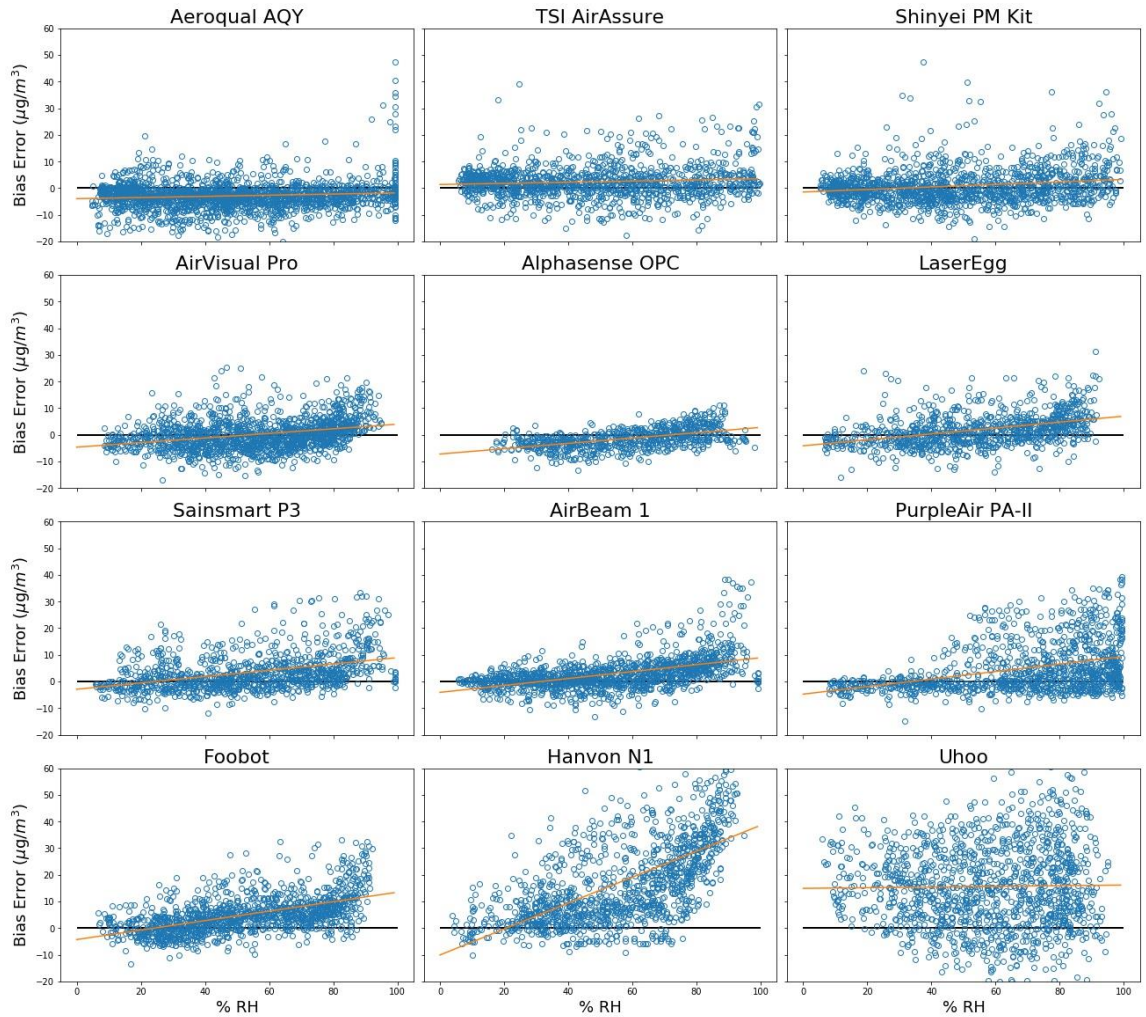
Figure 2.1 Impact of Relative Humidity (RH) on the bias error between Sensor and Met One BAM

Ideally, the slope of the best fit line would be zero and would be located on the y =

0 axis. The bias error by RH plot for the Aeroqual AQY, TSI AirAssure, and the Shinyei

indicate that these sensors are not strongly impacted by increasing RH. The remaining 9

sensors, except for the Uhoo, indicate increasingly positive bias error as RH increases and

are ordered from left to right and top to bottom by magnitude of slope of best fit line.

Addressing and correcting for the impact of RH on these optical devices, by either

advancing OPC hardware or by developing software corrections algorithms for RH, would

likely result in a reduction in the measurement error associated with low-cost sensors. Care should be taken when developing these software correction algorithms so that the model or algorithm developed is based on scientifically relevant inputs (i.e. ambient Temperature and RH collected in real-time) so as not to over-fit the models to limited training data sets and to ensure that the measurement is still a measurement (Hagler et al., 2018). Extensive field testing to capture seasonal variabilities for temperature and RH will help tremendously towards understanding the impacts of RH on low-cost optical particle counters. Additionally, laboratory testing with a sophisticated heating, ventilation, and air conditioning (HVAC) system to control temperature, RH, and the particles environment can provide valuable insights into the impacts of local weather conditions and interferants on these devices (Papapostolou et al., 2017).

To examine the potential impact of $PM_{2.5}$ concentrations on sensor response, hourly bias errors were plotted against the hourly BAM $PM_{2.5}$ for all 12 sensors (Figure 2.2). No consistent trends are seen across the 12 sensors as $PM_{2.5}$ concentrations increase. Individually though, Figure 2.2 provides a telling story of where shifts between systematic and random measurement error occur along the $PM_{2.5}$ measurement range. For example, the Purple Air sensor indicates predominant random error between 0-12 $\mu g/m^3$ with scatter almost evenly distributed between positive and negative bias. However, between 13-50 $\mu g/m^3$ the sensor indicates systematic positive bias error. On the other hand, the Aeroqual AQY indicates systematic negative error that increases as concentrations rise from 0 to 25 $\mu g/m^3$. Above 25 $\mu g/m^3$, the Aeroqual AQY bias is scattered around the y=0 line indicating random error. The Shinyei PM kit, AirVisual Pro, and Laser Egg indicate measurement

51

error dominated by random error with scatter evenly distributed between positive and negative bias. These sensors also exhibit lower MBE/MAE ratios. Understanding when measurement error shifts between systematic and random error, can provide insights on how to model sensor response to regulatory-grade equipment. It should be noted that these observations are limited to the PM$_{2.5}$ concentration range of 0-50 µg/m^3 and sensors may behave differently outside of this range.
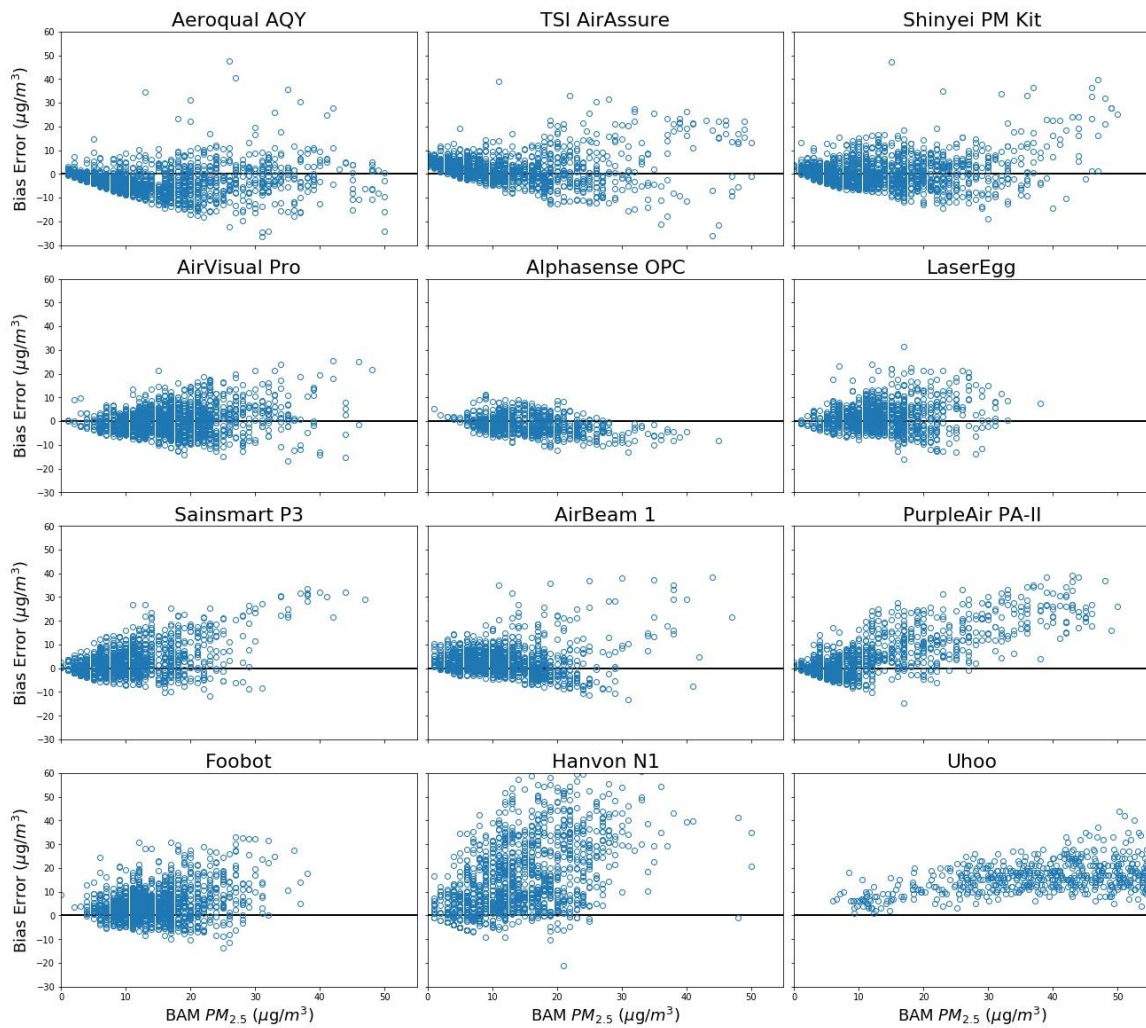
Figure 2.2 Impact of PM$_{2.5}$ concentration on bias error between Sensor and Met One BAM

2.3.6   Limitations and future work

Evaluating the performance of low-cost air quality sensors has limitations that must be acknowledged and understood. First, the ambient field environment is specific to location, time of year, weather conditions, and the pollutant physical/chemical properties experienced during the evaluation. The ambient environment experienced by a sensor within an evaluation time period cannot be controlled or duplicated for subsequent tests. The results of this limited evaluation provide an indication of the sensors performance under specific conditions at the RIVR AMS. A performance evaluation of a sensor under different environmental conditions and particle properties would likely provide similar but non-identical results. To address these limitations of field performance evaluations, sensors that perform well in the field are submitted to the AQ-SPEC laboratory for testing in a characterization chamber (Papapostolou et al., 2017). Secondly, a number of the sensors evaluated are designed for indoor air quality and are not ruggedized for ambient monitoring. These non-ruggedized sensors are installed inside an aluminum shelter enclosure which protects the units from ambient weather conditions. While the enclosure minimizes the effect of extreme weather conditions and is designed to provide a near ambient environment, the shelter environment is not identical to the ambient environment sampled by the FEM BAM $PM_{2.5}$ instrument.

The future development of performance targets for low-cost air quality sensors would drive technology advancement and provide a pathway to generate an increase in understanding and trust in low-cost sensors. A sensor certification program could perform more rigorous field testing that incorporates multiple sites across the country and multiple

seasons in a testing protocol similar to the process for instruments to achieve designation as a FRM or FEM. Rigorous field testing for PM sensors in various environments would be necessary as generating an aerosol environment in a laboratory identical to a local aerosol environment (e.g., in terms of particle count, shape, refractive index, speciation, source, size and mass distribution) is extremely difficult. A certification program with more rigorous field and laboratory studies can enhance the current understanding of how particle composition can impact low-cost sensor performance with understanding how these optical methods respond in environments dominated by regional specific aerosols like inland dust, course silt, coastline sea salt, secondary organic aerosol, and other regional specific aerosol compositions. A certification center could provide guidance and catalyze the evolution of this technology, identify key data quality indicators, set performance requirements, and increase trust in data generated by low-cost sensors.

2.4   Conclusions

This paper presents the results of 12 "low-cost" $PM_{2.5}$ sensors against reference instrumentation at the South Coast AQMD RIVR AMS in Southern California. The sensor products range in price from US$150.00 to US$3000.00 with varying performance for intra-model variability, linear regression statistics, and measurement errors. The high correlation coefficients between sensors and the FEM BAM indicate that a number of these low-cost units track the ambient PM concentrations of regulatory monitors well. For sensors that are highly correlated to the FEM BAM, the slope and intercept offsets of the regression statistics indicate that refinement or calibration of the sensors could be performed to improve sensor performance and reduce measurement error. Additionally,

sensors with a high MBE/MAE ratio are impacted predominantly by systematic error which could potentially be accounted for to reduce measurement error. The impacts of environmental conditions (RH and PM concentration) were investigated and indicate that the bias error for many low-cost optical particulate sensors on the market are impacted by changing environmental conditions. Future development by sensor manufacturers and sensor integrators that address the positive bias error associated with RH will likely produce sensors with less measurement error and that generate higher trust in data collected. Not accounting for RH effects may lead to the collection of measurements with a large bias error and may limit the usefulness of these low-cost tools and collected data. Due to the need for slope/intercept and potential RH corrections for some sensors, the actual utility of these devices may be limited to those who have access to reference grade instrumentation and the data science skill set to develop models and algorithms to correct the data. The technical requirements to develop and apply these corrections in real-time can potentially remove the usefulness of this technology from potential end-users and limit usefulness to those that are trained and able to perform the required corrections. For use by non-experts, low-cost sensors should be easily operated, installed, configured, and provide data with low measurement errors.

The overall state of the technology for measuring PM is improving and commercially available products have the potential to provide meaningful results to citizen scientists, communities, researchers, and regulatory agencies. As the market continues to expand, air quality measurement techniques and methodology is changing dramatically. Validating the performance of these sensors is a critical step as this new paradigm of low-

cost sensing takes effect. The potential applications for "low-cost" sensors are vast and properly characterizing of the performance of these devices will provide insights into interpreting their results and reduce confusion especially when low-cost sensor data does not agree with federally approved reference instruments.

References

Al-Thani, H., M. Koc and R. J. Isaifan (2018). "A Review on the Direct Effect of Particulate Atmospheric Pollution on Materials and its Mitigation for Sustainable Cities and Societies." Environmental Science and Pollution Research **25**(28): 27839-27857.

Apte, J. S., J. D. Marshall, A. J. Cohen and M. Brauer (2015). "Addressing Global Mortality from Ambient PM2.5." Environmental Science & Technology **49**(13): 8057-8066.

Apte, J. S., K. P. Messier, S. Gani, M. Brauer, T. W. Kirchstetter, M. M. Lunden, J. D. Marshall, C. J. Portier, R. C. H. Vermeulen and S. P. Hamburg (2017). "High-Resolution Air Pollution Mapping with Google Street View Cars: Exploiting Big Data." Environmental Science & Technology **51**(12): 6999-7008.

Austin, E., I. Novosselov, E. Seto and M. G. Yost (2015). "Laboratory Evaluation of the Shinyei PPD42NS Low-Cost Particulate Matter Sensor." Plos One **10**(9).

Badura, M., P. Batog, A. Drzeniecka-Osiadacz and P. Modzel (2018). "Evaluation of Low-Cost Sensors for Ambient PM2.5 Monitoring." Journal of Sensors **2018**: 1-16.

Borghi, F., A. Spinazze, D. Campagnolo, S. Rovelli, A. Cattaneo and D. M. Cavallo (2018). "Precision and Accuracy of a Direct-Reading Miniaturized Monitor in PM2.5 Exposure Assessment." Sensors **18**(9).

Bulot, F. M. J., S. J. Johnston, P. J. Basford, N. H. C. Easton, M. Apetroaie-Cristea, G. L. Foster, A. K. R. Morris, S. J. Cox and M. Loxham (2019). "Long-term field comparison of multiple low-cost particulate matter sensors in an outdoor urban environment." Scientific Reports **9**: 13.

Cohen, A. J., M. Brauer and R. Burnett (2017). "Estimates and 25-year trends of the global burden of disease attributable to ambient air pollution: an analysis of data from the Global Burden of Diseases Study 2015 (vol 389, pg 1907, 2017)." Lancet **391**(10130): 1576-1576.

Crilley, L. R., M. Shaw, R. Pound, L. J. Kramer, R. Price, S. Young, A. C. Lewis and F. D. Pope (2018). "Evaluation of a low-cost optical particle counter (Alphasense OPC-N2) for ambient air monitoring." Atmospheric Measurement Techniques **11**(2): 709-720.

Di Antonio, A., O. Popoola, B. Ouyang, J. Saffell and R. Jones (2018). "Developing a Relative Humidity Correction for Low-Cost Sensors Measuring Ambient Particulate Matter." Sensors **18**(9): 2790.

Feinberg, S., R. Williams, G. S. W. Hagler, J. Rickard, R. Brown, D. Garver, G. Harshfield, P. Stauffer, E. Mattson, R. Judge and S. Garvey (2018). "Long-term evaluation of air sensor technology under ambient conditions in Denver, Colorado." Atmospheric Measurement Techniques **11**(8): 4605-4615.

Gu, P. S., H. Li, Q. Ye, E. S. Robinson, J. S. Apte, A. L. Robinson and A. A. Presto (2018). "Intracity Variability of Particulate Matter Exposure Is Driven by Carbonaceous Sources and Correlated with Land-Use Variables." Environmental Science & Technology **52**(20): 11545-11554.

Hagler, G. S. W., R. Williams, V. Papapostolou and A. Polidori (2018). "Air Quality Sensors and Data Adjustment Algorithms: When Is It No Longer a Measurement?" Environmental Science & Technology **52**(10): 5530-5531.

Harris, G., W. D. Thompson, E. Fitzgerald and D. Wartenberg (2014). "The association of PM2.5 with full term low birth weight at different spatial scales." Environmental Research **134**: 427-434.

Hasheminassab, S., N. Daher, B. D. Ostro and C. Sioutas (2014). "Long-term source apportionment of ambient fine particulate matter (PM2.5) in the Los Angeles Basin: a focus on emissions reduction from vehicular sources." Environmental Pollution **193**: 54-64.

Hojaiji, H., H. Kalantarian, A. A. T. Bui, C. E. King and M. Sarrafzadeh (2017). "Temperature and Humidity Calibration of a Low-Cost Wireless Dust Sensor for Real-Time Monitoring." 2017 IEEE Sensors Applications Symposium (SAS).

Jayaratne, R., X. T. Liu, P. Thai, M. Dunbabin and L. Morawska (2018). "The influence of humidity on the performance of a low-cost air particle mass sensor and the effect of atmospheric fog." Atmospheric Measurement Techniques **11**(8): 4883-4890.

Jiao, W., G. Hagler, R. Williams, R. Sharpe, R. Brown, D. Garver, R. Judge, M. Caudill, J. Rickard, M. Davis, L. Weinstock, S. Zimmer-Dauphinee and K. Buckley (2016). "Community Air Sensor Network (CAIRSENSE) project: evaluation of low-cost sensor performance in a suburban environment in the southeastern United States." Atmospheric Measurement Techniques **9**(11): 5281-5292.

Johnson, K. K., M. H. Bergin, A. G. Russell and G. S. W. Hagler (2018). "Field Test of Several Low-Cost Particulate Matter Sensors in High and Low Concentration Urban Environments." Aerosol and Air Quality Research **18**(3): 565-578.

Kelly, K. E., J. Whitaker, A. Petty, C. Widmer, A. Dybwad, D. Sleeth, R. Martin and A. Butterfield (2017). "Ambient and laboratory evaluation of a low-cost particulate matter sensor." Environmental Pollution **221**: 491-500.

Kim, S., S. Park and J. Lee (2019). "Evaluation of Performance of Inexpensive Laser Based PM2.5 Sensor Monitors for Typical Indoor and Outdoor Hotspots of South Korea." Applied Sciences **9**(9): 14.

Lewis, A. and P. Edwards (2016). "Validate personal air-pollution sensors." Nature **535**(7610): 29-31.

Liu, H. Y., P. Schneider, R. Haugen and M. Vogt (2019). "Performance Assessment of a Low-Cost PM2.5 Sensor for a near Four-Month Period in Oslo, Norway." Atmosphere **10**(2): 18.

Magi, B. I., C. Cupini, J. Francis, M. Green and C. Hauser (2019). "Evaluation of PM2.5 measured in an urban setting using a low-cost optical particle counter and a Federal Equivalent Method Beta Attenuation Monitor." Aerosol Science and Technology: 13.

Morawska, L., P. K. Thai, X. T. Liu, A. Asumadu-Sakyi, G. Ayoko, A. Bartonova, A. Bedini, F. H. Chai, B. Christensen, M. Dunbabin, J. Gao, G. S. W. Hagler, R. Jayaratne, P. Kumar, A. K. H. Lau, P. K. K. Louie, M. Mazaheri, Z. Ning, N. Motta, B. Mullins, M. M. Rahman, Z. Ristovski, M. Shafiei, D. Tjondronegoro, D. Westerdahl and R. Williams (2018). "Applications of low-cost sensing technologies for air quality monitoring and exposure assessment: How far have they gone?" Environment International **116**: 286-299.

Moreno-Rangel, A., T. Sharpe, F. Musau and G. McGill (2018). "Field evaluation of a low-cost indoor air quality monitor to quantify exposure to pollutants in residential environments." Journal of Sensors and Sensor Systems **7**(1): 373-388.

Mukherjee, A., L. G. Stanton, A. R. Graham and P. T. Roberts (2017). "Assessing the Utility of Low-Cost Particulate Matter Sensors over a 12-Week Period in the Cuyama Valley of California." Sensors **17**(8).

Papapostolou, V., H. Zhang, B. J. Feenstra and A. Polidori (2017). "Development of an environmental chamber for evaluating the performance of low-cost air quality sensors under controlled conditions." Atmospheric Environment **171**: 82-90.

Polidori, A., B. Feenstra, V. Papapostolou and H. Zhang (2017). Field Evaluation of Low-Cost Air Quality Sensors - Field Setup and Testing Protocol. Diamond Bar, CA, South Coast Air Quality Management District.

Pope, C. A., R. T. Burnett, M. J. Thun, E. E. Calle, D. Krewski, K. Ito and G. D. Thurston (2002). "Lung cancer, cardiopulmonary mortality, and long-term exposure to fine particulate air pollution." Journal of the American Medical Association **287**(9): 1132-1141.

Pope, C. A., III, M. Ezzati and D. W. Dockery (2009). "Fine-Particulate Air Pollution and Life Expectancy in the United States." New England Journal of Medicine **360**(4): 376-386.

Sadighi, K., E. Coffey, A. Polidori, B. Feenstra, Q. Lv, D. K. Henze and M. Hannigan (2018). "Intra-Urban Spatial Variability of Surface Ozone in Riverside, CA: Viability and Validation of Low-cost Sensors." Atmospheric Measurement Techniques **11**(3): 1777-1792.

Sayahi, T., A. Butterfield and K. E. Kelly (2019). "Long-term field evaluation of the Plantower PMS low-cost particulate matter sensors." Environmental Pollution **245**: 932-940.

Snyder, E. G., T. H. Watkins, P. A. Solomon, E. D. Thoma, R. W. Williams, G. S. W. Hagler, D. Shelow, D. A. Hindin, V. J. Kilaru and P. W. Preuss (2013). "The Changing Paradigm of Air Pollution Monitoring." Environmental Science & Technology **47**(20): 11369-11377.

U.S. Environmental Protection Agency. "Summary of the Clean Air Act."   Viewed 11/20/18, from https://www.epa.gov/laws-regulations/summary-clean-air-act.

U.S. Environmental Protection Agency. (2019). "Air Sensor Toolbox."   Viewed 02/02/2019, from https://www.epa.gov/air-sensor-toolbox.

Williams, R., A. Kaufman, T. Hanley, J. Rice and S. Garvey (2014). Evaluation of Field-deployed Low Cost PM Sensors. Washington, DC, U.S. Environmental Protection Agency.

Williams, R., D. Nash, G. Hagler, K. Benedict, I. MacGregor, B. Seay, M. Lawrence and T. Dye (2018). Peer Review and Supporting Literature Review of Air Sensor Technology Performance Targets. Washington, DC, U.S. Environmental Protection Agency.

World Health Organization (2016). Ambient Air Pollution: a Global Assessment of Exposure and Burdent of Disease. W. H. Organization. Geneva, Switzerland.

Wu, J., W. Cheng, H. J. Lu, Y. Shi and Y. He (2018). "The Effect of Particulate Matter on Visibility in Hangzhou, China." Journal of Environmental Science and Management **21**(1): 100-109.

Ye, Q., P. Gu, H. Z. Li, E. S. Robinson, E. Lipsky, C. Kaltsonoudis, A. K. Y. Lee, J. S. Apte, A. L. Robinson, R. C. Sullivan, A. A. Presto and N. M. Donahue (2018). "Spatial Variability of Sources and Mixing State of Atmospheric Particles in a Metropolitan Area." Environmental Science & Technology **52**(12): 6807-6815.

Yong, Z. and Z. Haoxin (2016). PMS5003 Series Data Manual. <u>2016 Product Data Manual of Plantower</u>, Plantower.

Zamora, M., F. Xiong, D. Gentner, B. Kerkez, J. Kohrman-Glaser and K. Koehler (2019). "Field and Laboratory Evaluations of the Low-Cost Plantower Particulate Matter Sensor." <u>Environmental Science & Technology</u> **53**(2): 838-849.

Zheng, T. S., M. H. Bergin, K. K. Johnson, S. N. Tripathi, S. Shirodkar, M. S. Landis, R. Sutaria and D. E. Carlson (2018). "Field evaluation of low-cost particulate matter sensors in high-and low-concentration environments." <u>Atmospheric Measurement Techniques</u> **11**(8): 4823-4846.

Supplemental Information – Chapter 2

1. Air Quality – Sensor Performance Evaluation Center (AQ-SPEC)
2. Figure S2.1
3. Figure S2.2
4. Equations S2.1 to S2.3
5. Table S2.1
6. Table S2.2

1. Air Quality – Sensor Performance Evaluation Center (AQ-SPEC)

The South Coast Air Quality Management District (SCAQMD) established the Air Quality Sensor Performance Evaluation Center (AQ-SPEC) in July 2014 in an effort to provide the public with much-needed information about the actual performance of commercially available low-cost monitoring sensors. The performance of currently available low-cost sensors is characterized using both field- and laboratory-based testing. Evaluation results are communicated to the public through an information website (www.aqmd.gov/aq-spec). In the field, air quality sensors are operated at an air monitoring station (AMS) where FRM or FEM instruments measure the ambient concentration of gaseous or particle pollutants for regulatory purposes. Field testing is conducted, primarily, at one of SCAQMD's fully instrumented air monitoring sites in Rubidoux, California. Sensors are typically tested in triplicate for 8 weeks to evaluate the performance against FRM or FEM instruments, as well as sensor-specific parameters such as intra-model variability, data recovery, and sensor lifetime. Sensors that demonstrate an acceptable performance in the field are then brought back to the laboratory for laboratory chamber testing. (Paragraph adapted from Appendix A in Papapostolou et al., 2017)

While the AQ-SPEC field and laboratory testing results evaluates the performance of sensors, AQ-SPEC does not rank or endorse specific sensors. Nor does AQ-SPEC make recommendations as to which sensor devices should be used for specific applications. Sensor selection is application and project specific with the application defining performance requirements and the project defining requirements for connectivity (Wi-Fi, Bluetooth, etc.), data visualization (mobile application, screen display on sensor, web-based mapping application, etc.), power requirements (12v, 5v, or 120V), and sensor mobility (stationary vs. mobile).

2.

Figure S2.1 (a-e) Left to Right: (a) Rubidoux-Riverside (RIVR) Air Monitoring Station; (b) Met One BAM inlets; (c) Met One BAM 1020 FEM PM$_{2.5}$; (d) Sensor Shelter; (e) Sensor Shelter Mesh sides

3. Figure S2.2
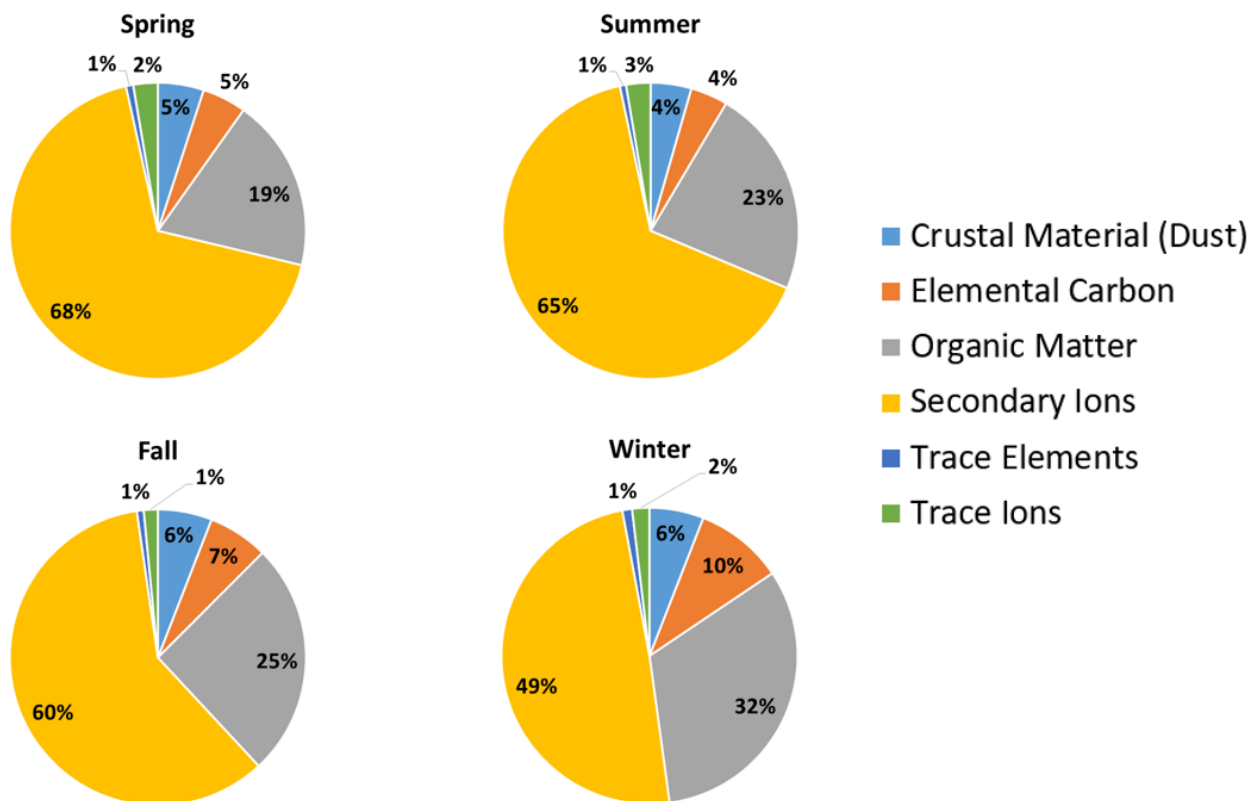
Figure S2.2 Seasonal average chemical composition of PM2.5 between 2002 and 2013 at Rubidoux monitoring station. Data adapted from Hasheminassab et al. (2014).

4. Equations S2.1 – S2.3

Eq. S2.1   Data Recovery (%) $= \dfrac{N_{\text{Valid Data}}}{N_{\text{Test Period}}} * 100$

where,
$N_{\text{Valid Data}}$ is the number of valid 1-hr data points generated during the testing period for sensor or reference
$N_{\text{Test Period}}$ is the total number of hourly of data points expected for the testing period (from start to end)

Eq. S2.2   Filtered Data Recovery (%) $= \dfrac{N_{\text{Valid Filtered Data}}}{N_{\text{test perid}}} * 100$

Where,
$N_{\text{Valid Filtered Data}}$ is the number of valid 1-hr time/date matched data points after the two data reduction filters are applied
$N_{\text{Test Period}}$ is the total number of hourly of data points expected for the testing period (from start to end)

Eq. S2.3 $Y = mX + b$

Where,
Y is the 1-hr average $PM_{2.5}$ measurement provided by a low-cost sensor
X is the 1-hr average $PM_{2.5}$ measurement provided by the Metone BAM 1020
m is the slope of the best fit line
b is the y-intercept of the best fit line

Table S2.1 Field conditions during sensor deployment and data recovery for BAM and Sensors.

Sensor Manufacturer & Model	Evaluation Dates	Temp. (°C) Mean ± SD	Humidity (%) Mean ± SD	BAM PM$_{2.5}$ (µg/m^3) Mean ± SD	Max	Data Recovery (%) BAM	Sensor*	Analysis (N) [†]
Aeroqual AQY	12/22/17 - 03/27/18	14.9 ± 5.6	48.2 ± 27.1	13.8 ± 14.4	133	88	99	84 (1917)
Airboxlab Foobot	07/14/16 - 09/15/16	25.2 ± 5.7	53.1 ± 21.6	14.4 ± 6.4	38	96	95	86 (1295)
Alphasense OPC-N2	07/10/15 - 08/10/15	24.7 ± 4.9	58.8 ± 19.5	15.6 ± 6.6	45	99	99	98 (732)
HabitatMap Air Beam 1	03/17/17 - 05/12/17	18.1 ± 5.3	53.5 ± 23.2	11.1 ± 6.6	47	98	99	98 (1317)
Hanvon N1	05/20/16 - 07/27/16	23.5 ± 6.7	54.1 ± 22.0	15.2 ± 10.3	131	98	88	77 (1264)
Kaiterra LaserEgg	08/01/16 - 09/26/16	24.2 ± 5.8	54.6 ± 21.6	14.0 ± 6.1	38	96	92	71 (951)
PurpleAir PA-II	12/08/16 - 01/26/17	12.3 ± 4.0	67.9 ± 25.3	12.1 ± 11.3	73	97	99	96 (1124)
SainSmart Pure Morning P3	03/17/17 - 05/12/17	18.1 ± 5.3	53.5 ± 23.2	11.1 ± 6.6	47	99	93	78 (1047)
Shinyei PM Evaluation Kit	02/05/15 - 04/08/15	18.0 ± 6.1	48.1 ± 26.3	15.2 ± 12.3	79	99	99	97 (1435)
TSI AirAssure	12/18/15 - 02/15/16	13.5 ± 5.7	47.6 ± 27.3	13.2 ± 11.3	69	96	93	91 (1299)
Uhoo	08/07/17 - 10/06/17	24.2 ± 6.3	55.7 ± 21.5	17.1 ± 7.3	51	99	79[§]	92 (1333)
IQAir Air Visual Pro	08/02/17 - 10/05/17	24.5 ± 6.2	55.9 ± 21.0	17.2 ± 7.3	51	99	99	98 (1535)
Mean of Means ± SD		20.1 ± 4.6	54.3 ± 5.3	14.2 ± 2.0				

* Average data recovery of the three sensors

[†] Data recovery % and (N) number of 1-hr time matched data points after the two filters applied time matched data set.

[§] Uhoo 1 (98.3%), Uhoo 2 (47%), and Uhoo 3 (91%); Uhoo 2 excluded from further analysis

Chapter 3: Development of a Network of Accurate Ozone Sensing Nodes for Parallel Monitoring in a Site Relocation Study

Contributing Authors: Brandon Feenstra, Vasileios Papapostolou, Berj Der Boghossian, David Cocker, and Andrea Polidori

Abstract

Recent technological advances in both air sensing technology and Internet of Things (IoT) connectivity have enabled the development and deployment of remote monitoring networks of air quality sensors. The compact size and low power requirements of both sensors and IoT data loggers allow for the development of remote sensing nodes with power and connectivity versatility. With these technological advancements, sensor networks can be developed and deployed for various ambient air monitoring applications. This paper describes the development and deployment of a monitoring network of accurate ozone (O_3) sensor nodes to provide parallel monitoring in an air monitoring site relocation study. The reference O_3 analyzer at the station along with a network of three O_3 sensing nodes were used to evaluate the spatial and temporal variability of O_3 across four Southern California communities in the San Bernardino Mountains which are currently represented by a single reference station in Crestline, CA. The motivation for developing and deploying the sensor network in the region was that the single reference station potentially needed to be relocated due to uncertainty that the lease agreement would be renewed. With the implication of siting a new reference station that is also a high O_3 site, the project required the development of an accurate and precise sensing node for establishing a parallel monitoring network at potential relocation sites. The deployment methodology included a pre-deployment co-location calibration to the reference analyzer at the air monitoring station with post-deployment co-location results indicating a mean absolute error (MAE) < 2 ppb for 1-hr mean O_3 concentrations. Ordinary least squares regression statistics between reference and sensor nodes during post-deployment co-location testing indicate

that the nodes are accurate and highly correlated to reference instrumentation with R2 values > 0.98, slope offsets < 0.02, and intercept offsets < 0.6 for hourly O_3 concentrations with a mean concentration value of 39.7 ± 16.5 ppb and a maximum 1-hr value of 94 ppb. Spatial variability for diurnal O_3 trends was found between locations within 5 km of each other with spatial variability between sites more pronounced during nighttime hours. The parallel monitoring was successful in providing the data to develop a relocation strategy with only one relocation site providing a 95% confidence that concentrations would be higher there than at the current site.

3.1   Introduction

3.1.1   Ozone Pollution

Ozone (O_3) is a highly reactive gas that is comprised of three oxygen atoms. In the stratosphere (10–50 km above the earth's surface), O_3 is generated naturally and provides a protective layer that shields the earth from harmful ultraviolet (UV) rays emitted by the sun. In the troposphere (0–10 km above earth's surface), O_3 is considered an air pollutant and harmful to public health and the environment. The effects of O_3 on human health include reducing lung function and irritation of the respiratory system. Increases in exposure to O_3 have been associated with increases in school absenteeism (Romieu et al., 1992; Gilliland et al., 2001; Park et al., 2002) and increases in the risk of death from respiratory causes (Jerrett et al., 2009; Turner et al., 2016; Cohen et al., 2017; Song et al., 2019). In a long-term study on children, reductions in air pollutants have been associated with statistically significant decreases in bronchitis symptoms like asthma (Gauderman et al., 2015; Berhane et al., 2016). High concentrations of O_3 have been recognized as a

phytotoxic threat to forests, crops, and vegetation (Ashmore 2005; Bytnerowicz et al., 2008).

Tropospheric O_3 or ground-level O_3 is formed by chemical reactions between oxides of nitrogen (NO_x) and volatile organic compounds (VOC) that occur in the presence of sunlight. This process is known as the photolytic cycle and is shown in Equations 3.1 to 3.3 (Godish 1997). Prime conditions for generating O_3 typically occur during the summer months when intense sunlight is coupled with mobile and stationary sources emitting carbon monoxide (CO), VOC, and NO_x. Without sunlight, photolysis of nitrogen dioxide (NO_2) in Eq. 3.1 ceases and Eq. 3.3 leads to the removal of O_3 from the atmosphere when fresh emissions of NO are present. Commuter traffic in the late afternoon and early evening typically provides a source of fresh NO emissions leading to O_3 titration. In rural communities, fewer sources of NO may cause less titration of O_3 by NO which may lead to higher nighttime O_3 concentrations than nearby urban environments (Duenas et al., 2004).

Eq 3.1 $NO_2 + hv \rightarrow NO + O \cdot$

Eq. 3.2 $O \cdot + O_2 \rightarrow O_3$

Eq. 3.3 $O_3 + NO \rightarrow NO_2 + O_2$
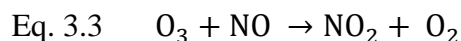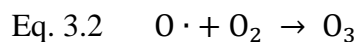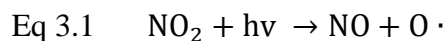
3.1.2 Regulation

In the United States, O_3 concentration levels are regulated by the United States Environmental Protection Agency (U.S. EPA) under the Clean Air Act (CAA). The U.S. EPA establishes National Ambient Air Quality Standards (NAAQS) for criteria pollutants which include CO, lead (Pb), NO_2, O_3, particulate matter (PM), and sulfur dioxide (SO_2).

The State of California further regulates these pollutants with the California Ambient Air Quality Standards (CAAQS) established by the California Air Resources Board (CARB). These standards are designed to protect public health and the environment. The latest federal and state standards for O_3 are shown in Table 3.1.

Standard for Ozone	1-hr Average	8-hr Average (Year Established)
National Ambient Air Quality Standard	120 ppb (1979)	70 ppb (2015) 75 ppb (2008) 80 ppb (1997)
California Ambient Air Quality Standard	90 ppb	-

Table 3.1 Federal and State standards for ozone (obtained September 2019).

3.1.3 Ozone Levels in the South Coast Air Basin and Monitoring in the San Bernardino Mountains

The South Coast Air Quality Management District (South Coast AQMD) is the air pollution agency for the South Coast Air Basin (SCAB) which is in Southern California and includes all of Orange County and the urban portions of Los Angeles, Riverside, and San Bernardino Counties. In order to determine regional attainment for ambient air quality standards, South Coast AQMD operates a network of air monitoring stations (AMS) equipped with EPA approved instrumentation that measures criteria air pollutants across the basin. South Coast AQMD operates 29 Federal Equivalent Method (FEM) O_3 instruments. Significant improvement has been achieved in reducing O_3 while population, vehicle miles traveled, economic activity, and goods movement in the region has been increasing. Large emissions of O_3 precursors (NO_x and VOCs) along with the topography and meteorology of the region lead to some of the worst O_3 pollution in the nation (Air Quality Management Plan (AQMP) 2016). The San Bernardino Mountain (SBM)

71

Communities (SBMCs) are especially at risk for severe O_3 episodes as polluted air travels inland with onshore wind from Los Angeles. Regional-scale temperature inversions that occur below the heights of the mountain crests lead to stagnant air conditions while clear skies and abundant sunlight provide conditions conducive for O_3 formation (Lu and Turco 1995). In 2015, one or more of the South Coast AQMD's O_3 reference analyzers exceeded the most current federal standard (2015 8-hr NAAQS: 70 ppb) on 113 days. Of the top ten monitoring sites in the nation for most frequently exceeding the 8-hr standard, seven are located within the SCAB. Monitoring sites within the San Bernardino County exceeded this standard 102 times in 2015 with the Central San Bernardino Mountains air monitoring site (Crestline AMS) exceeding the 8-hr O_3 standard 86 times; more than any other O_3 monitoring location in the basin. The maximum 8-hr average O_3 concentration recorded in the SCAB in 2015 was measured at the Crestline AMS at 127 ppb (AQMP, 2016).

The main goal of this study is to determine if a relocation site in a nearby community would experience the same or similar O_3 profile to the current monitoring site by testing the hypothesis that O_3 concentrations in nearby communities are consistent spatially and temporally. While O_3 is a secondary pollutant that is formed by reactions between primary pollutants (NO_x and VOC) in the presence of sunlight and is often considered a regional pollutant, a recent community level O_3 monitoring campaign in Riverside, CA found that O_3 concentrations vary spatially across a community (Sadighi et al., 2018). In early 2017, South Coast AQMD was faced with the potential need to relocate the Crestline AMS due to uncertainty that the lease agreement would be renewed. If the lease was terminated, circumstances may prevent the option to perform parallel monitoring or perform parallel

monitoring during the high O_3 season, typically occurring from July through September. At a minimum, parallel monitoring must be conducted during the season when maximum concentrations are expected (California Air Resources Board 1997). Since this monitoring station experiences some of the highest O_3 concentrations in the basin, parallel monitoring at the current and potential relocation monitoring sites was determined to be necessary to develop an appropriate relocation strategy. While parallel monitoring is not required via statute or regulation when relocating a monitoring site, not performing parallel monitoring may have regulatory consequences if the relocation site does not meet the same monitoring objectives of the current monitoring location. Parallel monitoring provides a mechanism to determine if the relocation site can meet the current monitoring objectives.

The current monitoring objectives of the Crestline AMS include evaluation of ambient air quality data, protection of public health, development and evaluation of control plans, and air quality research. The evaluation of ambient air quality provides data to determine the attainment of ambient air quality standards (NAAQS and CAAQS), assess progress in achieving standards, and track long term trends. The protection of public health is achieved through communicating the Air Quality Index (AQI) results to the public in a timely manner and documenting population exposure to air pollutants (AirNow). Data used for research involves long-term trend analysis and tracking impacts on the environment and the public health effects of air pollutants. Parallel monitoring can also provide insights into the continuity of measurements between an old and new monitoring site. Continuity of measurements in one location is ideal for tracking long term trends for assessing progress in achieving and maintaining national and state standards, developing and evaluating State

73

Implementation Plans (SIP) for attaining the standards, and providing long term data repositories for answering questions posed by researchers. The South Coast AQMD has been monitoring O_3 in Crestline, California since 1973 and maintaining the continuity of measurements is ideal for long-term trend analysis (Site Survey Report for Crestline 2018).

This study aims to investigate the spatial and temporal variability between Crestline and the three potential relocation sites by parallel monitoring during the high O_3 season. With the expected results impacting the relocation strategy of a monitoring site with high O_3 concentrations, the monitoring project required an accurate, precise, and reliable O_3 sensor that could be deployed in remote mountain locations with power and connectivity versatility.

3.1.4 Evaluation of Ozone Sensing Technology

In 2014, the South Coast AQMD established the Air Quality Sensor Performance Evaluation Center (AQ-SPEC) to evaluate the performance of consumer and research-grade sensors against federally approved instrumentation. AQ-SPEC evaluates gas-phase and particle-phase sensors under both ambient field and controlled laboratory conditions. Results from these performance evaluations are publicly available on the AQ-SPEC website at www.aqmd.gov/aq-spec. The methodology of low-cost sensors that measure O_3 is typically categorized as either metal-oxide or electrochemical methods. The performance of low-cost gas-phase sensors can be impacted by changing environmental factors (e.g., temperature and humidity), long-term drift, and interfering pollutants (Gerboles and Buzica 2009; Mead et al., 2013; Spinelle et al., 2016; Afshar-Mohajer et al., 2018). Electrochemical sensors for O_3 detection often experience inference from other oxidizing

gases commonly found in ambient environments (Afshar-Mohajer et al., 2018). When deployed for ambient air monitoring, the electrochemical O_3 sensors are often coupled with a NO_2 sensor in order to subtract out interference from local NO_2 concentrations. While metal-oxide O_3 sensors are selective to O_3, previous deployments of this technology have shown reduced sensitivity to O_3 concentrations over time in extended field deployment studies (Masey et al., 2018; Williams 2018).

AQ-SPEC evaluated the 2B Tech Personal O_3 Monitor (POM, 2B Technologies, Boulder, CO, USA) with the field and laboratory evaluation results indicating that the POM is capable of accurate and precise O_3 measurements. The POM is a miniature UV-absorption based monitor that uses a folded optical path ("U" shaped) to achieve a path length similar to that used in a regulatory-grade O_3 instrument that is designated as U.S. EPA FEM (Andersen et al., 2010). In August of 2015, the UV absorption methodology used in the POM was designated by the U.S. EPA as FEM for O_3: EQOA–0815–227. In the two-month AQ-SPEC field evaluation, the coefficient of determination (R^2) for a triplicate set of POMs was found to be 1.0 with a mean absolute error (MAE) less than 2 ppb (AQ-SPEC 2018a; Collier-Oxandale et al., 2019). In the AQ-SPEC laboratory evaluation, the performance of the POM was found not to be adversely affected by the NO_2 interferent or extreme environmental conditions (i.e., high/low temperature and relative humidity) (AQ-SPEC 2018b; Collier-Oxandale et al., 2019). In a previous study to monitor O_3 for the Hong Kong Marathon, the POM was selected due to its ability to measure O_3 without interferences from common oxidizing pollutants found in ambient air (Sun et al., 2016).

3.2 Materials and Methods

3.2.1 Node Design and Development

Based on project monitoring requirements, the POM was selected as the O_3 sensor to be incorporated into the sensing node. The POM weighs 0.3 kg with dimensions of $10 \times 7.6 \times 3.8$ cm and is shown in the Supplemental Information (SI) Figure S3.1. The POM is powered by 12-volt direct current (DC) and integrates well into battery, solar, or plugin (AC/DC converter) applications. Particular to this study, the POMs were equipped with a particulate filter at the sample inlet to prevent dust and aerosols from reaching the sensor optics. In contrast to many of the commercially available O_3 sensors that use a fan or passive sampling, the sampling mechanism of the POM is a small pump that controls sample flow through the unit. The pump is one of the factors affecting the commercial price of the device. Since only a small network of three sensors would be deployed, the cost was not a primary concern in sensor selection for this monitoring application. Enough monetary resources or access to loaning such sensors via a sensor library program would be required for other researchers to deploy similar types of sensor networks.

Due to the timeline requirements to build and deploy a network of O_3 monitors in the region during the high O_3 season, the decision was made to build a sensor network that would be easily deployed in contrast to deploying additional monitoring stations that would require constructing, building, and siting three additional ambient air monitoring shelters equipped with FEM O_3 analyzers, zero air generators, and gas calibrators. Constructing, building, and siting additional monitoring stations with required equipment would have

been time and cost-prohibitive to meet project timeline requirements to monitor O_3 in the region during the high O_3 season.

The POM is not an "Internet of Things" (IoT) connected device. Out of the box, POM data can be stored internally on the POMs internal memory (limited to ~6 days for 1-min averaged data) and/or data can be transmitted over a USB or serial port for logging data externally with a data acquisition solution. The POM was coupled with an IoT communications device for data acquisition, edge data processing, and data telemetry to a cloud-based platform for data storage and visualization. A remote IoT monitoring solution was selected, which included data acquisition hardware (i.e., model Thiamis 1000 (T1K), Netronix Inc., Philadelphia, PA, USA) and a cloud-based environmental monitoring software with web-based application functionality that provides access to real-time and historical monitoring data (i.e., Environet, Netronix Inc., Philadelphia, PA, USA). The T1K is equipped with both cellular and Wi-Fi data communication, a real-time clock, and 8 GB memory (see SI Figure S3.2). The real-time clock and internal memory allowed the T1K to continue recording data even if the data connection (Wi-Fi or cellular) was intermittent or unavailable for an extended period. The three POMs were configured to output data every 10 s. The 10-s data was transmitted to the T1K through the serial to 3.5 mm cable provided by 2B Technologies. The T1k recorded and performed edge data processing to average the 10-sec O_3 values to 1-min average O_3 concentrations and thus reduced the data transmission rate to 1/6 of the original data output from the sensor. These 1-min O_3 concentrations were then transmitted from the T1K via a cellular or Wi-Fi network to Environet for data storage and visualization. The 1-min data output was selected for this

monitoring network to allow the POM data to be time-matched with the output of the regulatory air monitoring station FEM ozone instrumentation for pre-deployment collocation calibration purposes.

The T1K and the POM were housed in a weatherproof polycarbonate enclosure (Fibox, Glen Burnie, MD, USA) with dimensions of $35.5 \times 30.5 \times 17.8$ cm. The box was fitted with the appropriate backing plate for mounting the components in the enclosure which allowed for easy access to remove hardware from the enclosure for potential repairs or replacement. Two vents were installed in the box for heat dissipation and to ensure that the sampling of the POM was not pumping air into a leak-tight box. The sensor node was powered via a 120/12V AC to DC power converter. The node could be optionally configured for solar power by adding a 12 V battery, 50 W solar panel, and charge controller. The total cost per node is roughly $6500 USD. The bill of materials (BOM) for the sensor node is shown in SI Table S3.1. Figure 3.1 shows the sensing node with the major components labeled. The result of this development was an accurate O_3 sensing node that could be successfully deployed in rural communities with varied access to power and connectivity to transmit real-time data and visualize data remotely.

Figure 3.1 Ozone sensor node with labeled components.

3.2.2 Nodes' Deployment

Three O_3 sensor nodes were constructed and deployed for this parallel monitoring application. Prior to deployment, the POMs were calibrated against a calibration transfer standard (CTS) at South Coast AQMD headquarters in Diamond Bar, CA. The CTS, Thermo Scientific Model 49i O_3 analyzer, was connected to a manifold along with the three POMs. The manifold was then inundated with varying O_3 concentrations by an O_3 generator. The POMs were calibrated with the in-line particulate filter upstream of the sampling inlets to ensure that the calibration configuration matched the deployment configuration. The initial calibration was a 2-point calibration with a zero and span at 250 ppb of O_3. The calibration parameters, slope (S) and offset (Z), derived from the 2-point calibration were inputted into the POM via the POM's user interface as outlined in the 2B Technology operational manual (POM Operational Manual 2015). After calibration, the POMs were verified against the CTS with ramping O_3 in the following sequence: 0, 250, 200, 150, 100, and 50 ppb (see SI Figure S3.3 a–c). The slopes ranged from 0.98 to 1.00 with R^2 values greater than 0.99. The intercepts ranged from 0.3 to 2.1 ppb. The results of

79

the verification indicate that the POMs accurately and precisely measured O_3 over a wide range of concentrations that were inclusive of ambient levels not exceeding 200 ppb during the study.

The experimental deployment design incorporated three phases: pre-deployment co-location, deployment, and post-deployment co-location. The three phases of deployment are summarized in Table 3.2. The pre- and post-deployment co-location took place at the Crestline AMS, which is equipped with a FEM O_3 reference analyzer (model 49i, Thermo Scientific, Waltham, MA, USA). The pre-deployment co-location at the AMS allowed for the implementation of an in-situ field calibration of the 3 POMs to the station reference analyzer. The post-deployment co-location at the AMS allowed for a verification of POM performance at the conclusion of the study in order to verify the in-situ field calibration and the deployment results.

Period	Dates	# of Days
Pre-deployment co-location	7/11/17 to 7/19/17	8
Deployment	7/19/17 to 9/19/17	62
Post-deployment co-location	9/19/17 to 9/29/17	10

Table 3.2 Deployment dates and number of days per deployment period.

The three additional deployment locations were selected based on their potential to serve as a possible relocation site for the current Crestline AMS. The deployment locations are shown on a map of the San Bernardino Mountains in Figure 3.2 (larger extent map in SI Figure S3.4). The three additional locations are on the south slope of the San Bernardino Mountains and located near the California State Route 18 (SR-18). SR-18 begins in San Bernardino at State Route 210 (SR-210) and travels to Big Bear City and then out to the

high desert region near Victorville and Interstate 15 (I-15). SR-330 which also originates in San Bernardino and merges with SR-18 in Running Springs.
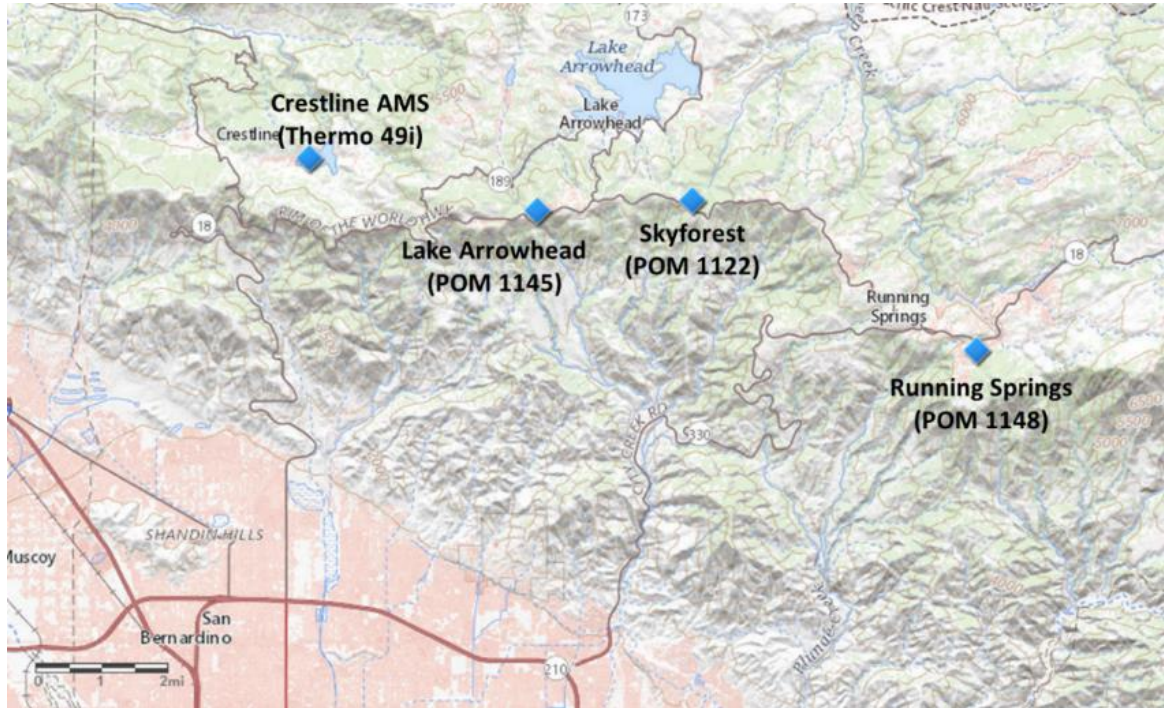
Figure 3.2 Map of deployment locations in Eastern San Bernardino Mountains.

3.2.3 Data Processing and Analysis

When examining the POMs during the co-location time periods, ordinary least squares (OLS) regression statistics along with mean bias error (MBE) and MAE were utilized to characterize the POMs performance against the Thermo 49i O_3 measurements from the Crestline AMS. Information on the measurement error calculations and equations for MBE and MAE can be found in the SI with Eq. S3.1 and S3.2.

When examining the POMs and the Crestline Thermo 49i during the deployment periods, OLS regression statistics and bias deviations between Crestline and the three alternative locations were utilized to characterize spatial and temporal differences between

sites. Equations for mean bias deviation (MBD) and mean absolute deviation (MAD) are found in SI Eq. S3.3 and S3.4. The MBD between the relocation sites and the Crestline location provides a metric that indicates the tendency of a relocation site to either under- or over-estimate O_3 concentrations when compared to the Crestline AMS location. The MBD is a relative measure that can be either positive or negative based on whether the relocation site under- or over-estimates O_3 concentrations when compared to the Crestline location. Care should be taken when examining the MBD since the positive and negative errors will cancel each other out. The MAD provides a better metric for examining the absolute deviations between the Crestline location and potential relocation sites.

The 1-min data collected during the deployment phase was calibrated according to the OLS calibration factors derived from the pre-deployment co-location period. The 1-min data was processed to remove negative and extremely high concentrations (> 250 ppb) from the data set. The 1-min data was then run through a Hampel outlier detection algorithm to remove and replace temporal outliers (see SI Section S7). The rolling Hampel filter compares each data point to a rolling median value of the last 10 consecutive data points in a data series. A threshold of six standard deviations was used to characterize a value as an outlier and replace it with the rolling median value. The cause of the outliers may have been power surges or temporary glitches with the POM or data transmission. Data were then averaged to 1-hr mean O_3 concentrations with a requisite of 42 or more 1-min data points to generate a valid 1-hr mean O_3 concentration. These 1-hr averages for the three POMs and Crestline reference monitors were then matched on date and time to enable the parallel monitoring comparisons between the reference site and three relocation

sites. Any row with a missing concentration value for either Crestline or the three relocation sites was removed from the analysis so the four locations could be compared across a complete matching data set.

In following the CARB Air Monitoring Technical Advisory Committee (AMTAC) document providing guidelines for site relocation and parallel monitoring, a data set of high values was created by finding the daily maximum 1-hr O_3 concentration for each location and then filtering to keep values that exceed a threshold value. The threshold value was set at 87.4 ppb which represents the top 20% of the prior three years of daily maximum 1-hr O_3 concentrations collected at the Crestline AMS. From this data set, MBD could be calculated to determine if a relocation site would be higher or lower than the current monitoring site with calculating the upper and lower limits of the 95% confidence interval (CI) on the MBD. Calculations for the 95% CI on the MBD have been adapted from the CARB's Guidelines for Parallel Monitoring (California Air Resources Board 1997) (SI Equation S3.5–S3.8).

3.3   Results and Discussion

3.3.1   Pre-Deployment Co-location Period at Crestline

Data collection for the pre-deployment co-location at the Crestline AMS took place from 11 July to 19 July 2017, which provided for nearly eight days of co-location data. During the pre-deployment co-location, ambient temperature ranged from 16 to 30 °C with a mean temperature of 23.4 ± 3.3 °C and ambient relative humidity (RH) ranged from 21% to 70% with a mean RH of $46.4\% \pm 11.2\%$, as measured by the AMS meteorological equipment (model HC2-S3, Rotronic, Hauppauge, NY, USA). During these eight days, the

range of 1-min O_3 concentration was 110 ppb with a maximum of 141 ppb measured on 15 July, as recorded by the Crestline AMS FEM O_3 instrument. The 1-min datasets from the POMs and FEM were filtered for values < -5 ppb and > 250 ppb. The 1-min data was then time-matched and OLS regression analysis was performed for the POMs against the Thermo 49i reference analyzer to perform an in-situ field calibration. The co-location OLS calibration offsets for the POMs were small with slope offsets < 0.07 and intercept offsets < 1.6 ppb (see SI Table S3.2). The in-situ field calibration is effective in correcting for slope and intercept offsets and reducing the MBE between the POMs and the Thermo 49i. The MAE calculated for the three POMs at the 1-min time interval is <4 ppb. Due to the inherent fluctuations of 1-min data points, the MAE was not effectively reduced by the in-situ field calibration. By averaging to 1-hr mean O_3 concentrations, the MAE between the three POMs and the Crestline O_3 monitor was reduced to less than 1 ppb. Figure 3.3 shows the time-series for the pre-deployment co-location time period with Figure 3.4 showing the correlation plots of the POMs against the Thermo 49i after the in-situ field calibration was performed. The low measurement error of the POMs against the reference instruments indicates that these units are not adversely affected by weather fluctuations (temperature or RH) or interfering pollutants.
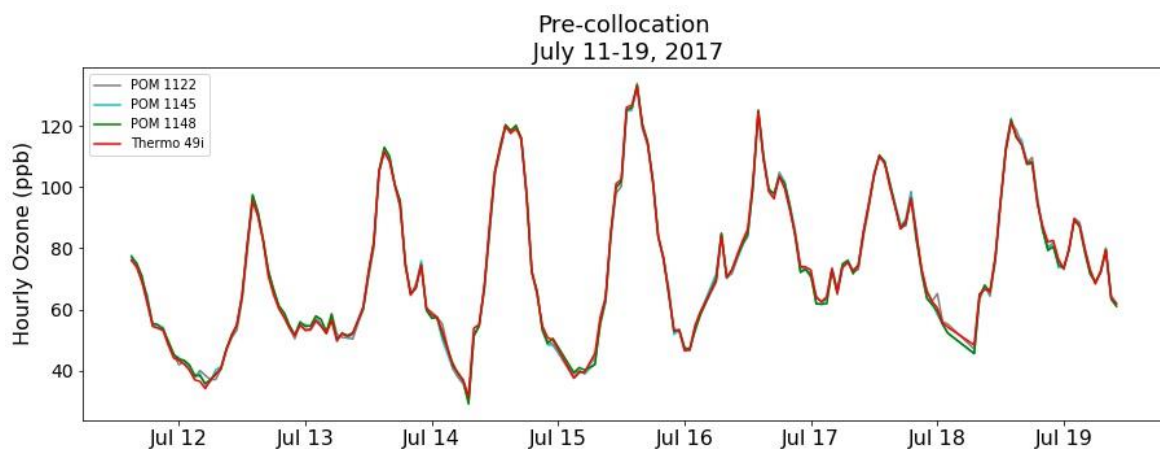
Figure 3.3 Pre-deployment co-location at Crestline time series for 1-hr mean O_3 concentrations after the in-situ field calibration was performed.
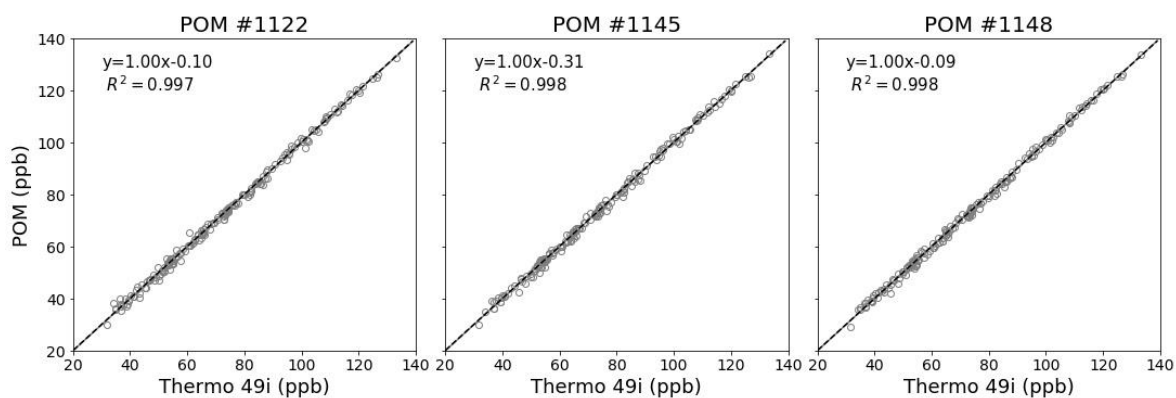
Figure 3.4 Pre-deployment co-location correlation plots for 1-h O_3 concentrations after the in-situ field calibration was performed.

3.3.2　Post-Deployment Co-location Period at Crestline

The post-deployment co-location at Crestline AMS took place for 10 days from 19–29 September 2017. The post-deployment co-location results provide a mechanism to verify that the POMs maintained their calibration and collected valid and accurate O_3 measurements throughout the deployment period. Temperature conditions during the pre-deployment co-location ranged between 4 and 25 °C with a mean temperature of 13.3 ± 5.1 °C. The RH ranged between 13% and 99% with a mean RH of 54.3% ± 28.9%. The range for 1-hr mean O_3 concentrations experienced in the post-deployment co-location was 86 ppb with a maximum 1-hr value of 91.6 ppb measured on September 29th by the Crestline AMS Thermo 49i. For hourly mean concentrations, R^2 values were greater than 0.98 with slopes ranging from 0.98 to 1.02 and intercepts ranging from −0.03 to −0.57. The calculated MAE was less than 2 ppb with MBE calculated at −0.83, −1.24, and 1.30 ppb for POM 1122, 1145, and 1148, respectively. Figure 3.5 shows the time series for the post-deployment co-location and Figure 3.6 shows the scatter plots for the POMs vs. the Thermo 49i. These post-deployment co-location results indicate that the individual POMs maintained their calibration throughout the deployment period and collected accurate measurements with MAEs less than 2 ppb. Additionally, the performance was not adversely affected by changing weather conditions, interfering pollutants, or length of deployment.
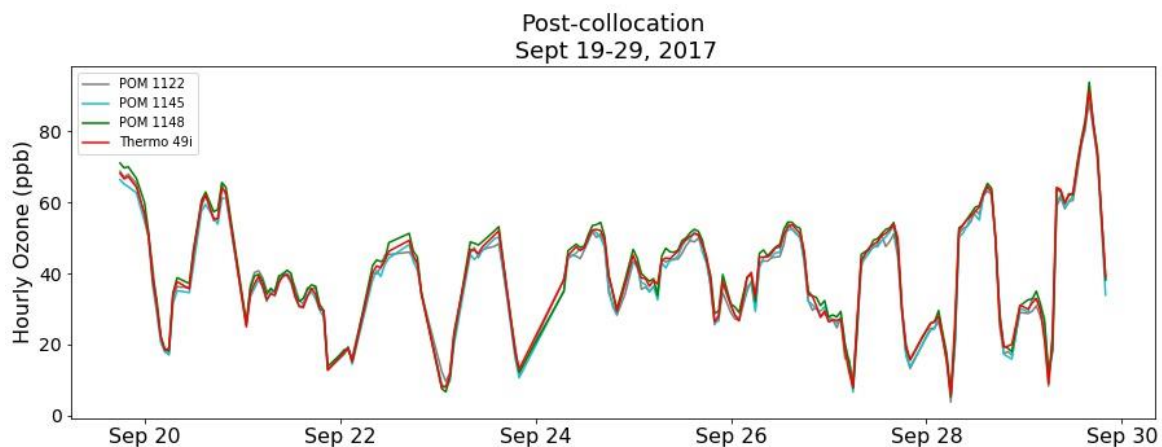
Figure 3.5 Post-deployment co-location time series for 1-hr mean O_3 concentrations.
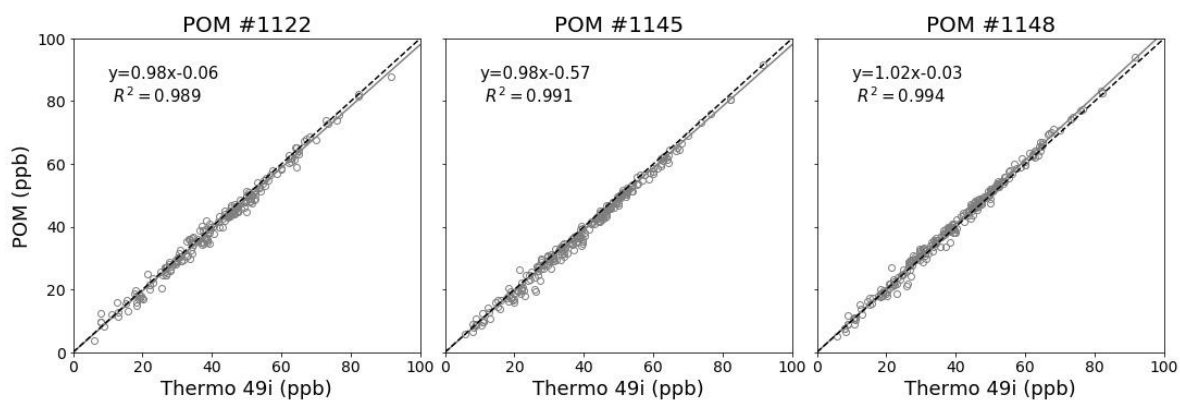
Figure 3.6 Post-deployment co-location at Crestline correlation plots for 1-hr O_3 concentrations.

3.3.3 Results from Deployment

The deployment of the sensors across the San Bernardino Mountains took place during the high O_3 season for two months (17 July to 18 September 2017). Performing parallel monitoring during the high O_3 season is critical for obtaining enough high concentration values to examine the relocation sites with the current monitoring site. Data recovery at the 1-h time average was found to be 99.9%, 96.5%, 73.4%, and 100% for the Thermo 49i, POM 1122, POM 1145, and POM 1148, respectively. POM 1145 in Lake Arrowhead, CA experienced a power outage due to an unforeseen water leak requiring the power outlet supplying the node to be turned off. As a result, data was not collected from 8:00 a.m. on 2 August 2017, to 4:00 p.m. on 18 August 2017, when the unit was outfitted with a solar panel, charge controller, and a 12-volt battery to provide power. Data rows with a missing value for any location were filtered out so a comparison between sites would have the same number of data points. After all rows with a missing value were dropped from further analysis, data recovery for the 1-hr matched data was 70.4% (1032 rows) by which the four sites are characterized and compared. Temperature conditions for Crestline AMS during the deployment ranged from 8 to 34 °C with a mean temperature of 21.6 ± 4.8 °C. The RH ranged from 9% to 99% with a mean RH at 49.0% $\pm$ 18.5%. Table 3.3 provides the summary statistics, OLS regression statistics, and the mean measurement deviations calculated for the monitoring locations during the deployment period. The difference in mean O_3 concentration between Crestline (54.2 ppb) and the three locations varied with Skyforest, CA (54.2 ppb) being identical, Running Springs, CA (56.7 ppb) being slightly higher on average, and Lake Arrowhead, CA (64.0 ppb) being about 10 ppb higher on

average than the Crestline location. These spatial variations in O_3 concentrations between locations could likely not have been predicted a priori without monitoring, highlighting the importance of developing less-expensive monitoring solutions to supplement the spatial resolution of current monitoring networks. The largest range of O_3 concentrations was seen at the Crestline AMS which had the highest maximum and lowest minimum hourly concentration values. The summary statistics between the four locations are shown in Figure 3.7 by box plots for each of the sampling locations. The horizontal dotted line and dotted diamond indicate the mean and standard deviation of the sample. Note that the following figures and tables are ordered from left to right by distance from the Crestline AMS.
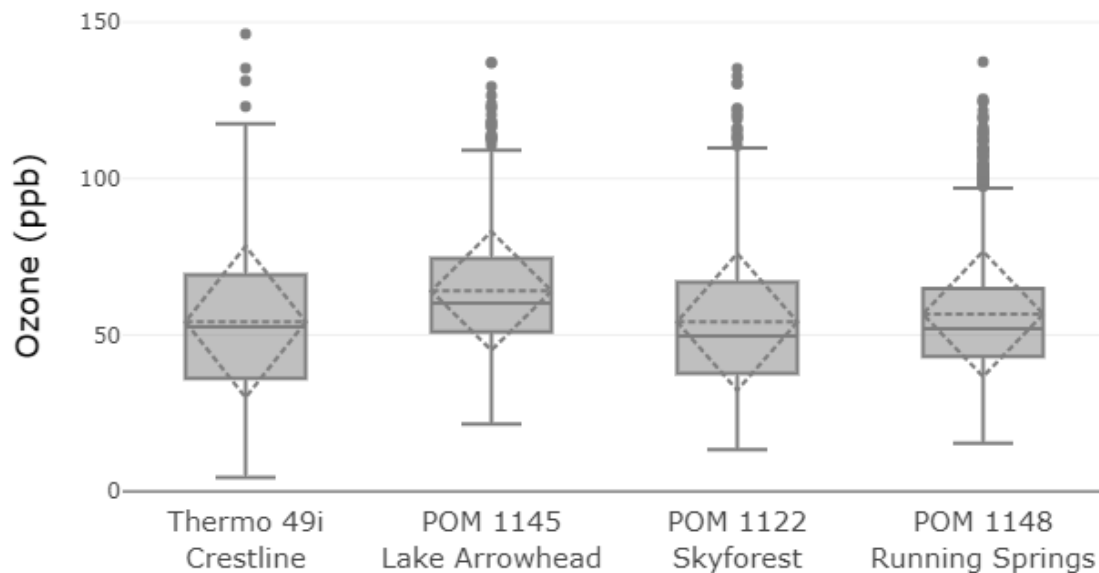
Figure 3.7 Box plots for the 1-hr mean O_3 concentrations for the four deployment locations.

Location	Crestline	Lake Arrowhead	Skyforest	Running Springs	
Instrument	Thermo 49i	POM 1145	POM 1122	POM 1148	Units
Population	10,700	12,400	300	4800	no. residents
Elevation	1390	1753	1733	1858	m
Distance from Crestline AMS	0	5.8	9.5	17.1	km
Statistics (1-hr average)					
Mean Ozone Conc.	54.2	64.0	54.2	56.7	ppb
Standard Deviation	24.2	18.9	21.8	20.0	ppb
Minimum Conc.	4.5	21.5	13.4	15.4	ppb
Maximum Conc.	146.2	137.1	135.2	137.3	ppb
Hourly data points	1032	1032	1032	1032	count
Slope	-	0.65	0.81	0.62	-
Intercept	-	28.8	10.5	22.8	-
R^2	-	0.69	0.80	0.57	-
Mean Bias Deviation (MBD)	-	9.8	0.0	2.5	ppb
Mean Absolute Deviation (MAD)	-	11.7	8.3	12.1	ppb
MAD—Daytime		7.1	6.7	8.7	ppb
MAD—Nighttime		16.7	10.0	15.9	ppb

Table 3.3 Summary information and 1-hr statistics for the four monitoring locations.

The OLS regression statistics for the 1-hr matched data sets compare each of the potential relocation sites (*y*-axis) to the current Crestline AMS (*x*-axis) and provides insights into the similarity between the four locations. Immediately, the large intercept bias between the three locations stands out with intercepts at 28.8, 10.5, and 22.8 for Lake Arrowhead, Skyforest, and Runnings Springs, respectively. This intercept offset is primarily due to the night-time differences between Crestline and the relocation sites likely caused by varying degrees of available local NO emission to scavenge O_3. Regarding

correlation, the three relocation sites correlate with Crestline with R^2 values at 0.69, 0.80, and 0.57 for Lake Arrowhead, Skyforest, and Runnings Springs, respectively. Slope offsets between Crestline and the three relocation sites were found to be 0.65, 0.81, and 0.62 for Lake Arrowhead, Skyforest, and Runnings Springs, respectively. Of the three relocation sites, the Skyforest location most closely matches the Crestline location with the highest correlation and the smallest slope/intercept offset. If finding the location that most closely matches the diurnal trends of the Crestline AMS is required for relocation, then the Skyforest location would be the chosen relocation site as this site was found to have an identical mean O_3 concentration throughout the deployment and regression statistics indicating the strongest commonality between Skyforest and the current monitoring site.

The MBD and MAD of the three locations with respect to Crestline provided insights on the spatial variability in O_3 between locations. The MBD between Crestline and the three alternative locations was found to be 9.8, 0.0, and 2.5 ppb bias for Lake Arrowhead, Skyforest, and Running Springs, respectively. The MAD from Crestline was found to be 11.7, 8.3, and 12.1 ppb for Lake Arrowhead, Skyforest, and Running Springs, respectively. Looking at the MBD, the Skyforest location appears to be the most suitable location for relocation as this location matched the mean of the Crestline location. However, when examining the MAD, all three sites deviate from Crestline AMS with MAD > 8.0 ppb; indicating spatial variability between Crestline and these relocation sites. When separating the MAD between day and night hours, the predominant deviation between Crestline and the three locations takes place during nighttime hours. The MAD values for nighttime hours are 135%, 50%, and 83% higher than daytime MAD for Lake Arrowhead, Skyforest,

and Running Springs, respectively. The cause for the increased nighttime deviation from the Crestline AMS is likely due to local factors affecting the titration of ozone between locations during nighttime conditions. Local factors including topography, populations, and traffic counts are discussed below to better understand these local factors and their impact on the spatial variation of O_3 between Crestline and the relocation sites.

Since the Crestline AMS experiences some of the highest O_3 concentrations in the SCAB, comparing the daily maximum O_3 concentrations between the current monitoring site and the potential relocation sites is important to understand the difference between the locations with regard to daily 1-hr maximum concentrations that could lead to exceedances of the 1-hr standard. When considering relocating a site that experiences high O_3 concentrations, care needs to be taken to ensure that the relocation site experiences O_3 concentrations as high as or higher than the existing monitoring site. A data set of high values of the daily maximum 1-hr O_3 concentration was created and after filtering for the threshold value and missing data, 30 daily maximum values remained with data summarized in Table 3.4. The mean of the high values in the data set for Crestline, Lake Arrowhead, Skyforest, and Running Springs was 100.8, 106.9, 101.9, and 104.6 ppb, respectively. While each of the relocation sites experienced higher O_3 concentrations than Crestline on average, only the Lake Arrowhead location provides a relocation site with a 95% confidence that the MBD would be greater than Crestline with a positive lower limit of MBD at 2.1 ppb, indicating that this location would likely be at least 2.0% higher than the Crestline AMS. Both Skyforest and Running Springs have negative values for the lower limit of the 95% CI of MBD at -2.6 and -1.5 ppb, respectively. These negative values

indicate that these relocation sites, Skyforest and Running Springs, could potentially yield

O_3 concentrations lower than the current monitoring site by 2.6% and 1.5% respectively.

If the requirement were set that the relocation site must on average experience higher

concentrations than the existing site with a 95% CI on the MBD, then the Lake Arrowhead

location would be chosen as the relocation site to meet this criterion. The regression

statistics of the high values data set ($n = 30$) are similar in nature with the 1-hr regression

statistics ($n = 1032$) shown in the preceding section. Between the three relocation sites,

Skyforest has the highest R^2 value (0.70), slope nearest to one (0.90), and lowest intercept

(11.3) which indicates this location most closely matches the diurnal trends experienced at

Crestline.

Location	Crestline	Lake Arrowhead	Skyforest	Running Springs	
Instrument	Thermo 49i	POM 1145	POM 1122	POM 1148	Units
Mean Conc.	100.8	106.9	101.9	104.6	ppb
MBD	-	6.08	1.08	3.81	ppb
SD MBD	-	8.89	8.29	11.93	ppb
Lower limit of MBD (95% CI)	-	2.10	−2.63	−1.53	ppb
Upper Limit of MBD (95% CI)	-	10.05	4.79	9.15	ppb
Lower Limit %	-	2.0	−2.6	−1.5	%
Upper Limit %	-	9.7	4.7	8.9	%
Slope	-	0.61	0.90	0.63	-
Intercept	-	45.7	11.3	41.5	-
R^2	-	0.59	0.70	0.40	-

Table 3.4 Summary Statistics and 95% confidence interval for the daily 1-hr maximum O_3 concentration.

The temporal differences between locations are shown in the time series plot shown in Figure 3.8 that is a subset from 21 August to 1 September 2017. The time series indicates that the three locations deviate from Crestline AMS predominantly during nighttime conditions when O_3 concentrations are typically decreasing. The typical wind patterns of the region with daytime onshore winds blowing in from the west/southwest and daytime upslope flow for the mountains provide a steady source of O_3 precursors for the elevated mountain communities. During the day, these upslope air masses are pushed up towards the boundary layer. In Figure 3.9, the timing of daily peak values between locations differs from the western sites (Crestline and Lake Arrowhead) peaking around 3 p.m. while the more eastern sites (Skyforest and Running Springs) peak an hour later around 4 p.m. During the evening time, wind patterns typically shift to an offshore direction with winds blowing from the northeast. These nighttime wind patterns lead to downslope air movement on the mountain which can lead to potential increases in O_3 concentrations as polluted air masses near the boundary layer fall in elevation and pass through the mountain communities. An example of this can be seen in Figure 3.9 with O_3 concentrations increasing in nighttime conditions on 25 August at 9 p.m. when hourly O_3 concentrations increase by 10 and 15 ppb from the previous hour at Lake Arrowhead and Skyforest, respectively. A similar trend with regional-scale air flows and increasing nighttime O_3 concentrations in mountain communities has been seen in the Front Range of the Colorado Mountains (Sullivan et al., 2016).

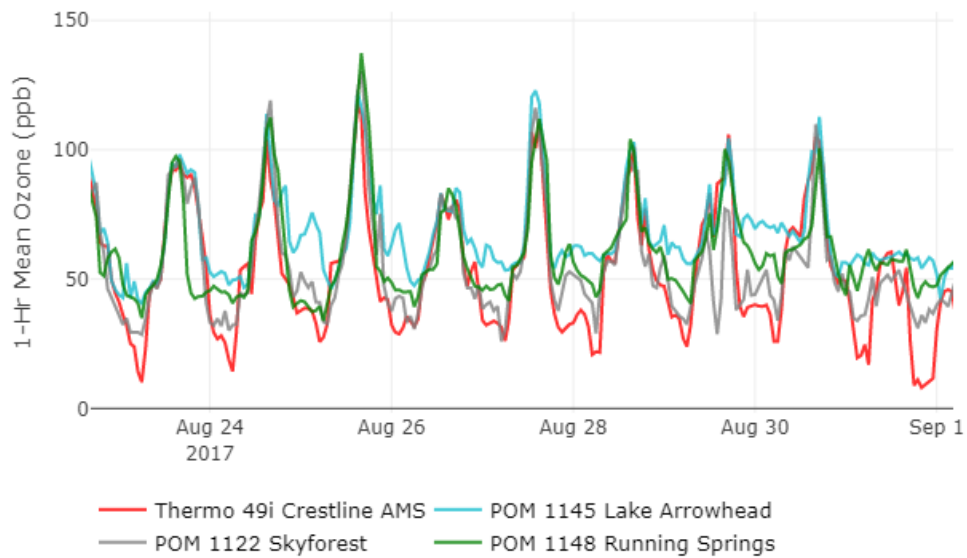Figure 3.8 Timeseries for deployment, subset between August 22 and September 1, 2017.
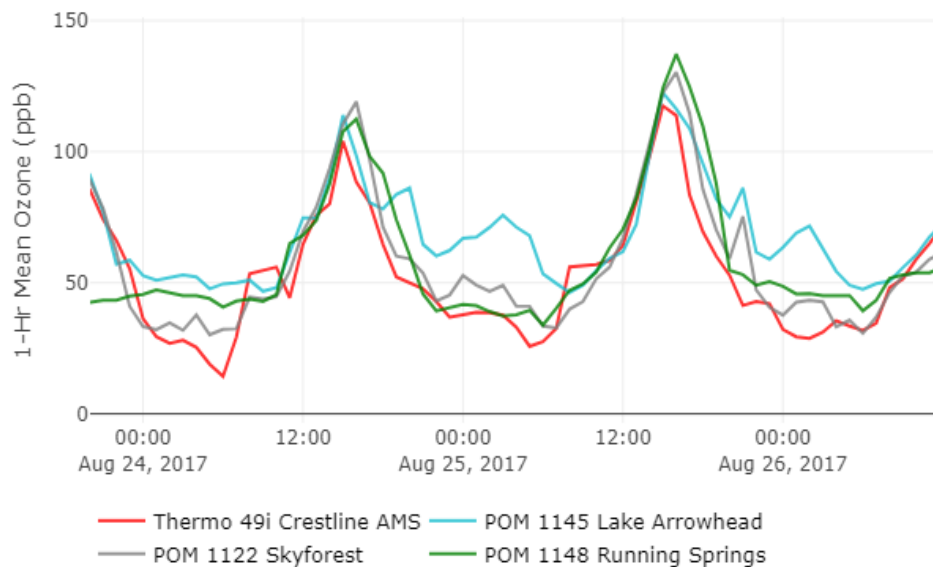

Figure 3.9 Time series for deployment subset between August 24 and 26, 2017.

Comparing the four locations regarding the number of exceedances of the 2015 U.S. EPA 8-h O_3 standard (70 ppb) provides another way for understanding the spatial variability of O_3 between these locations. For the time-matched deployment data set, the

Crestline location exceeded the 8-hr O_3 NAAQS standard 35 times while Lake Arrowhead, Skyforest, and Running Springs exceeded the standard 38, 27, and 28 times, respectively (Table 3.5).

Location—Unit	No. of Exceedances (Days)
Crestline—Thermo 49i	32
Skyforest—POM 1122	27
Lake Arrowhead—POM 1145	38
Running Springs—POM 1148	28

Table 3.5 Exceedances of the U.S. EPA 2015 8-hr ozone standard of 70 ppb.

In comparison to Crestline, the Arrowhead location experienced six additional exceedance days, while Skyforest and Running Springs had five and four fewer days exceeding the standard, respectively. These differences indicate the spatial variability of O_3 across the San Bernardino Mountains and provide an indication of how relocating the site may impact the number of 8-hr exceedances recorded for the region. The O_3 spatial variability with 10 additional days exceeding the standard at Lake Arrowhead in comparison with Skyforest is surprising as these two sites are located less than 5 km apart. This significant difference between locations in close proximity was surprising, not expected prior to monitoring, and could likely not have been predicted by simulation prior to monitoring. Many physical and chemical processes influence ambient O_3 concentrations. Models that predict O_3 concentrations simulate these physical and chemical processes. The simulation of atmospheric processes is challenging with the introduction of errors due to a lack of understanding of the physical and chemical processes, model assumptions, and data limitations (Kang et al., 2008). Chemical process simulations include but are not limited to

photolytic reactions and radical chemistry, while physical process simulations include but are not limited to emission sources and sinks, dispersion and diffusion, and meteorological conditions. An important physical process for air quality forecasting is the planetary boundary layer (PBL) which is the lowest layer of the atmosphere starting at the earth's surface and capped by a stable layer (Lee and Ngan 2011). The PBL layer height is difficult to predict when frontal boundaries (i.e., mountains) are present or multiple level thermal inversions are formed (Dabberdt et al., 2000). When the sun is setting, a second thermal inversion can form with the rapid loss of solar flux at the surface of the earth. This second layer forms the stable nocturnal boundary layer leaving a residual layer above that can potentially trap pollutants aloft. Simulations can be performed at varied spatial (regional to neighborhood) and temporal resolutions (yearly to hourly). The National Weather Service provides a national air quality forecast for the United States hour by hour at a spatial resolution of 12 km for O_3 to provide advance notice of air pollution events (National Weather Service 2019). In an active open-source development project, the U.S. EPA has developed the Community Multiscale Air Quality Modeling System (CMAQ) that consists of a suite of programs for creating air quality simulations (U.S. Environmental Protection Agency 2019). The CMAQ model has been used to simulate air quality at finer spatial scales. With the addition of high-resolution input data, ozone concentrations were simulated for the Baltimore/Washington region at a 1 km spatial resolution. The bias between the simulation and surface ozone monitoring sites was found to follow a similar diurnal pattern with a positive mean bias in the early morning hours that decreases throughout the day until sunset when the bias starts increasing (Garner et al., 2015). CMAQ

was used in more complex topography in the San Joaquin Valley in California at 2–12 km and in the Colorado Front range at 4 km spatial resolution (Flynn et al., 2016). During O_3 exceedances in Colorado, the simulation was found to capture the timing and rate of the initial rapid O_3 production well, but largely underestimated the persistence of elevated concentrations when compared to surface O_3 measurements. While the model correctly simulated regional O_3 concentrations, verification with the local air monitoring stations revealed under- and over-estimation errors (Sullivan et al., 2016). The spatial variability in O_3 concentrations found between the locations in this study and the potential bias of O_3 simulations indicates the importance of developing accurate sensing nodes and monitoring air pollutants in spatially dense networks to investigate the spatial variability of air pollutants and identify such spatial phenomena. This is especially true for regions with complex topography, meteorology, and atmospheric chemistry.

The topography and population of the distinct locations may have a factor in the differences in O_3 concentrations between the four monitoring locations. The Crestline community has a population of roughly 10,000 residents with a valley topography with homes distributed around Lake Gregory and the Crestline AMS. The Lake Arrowhead and the Skyforest monitoring locations are at the outer southern edge of the populated Lake Arrowhead region (12,400 population) and are located along the SR-18 highway. Both Lake Arrowhead and the Skyforest location are higher in elevation by an estimated 350 m when compared to the Crestline location and have views looking into the lower San Bernardino County valley communities. This topography with an overlooking view is quite different than the valley topography of the Crestline location. Running Springs has a

population of roughly 4800 residents with the monitor located at the southeastern edge of the community near an elementary school. The location of the Crestline AMS in the middle of a mountain community in contrast to the other three monitoring locations may potentially explain the differences in evening O_3 concentrations. As commuters return home in the late afternoon/early evening, vehicle tailpipe emissions of NO titrate O_3 from the Crestline community. Other stationary sources located within a mile of the Crestline AMS that may potentially play a role in O_3 production and/or titration include two gasoline fuel stations, a wastewater treatment plant, and other establishments that may increase local traffic. The Crestline valley topography may also contribute to the stagnation of air which in turn leads to higher maxima during the day and lower minima concentrations at night. Prior research between urban and rural sites show similar trends seen in this work with a nighttime minimum for O_3 more pronounced in urban locations (Duenas et al., 2004). These differences in topology, population, and siting location provide an explanation for why nighttime MAD is larger than daytime MAD between Crestline and the potential relocation sites.

The local traffic patterns in the region may also have an impact on O_3 patterns and evening titration of O_3 from the atmosphere. The California Department of Transportation (Caltrans) provides Annual Average Daily Traffic (AADT) estimates for state highways. AADT data for 2017 was retrieved from www.data.ca.gov as a geodatabase (GDB) with shapefiles for AADT which were viewed using ESRI ArcGIS Pro mapping software. Figure 3.10 shows the AADT estimates for relevant locations within the monitoring region. From the base of the mountains, AADT for California State Route 18 (SR-18) near

Waterman Canyon is estimated at 16,800 daily counts. SR-18 is a common route for daily commuters who live in the mountain communities and work in the valley communities below. Roughly 40% of the AADT heading into the mountain communities on SR-18 diverts into Crestline via SR-138 with traffic counts estimated at 6800 counts for SR-138. The remaining 60% of the daily traffic continues along SR-18 towards Arrowhead with AADT estimated at 10,000 counts along SR-18 past Crestline. While Crestline has two significant corridors into the city from SR-18 with SR-138 and Lake Gregory Dr., Lake Arrowhead has four significant corridors into the community with Daley Canyon Rd to SR-189, SR-173, Arrowhead Villa Rd., and Kuffel Canyon Rd. These additional entrance/exit routes serve to spatially spread out the daily commuter traffic and may reduce the impact of evening commuter traffic emissions scavenging O_3. The SR-330 travels from the valley in San Bernardino and merges with SR-18 in Running Springs. SR-330 is the primary route for commuters heading into Running Springs and one of several routes that lead to the Big Bear region. AADT measured at the base of the mountain at SR-330 and Highland Ave. indicates AADT at the base of the mountain is estimated at 11,500. After the merging of SR-18 and SR-330 in Running Springs, SR-18 has increased traffic counts with AADT estimated at 10,700. This increased traffic flow on SR-18 with the merging with SR-330 in the Running Springs community contrasts with the Crestline monitoring location that is embedded in the community and located away from the SR-18.
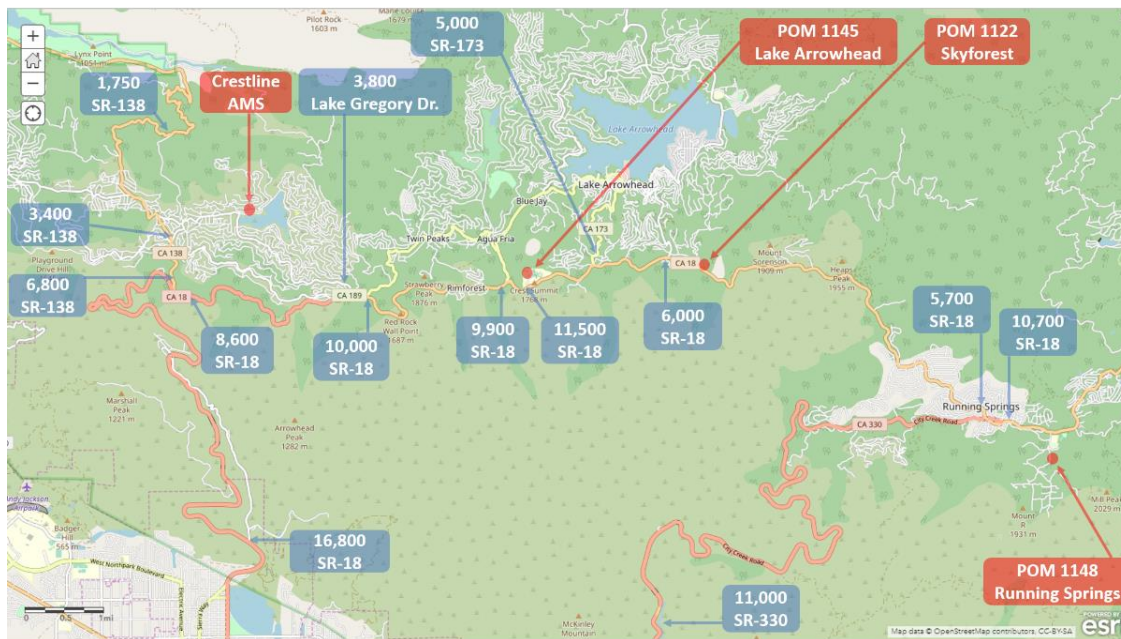
Figure 3.10 Annual Average Daily Traffic estimates by location for the monitoring region of interest. * SR: State Route.

The spatial scale of the Crestline AMS is considered to be a neighborhood scale monitoring site (Site Survey Report for Crestline 2018). A neighborhood scale monitoring station is one that is defined to extend throughout an area of a city with relatively uniform land use with a range of 0.5 to 4.0 km (40 CFR Part 58 2017). The spatial variability of O_3 between the Crestline AMS and the three sites (5.8 to 17.1 km from Crestline) supports this scale with the changing topography, population, and local land use between the mountain communities. When relocating a site, the data uses of the current site need to be examined to ensure the relocation site meets the desired data uses. The primary data uses for the Crestline O_3 data are the evaluation of ambient air quality, protection of public health, and scientific research. Since Crestline is a site were high O_3 concentrations are recorded in the SCAB, the evaluation of ambient air quality and determination of the NAAQS and CAAQS stands in the forefront. Therefore, the Lake Arrowhead location,

which was the only site with a 95% CI on the MBD to be on at least 2% higher than the current site, would be the best choice for a relocation site. The Lake Arrowhead relocation option with higher O_3 concentrations also suits the monitoring purpose of protecting public health as this location would likely indicate higher calculated AQI values and provide the associated AQI health messaging to warn residents during high O_3 pollution events. Relocating to the Lake Arrowhead site would likely yield O_3 monitoring data between 2.0% and 9.7% higher on average (95% confidence on MBD) than the Crestline AMS. This lack of continuity between measurement locations with higher concentrations at the relocation site would not be beneficial for the tracking of long-term air quality trends. Since the Lake Arrowhead relocation site would likely experience more O_3 exceedances than the Crestline location, assessing the progress in achieving the air quality standards, with regard to regulatory or incentive actions taken to meet the standard, would not be measurable until several years of monitoring data is collected for trend tracking. Data uses involving long-term trend analysis and tracking of impacts on the environment and public health effects are benefited from long-term continuous measurements in one location. With that in mind, other than maintaining the site in Crestline, relocating to the Skyforest location would be the most likely relocation option since this site nearly matches the average concentrations at Crestline and most closely tracks the Crestline diurnal trends with the best regression statistics between the three relocation sites. With protecting public health and welfare as one of the ultimate goals of monitoring air quality, monitoring stations are strategically placed in locations with high population density. The current monitoring site in Crestline is the most strategically located as this location is situated near the center of a mountain

community in contrast to the potential relocation sites located at the edges of their respective population centers.

In this study, the sensor nodes were developed to obtain O_3 concentration across a region to determine potential alternative siting locations for an ambient air monitoring station with uncertainty around the renewal of the lease agreement for the current monitoring site. While these sensing nodes were purposely built for parallel monitoring of O_3, the sensing platform could be used in other ambient applications due to the ease of installation, versatility with power and connectivity options, and accuracy of the O_3 monitors. Each of the four locations monitored in this work included areas where the physical activity took place and ranged from water sports activities, high school athletics, biking/mountain biking, ice-skating, and softball/baseball. Two of the locations are adjacent to schools where physical education classes and school sporting events are conducted. Deployment of real-time O_3 sensors in O_3 pollution impacted communities at schools could provide data to school administrators and coaches on their current hyper-local O_3 concentrations that could be used to make determinations on the appropriateness of conducting physical activities. Threshold values based on health and exposure studies could be established to set up alert notifications to inform decision-makers when O_3 concentrations reach unhealthy or unsafe conditions.

3.4 Conclusions

This paper presents the development and deployment of a small network of a highly accurate remote O_3 sensor node for performing parallel monitoring to examine three potential relocation sites for a regulatory air monitoring site. The deployment methodology

of the three O_3 sensing nodes included a pre-deployment co-location calibration to a reference O_3 analyzer with post-deployment co-location results indicating a MAE for 1-hr O_3 concentrations to be less than 2 ppb between the POMs and the O_3 reference instrument at the monitoring site. The O_3 sensing nodes provided accurate, precise, and real-time O_3 measurements that were displayed on an online dashboard for real-time viewing and reporting. The high-level of confidence in the data generated by these sensing nodes allows for investigating the spatial and temporal trends across the distinct locations that could serve as a relocation site for the current regulatory monitoring station in the San Bernardino Mountains. The results indicate that spatial variability exists between these locations with differences more pronounced in the evening hours. When examining exceedances of the 2015 8-hr standard at 70 ppb, locations within 5 km from each other differed by more than 10 exceedance days over the deployment period. The parallel monitoring was successful in providing the data to adequately defend a relocation strategy for the current O_3 monitoring site with only one site providing a 95% confidence that concentrations would be higher than the current monitoring location.

References

40 CFR Part 58 (2017). Appendix D - Network Design Criteria for Ambient Air Quality Monitoring, US EPA.

Afshar-Mohajer, N., C. Zuidema, S. Sousan, L. Hallett, M. Tatum, A. M. Rule, G. Thomas, T. M. Peters and K. Koehler (2018). "Evaluation of low-cost electro-chemical sensors for environmental monitoring of ozone, nitrogen dioxide, and carbon monoxide." Journal of Occupational and Environmental Hygiene **15**(2): 87-98.

Air Quality Management Plan (AQMP) (2016). South Coast Air Quality Management District. Diamond Bar, CA.

AirNow. (06/18/19). "Air Quality Index (AQI) Basics."   Viewed 07/20/19, from www.airnow.gov/index.cfm?action=aqibasics.aqi.

Andersen, P. C., C. J. Williford and J. W. Birks (2010). "Miniature Personal Ozone Monitor Based on UV Absorbance." Analytical Chemistry **82**(19): 7924-7928.

AQ-SPEC (2018a). Field Evaluation: 2B Technologies Personal Ozone Monitor (POM). Air Quality Sensor Performance Evaluation Center (AQ-SPEC), South Coast Air Quality Management District.

AQ-SPEC (2018b). Laboratory Evaluation: 2B Technologies Personal Ozone Monitor (POM). Air Quality Sensor Performance Evaluation Center (AQ-SPEC), South Coast Air Quality Management District.

Ashmore, M. R. (2005). "Assessing the future global impacts of ozone on vegetation." Plant Cell and Environment **28**(8): 949-964.

Berhane, K., C. C. Chang, R. McConnell, W. J. Gauderman, E. Avol, E. Rapapport, R. Urman, F. Lurmann and F. Gilliland (2016). "Association of Changes in Air Quality With Bronchitic Symptoms in Children in California, 1993-2012." Journal of the American Medical Association **315**(14): 1491-1501.

Bytnerowicz, A., M. Arbaugh, S. Schilling, W. Fraczek and D. Alexander (2008). "Ozone distribution and phytotoxic potential in mixed conifer forests of the San Bernardino Mountains, Southern California." Environmental Pollution **155**(3): 398-408.

California Air Resources Board (1997). Site Relocation and Parallel Monitoring Guidelines, Air Monitoring Technical Advisory Committee.

Cohen, A. J., M. Brauer, R. Burnett, H. R. Anderson, J. Frostad, K. Estep, K. Balakrishnan, B. Brunekreef, L. Dandona, R. Dandona, V. Feigin, G. Freedman, B.

Hubbell, A. Jobling, H. Kan, L. Knibbs, Y. Liu, R. Martin, L. Morawska, C. A. Pope, H. Shin, K. Straif, G. Shaddick, M. Thomas, R. van Dingenen, A. van Donkelaar, T. Vos, C. J. L. Murray and M. H. Forouzanfar (2017). "Estimates and 25-year trends of the global burden of disease attributable to ambient air pollution: an analysis of data from the Global Burden of Diseases Study 2015." Lancet **389**(10082): 1907-1918.

Collier-Oxandale, A., B. Feenstra, V. Papapostolou, H. Zhang, M. Kuang, B. Der Boghossian and A. Polidori (2019). "Field and laboratory performance evaluations of 28 gas-phase air quality sensors by the AQ-SPEC program." Atmospheric Environment **220**: 117092.

Dabberdt, W. F., J. Hales, S. Zubrick, A. Crook, W. Krajewski, J. C. Doran, C. Mueller, C. King, R. N. Keener, R. Bornstein, D. Rodenhuis, P. Kocin, M. A. Rossetti, F. Sharrocks and E. M. Stanley (2000). "Forecast issues in the urban zone: Report of the 10th Prospectus Development Team of the US Weather Research Program." Bulletin of the American Meteorological Society **81**(9): 2047-2064.

Duenas, C., M. C. Fernandez, S. Canete, J. Carretero and E. Liger (2004). "Analyses of ozone in urban and rural sites in Malaga (Spain)." Chemosphere **56**(6): 631-639.

Flynn, C. M., K. E. Pickering, J. H. Crawford, A. J. Weinheimer, G. Diskin, K. L. Thornhill, C. Loughner, P. Lee and S. A. Strode (2016). "Variability of O3 and NO2 profile shapes during DISCOVER-AQ: Implications for satellite observations and comparisons to model-simulated profiles." Atmospheric Environment **147**: 133-156.

Garner, G. G., A. M. Thompson, P. Lee and D. K. Martins (2015). "Evaluation of NAQFC model performance in forecasting surface ozone during the 2011 DISCOVER-AQ campaign." Journal of Atmospheric Chemistry **72**(3-4): 483-501.

Gauderman, W. J., R. Urman, E. Avol, K. Berhane, R. McConnell, E. Rappaport, R. Chang, F. Lurmann and F. Gilliland (2015). "Association of Improved Air Quality with Lung Development in Children." New England Journal of Medicine **372**(10): 905-913.

Gerboles, M. and D. Buzica (2009). Evaluation of Micro-Sensors to Monitor Ozone in Ambient Air. EUR 23676 EN, Joint Research Center for Environment and Sustainability.

Gilliland, F. D., K. Berhane, E. B. Rapaport, D. C. Thomas, E. Avol, W. J. Gauderman, S. J. London, H. G. Margolis, R. McConnell, K. T. Islam and J. M. Peters (2001). "The effects of ambient air pollution on school absenteeism due to respiratory illnesses." Epidemiology **12**(1): 43-54.

Godish, T. (1997). Air Quality Boca Raton, New York, Lewis Publishers.

Jerrett, M., R. T. Burnett, C. A. Pope, K. Ito, G. Thurston, D. Krewski, Y. L. Shi, E. Calle and M. Thun (2009). "Long-Term Ozone Exposure and Mortality." New England Journal of Medicine **360**(11): 1085-1095.

Kang, D. W., R. Mathur, S. T. Rao and S. C. Yu (2008). "Bias adjustment techniques for improving ozone air quality forecasts." Journal of Geophysical Research-Atmospheres **113**(D23): 17.

Lee, P. and F. Ngan (2011). "Coupling of Important Physical Processes in the Planetary Boundary Layer between Meteorological and Chemistry Models for Regional to Continental Scale Air Quality Forecasting: An Overview." Atmosphere **2**(3): 464-483.

Lu, R. and R. P. Turco (1995). "Air Pollutant Transport in a Coastal Environment - II. 3-Dimensional Simulations over Los Angeles Basin." Atmospheric Environment **29**(13): 1499-1518.

Masey, N., J. Gillespie, E. Ezani, C. Lin, H. Wu, N. S. Ferguson, S. Hamilton, M. R. Heal and I. J. Beverland (2018). "Temporal changes in field calibration relationships for Aeroqual S500 O-3 and NO2 sensor-based monitors." Sensors and Actuators B-Chemical **273**: 1800-1806.

Mead, M. I., O. A. M. Popoola, G. B. Stewart, P. Landshoff, M. Calleja, M. Hayes, J. J. Baldovi, M. W. McLeod, T. F. Hodgson, J. Dicks, A. Lewis, J. Cohen, R. Baron, J. R. Saffell and R. L. Jones (2013). "The use of electrochemical sensors for monitoring urban air quality in low-cost, high-density networks." Atmospheric Environment **70**: 186-203.

National Weather Service. (2019). "National Air Quality Forecast Capability Summary." Office of Science and Technology Integration Viewed 11/26/2019, from https://www.weather.gov/sti/stimodeling_airquality_summary.

Park, H., B. Lee, E. H. Ha, J. T. Lee, H. Kim and Y. C. Hong (2002). "Association of air pollution with school absenteeism due to illness." Archives of Pediatrics & Adolescent Medicine **156**(12): 1235-1239.

POM Operational Manual (2015). Personal Ozone Monitor Operational Manual, 2B Technologies**:** 41.

Romieu, I., M. C. Lugo, S. R. Velasco, S. Sanchez, F. Meneses and M. Hernandez (1992). "Air-Pollution and School Absenteeism Among Children in Mexico City." American Journal of Epidemiology **136**(12): 1524-1531.

Sadighi, K., E. Coffey, A. Polidori, B. Feenstra, Q. Lv, D. K. Henze and M. Hannigan (2018). "Intra-Urban Spatial Variability of Surface Ozone in Riverside, CA: Viability and

Validation of Low-cost Sensors." <u>Atmospheric Measurement Techniques</u> **11**(3): 1777-1792.

Site Survey Report for Crestline (2018). South Coast Air Quality Management District. Diamond Bar, Ca.

Song, W. M., Y. Liu, J. Y. Liu, N. N. Tao, Y. F. Li, Y. Liu, L. X. Wang and H. C. Li (2019). "The burden of air pollution and weather condition on daily respiratory deaths among older adults in China, Jinan from 2011 to 2017." <u>Medicine</u> **98**(10): 9.

Spinelle, L., M. Gerboles, M. Aleixandre and F. Bonavitacola (2016). "Evaluation of Metal Oxides Sensors for the Monitoring of O3 in Ambient Air at Ppb Level." <u>Chemical Engineering Transactions</u> **54**.

Sullivan, J. T., T. J. McGee, A. O. Langford, R. J. Alvarez, C. J. Senff, P. J. Reddy, A. M. Thompson, L. W. Twigg, G. K. Sumnicht, P. Lee, A. Weinheimer, C. Knote, R. W. Long and R. M. Hoff (2016). "Quantifying the contribution of thermally driven recirculation to a high-ozone event along the Colorado Front Range using lidar." <u>Journal of Geophysical Research-Atmospheres</u> **121**(17): 10377-10390.

Sun, L., K. C. Wong, P. Wei, S. Ye, H. Huang, F. H. Yang, D. Westerdahl, P. K. K. Louie, C. W. Y. Luk and Z. Ning (2016). "Development and Application of a Next Generation Air Sensor Network for the Hong Kong Marathon 2015 Air Quality Monitoring." <u>Sensors</u> **16**(2): 18.

Turner, M. C., M. Jerrett, C. A. Pope, D. Krewski, S. M. Gapstur, W. R. Diver, B. S. Beckerman, J. D. Marshall, J. Su, D. L. Crouse and R. T. Burnett (2016). "Long-Term Ozone Exposure and Mortality in a Large Prospective Study." <u>American Journal of Respiratory and Critical Care Medicine</u> **193**(10): 1134-1142.

U.S. Environmental Protection Agency. (2019). "CMAQ: The Community Multiscale Air Quality Modeling System."   Viewed 11/27/2019, 2019, from https://www.epa.gov/cmaq.

Williams, R., D. Vallano, A. Polidori, S. Garvey (2018). Spatial and Temporal Trends of Air Pollutants in the South Coast Basin Using Low Cost Sensors. U.S. Environmental Protection Agency. Washington, DC, U.S. Environmental Protection Agency,. **EPA/600/R-17/463**.

Supplemental Information - Chapter 3

1. Tech Personal Ozone Monitor (POM)

Figure S3.1 2B Tech Personal Ozone Monitor (POM)

Source: https://twobtech.com/docs/manuals/model_POM_revF-4.pdf

2. Netronix Thiamis 1000

Figure S3.2 Netronix Thiamis 1000

3. Bill of Materials for O_3 Sensing Node

Materials	Manufacturer	Part number	Est. Cost (USD)
POM	2B Technologies	MODELPOM	$5,000
Filter housing	2B Technologies	FILTERHS (25mm)	$150
Thiamis 1000	Netronix	T1K	$1,000
Enclosure + pole mount kit + back panel kit	Fibox	AR14127CHSSL	$100
Vent	Attabox	AH-V60	$10
120V to 12V converter	Aiposen	S-60-12	$15
50-watt solar panel	Renogy	RNG-50D	$75
Charge controller	Renogy	CTRL-PWM10	$20
12V 15 AHR Battery	Bioenno	BLF-1215AS	$130
Total Est. Cost:			**$6,500**

Table S3.2 Bill of Materials for O_3 Sensing Node

4. Figure S3.3 (a-c) Calibration Verification of 2B POMs

POM 1122 Calibration Verification
Ozone (ppb)

$y = 0.9796x + 2.0713$
$R^2 = 0.9999$

POM 1145 Calibration Verification
Ozone (ppb)

$y = 0.9897x + 1.4309$
$R^2 = 0.9999$
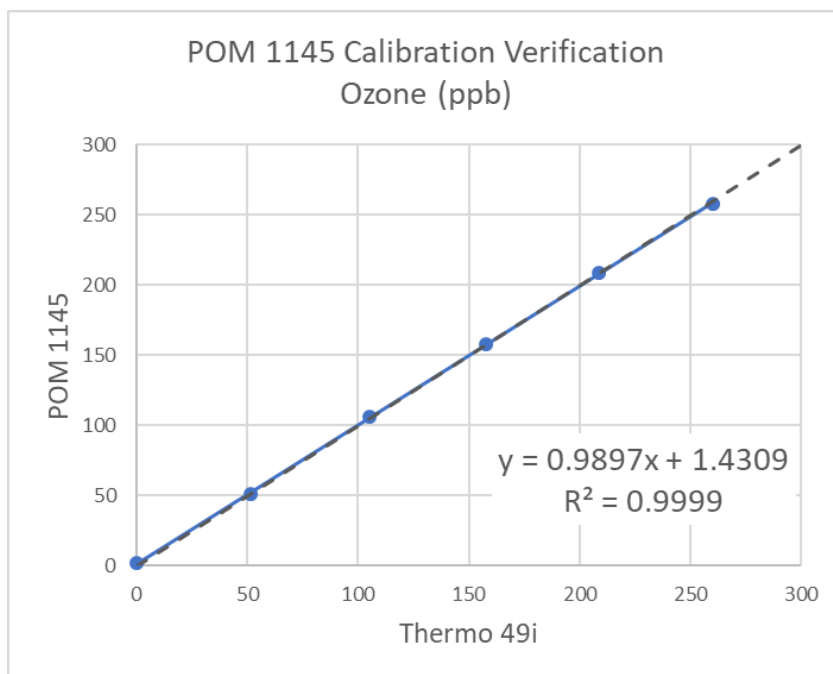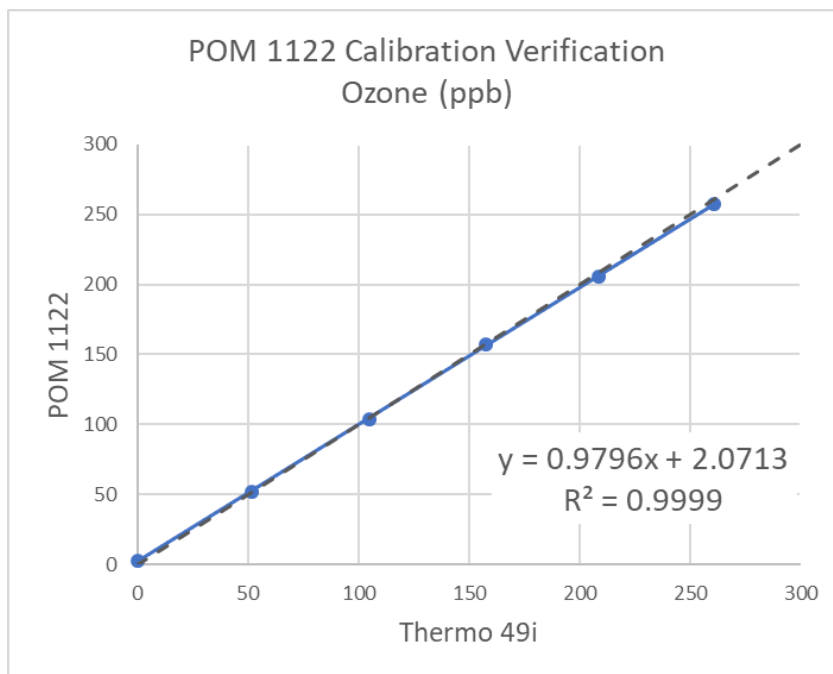
Figure S3.3 (a-c) Calibration Verification of 2B POMs

5. Figure S3.4. Extended Map of Southern California with Deployment Locations.
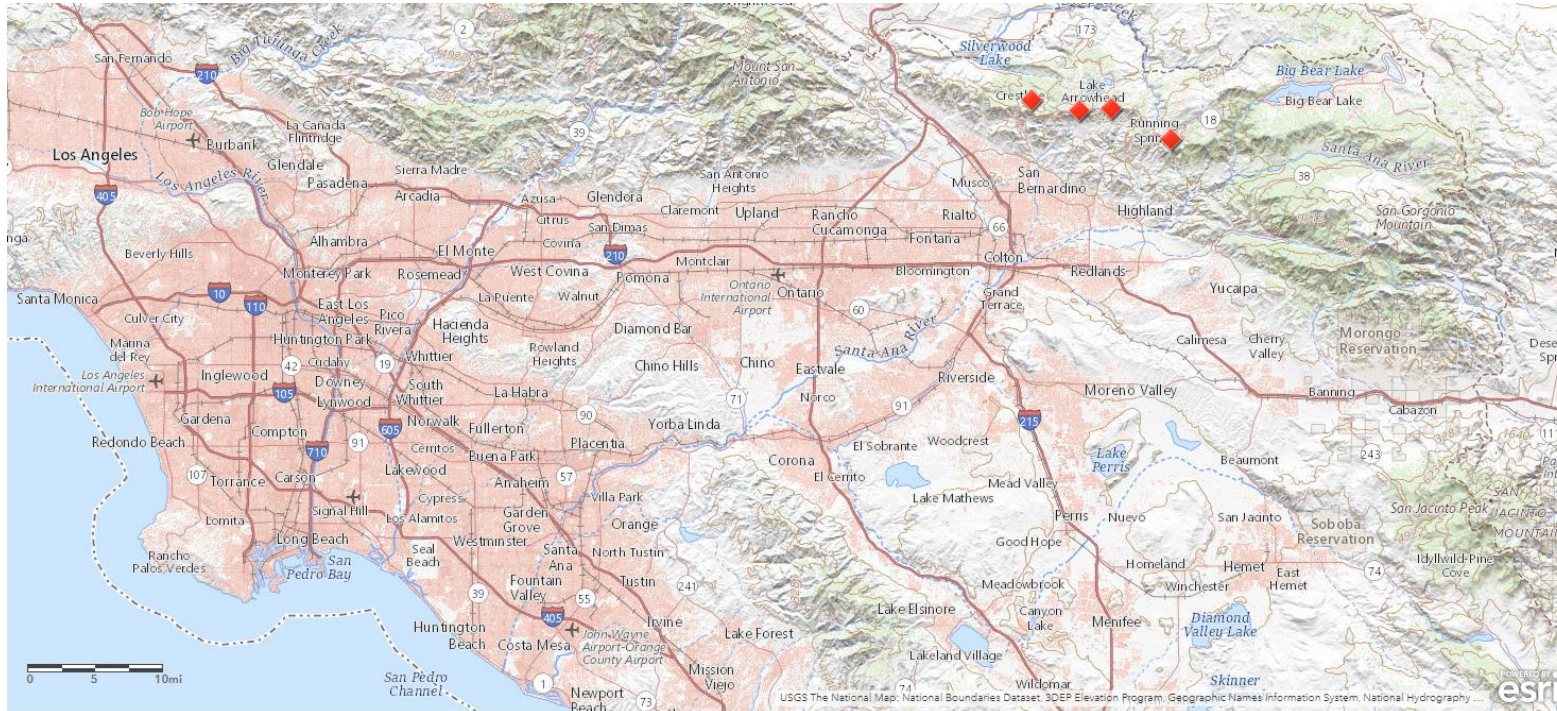
Figure S3.4 Extended Map of Southern California with Deployment Locations.

6. Calculations and Equations

Mean Bias Error (MBE) and Mean Absolute Error (MAE) calculate the measurement error by examining the hourly differences between the 2B POM and the Crestline AMS Thermo 49i O_3 measurement. The MBE between the sensor and the reference O_3 instrument provides a metric that indicates the tendency of the sensor to either under- or over-estimate the reference O_3 concentrations during the pre- and post-deployment collocation periods. The units of both MBE and MAE are calculated in ppb, which is identical to the units of measurement. Care must be taken with the MBE statistic, as over-estimated errors will c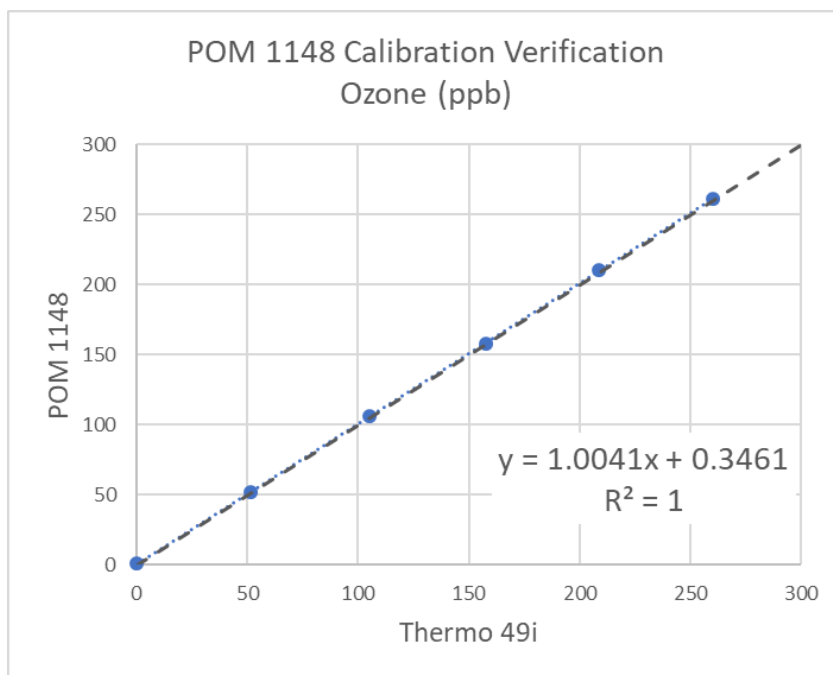ancel out under-estimated errors in the calculation of the bias error. The MAE provides a better metric for actual measurement error between sensor and reference. The equations for MBE and MAE are found in equation S1 and S2, respectively.

Equation S3.1 $\text{Mean Bias Error (MBE)} = \dfrac{1}{n} \sum_{i=1}^{n} (X_i - X_t)$

Equation S3.2 $\text{Mean Absolute Error (MAE)} = \dfrac{1}{n} \sum_{i=1}^{n} |(X_i - X_t)|,$

where,
   X_i is the 1-hr average measurement provided by the low-cost sensor
   X_t is the 1-hr average measurement provided by the Crestline Thermo 49i
   n is the number of 1-hr time-matched data pairs

Mean Bias Deviation (MBD) and Mean Absolute Deviation (MAD) calculate the deviation in O_3 concentrations between deployment locations by examining the hourly differences between the POM unit and the Crestline AMS Thermo 49i O_3 measurements. The MBD between the POM and Crestline provides a metric that indicates the tendency of a relocation site to either under- or over-estimate O_3 concentrations when compared to the

Crestline AMS. The equations for MBD and MAD are found in equation S3 and S4, respectively.

Equation S3.3 $\text{Mean Bias Deviation (MBD)} = \dfrac{1}{n} \sum_{i=1}^{n} (X_i - X_t)$

Equation S3.4 $\text{Mean Absolute Deviation (MAD)} = \dfrac{1}{n} \sum_{i=1}^{n} |(X_i - X_t)|,$

    where,
        X_i is the 1-hr average measurement provided by the POM
        X_t is the 1-hr average measurement provided by the Crestline Thermo 49i
        n is the number of 1-hr time-matched data pairs

7. Hampel Filter

The Hampel Filter function applies a filter along a rolling sample of an input vector. The median and standard deviation of the median are computed for the rolling sample window. Points that exceed a set threshold for the standard deviation of the median of the rolling sample window are characterized as outliers and replaced with the rolling median value. The sample window consists of ten data points which would constitute 10 min of data. If a sample value differed from the rolling median by more than six standard deviations, the sample value was replaced with the median value for the rolling window.

8. 95 % Confidence Interval Calculations

These calculations are adapted from the California Air Resources Board's (CARB's) Air Monitoring Technical Advisory Committee (AMTAC) document that provides guidelines for site relocation and Parallel Monitoring.

Equation S3.5 $\text{Lower Limit of 95\% CI (L)} = \bar{d} - \left(t * \dfrac{s}{\sqrt{n}} \right)$

Equation S3.6 $\text{Upper Limit of 95\% CI (U)} = \bar{d} + \left(t * \dfrac{s}{\sqrt{n}} \right),$

where,

$\bar{d}$ = Mean Bias Deviation (Eq. S3)

s = standard deviation of the MBD

n = number of matching pairs

df = degree of freedom = n-1

t = T score found in from at T-score distribution table, specific to degree of freedom and confidence interval level of certainty

Equation S3.7   Lower Limit % $= \dfrac{L}{(\bar{X} + \bar{Y})/2} * 100$

Equation S3.8   Upper Limit % $= \dfrac{U}{(\bar{X} + \bar{Y})/2} * 100$,

where,

L = Lower Limit of Confidence Interval (Eq. S5)

U = Upper Limit of Confidence Interval (Eq. S6)

$\bar{X}$ = Mean of Existing Monitoring Site

$\bar{Y}$ = Mean of Relocation Site

9. Table S3.2 Ordinary Least Squares Calibration Offsets

POM #	Slope offset	Intercept offset
1122	1.066	-1.566
1145	1.002	0.679
1148	1.039	1.207

Table S3.3 In-situ collocation calibration offsets based on ordinary least squares regression

Chapter 4: The AirSensor Open-source R-package and DataViewer Web Application for Interpreting Community Data Collected by Low-cost Sensor Networks

An edited version of this chapter is under review at Environmental Modelling & Software Journal. Contributing Authors: Brandon Feenstra, Ashley Collier-Oxandale, Vasileios Papapostolou, David Cocker, and Andrea Polidori.

Abstract

While large-scale low-cost sensor networks are now recording air pollutant concentrations at finer spatial and temporal scales than previously measured, the large environmental data sets generated by these sensor networks can become overwhelming when considering the scientific skills required to analyze the data and generate interpretable results. This paper summarizes the development of an open-source R package (*AirSensor)* and interactive web application (*DataViewer*) designed to address the environmental data science challenges of visualizing and understanding local air quality conditions with community networks of low-cost air quality sensors. *AirSensor* allows users to access historical data, add spatial metadata, and create maps and plots for viewing community monitoring data. The *DataViewer* application was developed to incorporate the functionality and plotting functions of the R package into a user-friendly web experience that would serve as the primary source for data communication for community-based organizations and citizen scientists.

4.1 Introduction

A paradigm shift in air quality monitoring is occurring with community scientists able to develop hyper-local community monitoring networks to supplement the established regulatory monitoring networks that are designed for regional monitoring (Snyder et al., 2013). These environmental monitoring networks are increasing in complexity, size, and resolution (both spatial and temporal) due to technological advances and cost reductions for environmental monitoring hardware, connected Internet of Things (IoT) devices, and cloud computing. Community scientists can take an active role in monitoring air quality at

the neighborhood level by installing low-cost air quality sensors that collect and report air pollutant data. The ability to record and visualize hyper-local data in an intuitive and informative interface will likely spawn an increase in interest and interaction with environmental data sets due to the locally relevant nature of the information. On the other hand, non-intuitive user interfaces and confusing user experiences may discourage community scientists from interacting with the collected data. The increasing complexity, size, and resolution of today's environmental monitoring networks have created big data challenges leading to the emergence of a new field of study: Environmental Data Science (Gibert et al., 2018). Data science combines computer programming skills, math and statistical knowledge, and subject matter expertise (Conway 2013). Free Open Source Software (FOSS) platforms play a vital role in the progress of research towards developing new methods for addressing environmental data science challenges. The R-environment and Python are two FOSS programing languages that are often used in environmental data science applications (Kadiyala and Kumar 2017a; Kadiyala and Kumar 2017b). Open access to air monitoring data and related tools is foundational for environmental data science to thrive and develop. Environmental monitoring data can be considered open access when the data is available through a stable and consistent Application Programming Interface (API) that allows software and application developers to build systems to display and report that data in transparent and meaningful ways.

Open access to regulatory-grade air monitoring data is available through APIs. These open-access data resources provide the opportunity for the development of web-based graphical user interfaces (GUIs) to view the regulatory-grade air monitoring data. For

access to regulatory-grade data within the United States (U.S.), the AirNow API provides access to real-time data while the Air Quality System (AQS) Data Mart API provides access to historical data (AirNow 2020; U.S. Environmental Protection Agency 2020a). The *raqdm* R package provides access to the U.S. EPA AQS data mart for further analysis in R (Bailey 2015). For access to regulatory data collected internationally, OpenAQ aggregates, standardizes, and provides open API access to air monitoring data from over 92 different countries (Hasenkopf 2016; OpenAQ 2020). The *ropenaq* R package and the *py-openaq* python package provide software tools to access data from the OpenAQ API and perform data analysis and create plots (Hagan 2017; Salmon 2019).

Environmental data scientists with programming experience can access regulatory data via these open API's to create custom web applications for displaying air monitoring data. These data view sites are useful and provide information to the public at varying granularity spatially and temporally. The OpenAQ map and the World's Air Pollution: Real-time AQI (WAQI) map display international air quality monitoring data (OpenAQ 2020; World Air Quality Index Project 2020). OpenAQ uses a color scale to display air pollution concentrations that deviate from the common AQI color scale found on many air monitoring sites and is shown in the Supplemental Information (SI) Figure S4.1. A special feature in the WAQI site is their use of calendar plots to display air monitoring information. Data view sites that display maps with modeled or interpolated air pollutant or AQI values with additional data inputs are also available (BreezoMeter 2020; IQAir 2020; Plume Labs 2020). The IQAir AirVisual Map provides a global heat map for air quality and weather information and includes both regulatory and low-cost PM sensor data. The Plume Labs

map provides street-by-street air quality maps for several large cities while the Breezometer air quality map provides a high spatial resolution air quality heat map for much of the world. When displaying both regulatory- and consumer-grade data on a map, the source and type of data displayed for individual sites needs to be readily apparent. A lack of differentiating and identifying data sources may cause confusion for the end-user, especially if the regulatory- and consumer-grade measurements do not agree. With interpolated or modeled maps, often the user is not readily aware of the input parameters used to model air quality data at these fine spatial resolutions. When viewing such maps, the viewer should be cautious especially when data sources are not readily apparent and input parameters, whether defendable or questionable, for the data model are unknown to the end-user/viewer (Hagler et al., 2018). Broadly, these platforms are map-centric with point values or interpolated modeled data displayed with options for viewing recent time series data.

The available international regulatory monitoring data is spatially limited by the distribution of the regulatory monitoring instrumentation and partnering data providers. Only 24 of 234 countries have more than 3 monitors per million inhabitants and nearly 60% of countries have no regular particulate matter (PM) monitoring (Martin et al., 2019). While regulatory air monitoring data is essential for the determination of regional attainment of the established national or international air quality standards, the spatial extent of these measurements may be limited especially for communities impacted by nearby air pollution sources (i.e. freeway) requiring spatial resolution in the tens of meters

(Ahangar et al., 2019). To fill this spatial gap, online resources for accessing and displaying data collected from networks of sensors have emerged.

Resources for accessing and displaying data collected from networks of air quality sensors are available, though they vary in terms of software (FOSS or proprietary), what they provide, and whether they are provided by the manufacturer, a project team, or through a citizen science model. While many sensor manufacturers have software and platforms in place for ingesting, storing, and analyzing data that is generated from their respective sensors, these are often proprietary and offered as a Software as a Service (SaaS) or Platform as a Service (PaaS) requiring accounts with monthly or yearly subscriptions costs. In contrast to the SaaS and PaaS business model, several sensor resources are available for open-access viewing of data collected from low-cost sensor networks. These platforms include but are not limited to the HabitatMap AirCasting map, Air Quality Egg Portal, Luft Daten project map, PurpleAir Map, Smart Citizen Kit Map, and the uRADMonitor Network map (Air Quality Egg 2020; HabitatMap 2020; Luftdaten 2020; PurpleAir 2020; Smart Citizen Kit 2020; uRADMonitor 2020). PurpleAir provides open access to the data collected by the PurpleAir network of sensors through an API and provides open viewing and downloading of sensor data through the PurpleAir map. The Luft Daten project is a citizen science project with citizen scientist sensors reporting to a map and invites programmers to collaborate in this FOSS development through GitHub (OK Lab Stuttgart 2020). When selecting a sensor in either the PurpleAir or Luftdaten GUI, the user is currently limited to viewing only the last seven days of data in a time series plot and current data on the map (accessed January 2020), which means they do not provide the end-user

with historic data to understand the spatial and temporal trends of air pollutants in their community. The Breathe London project-specific website provides a GUI with a map displaying sensor monitoring data along with the option to add the regulatory network data to the map (Breathe London 2020). Other community-oriented project websites to note are the IVAN network in the Imperial Valley, CA and the AirWatch San Francisco Bay area site which provide access to air monitoring data and allow community members to report environmental issues through the website (Air Watch 2020; IVAN Imperial 2020). While concentration maps provide a great tool for viewing real-time data and understanding current spatial variability between locations, they do not provide substantive information to guide community members on how to reduce their exposure to local air pollution. Additionally, these sensor-specific online resources for viewing air monitoring sensor data often do not include the regulatory monitoring data that may be publicly available through the AirNow or OpenAQ API. Additionally, often the online data websites for low-cost sensors do not indicate what, if any, quality control (QC) measures are taking place on the collected data before displaying.

A more in-depth analysis of historical data is required to understand local pollution trends to provide community members the information needed to make actionable decisions to reduce their exposure based on historical air monitoring data. While map-centric GUIs work well for viewing real-time data, communities that are monitoring air quality in long-term deployments need additional plotting and viewing capabilities to access and understand their local historical air monitoring data. A data dashboard for viewing and analyzing historical data would provide a better understanding of local air

pollution levels, particularly spatial and temporal air pollutant trends for a community. For those with varying levels of technical programming skill, there are software resources available that support individual data analysis of air quality data. If data can be organized and loaded into a software system, then a more in-depth analysis can occur, and custom visualizations can be produced. The U.S. EPA developed a web-based tool to explore stationary or mobile environmental data; named Real Time Geospatial Data Viewer (RETIGO) that allows users to upload data and create interactive plots and maps (U.S. Environmental Protection Agency 2020b). While RETIGO offers an interactive way for users to explore sensor data, there are several types of plots that are effective for engaging citizen scientists that are not currently available through the RETIGO tool, for example calendar plots. FOSS software packages have been developed in the R and Python environments specifically for accessing and visualizing freely available air monitoring data. These include the R packages *openair*, *PWFSLSmoke*, *ropenaq*, and *raqdm*. *OpenAir* provides a useful package for developing visualizations from collected air monitoring data. When air monitoring data is properly formatted and loaded into R, that data can be visualized by *openair* plotting capabilities to create plots like calendar plots, scatter plots, and time variation plots along with wind roses, pollution roses, and bivariate polar plots when wind speed and direction data is available (Carslaw and Ropkins 2012; Carslaw and Beevers 2013).

If we leverage advanced analysis tools and the air quality data more directly, then we can facilitate more organized, robust, systematic, and repeatable data processing, analysis, and visualization of this data. Furthermore, using FOSS tools allows for increased iteration

and development. An example of this would be the U.S. Forest Service (USFS) led Wildland Fire Air Quality Response Program (WFAQRP) AirFire tools development of the *PWFSLSmoke* R package and the associated PM$_{2.5}$ Monitoring Site web application (Air Fire Tools 2020). These tools were developed to access regulatory grade air monitoring data via the AirNow API and display that data graphically to assist the USFS Air Resource Advisors (ARAs) to gather air quality data and create air quality reports during wildfire smoke events. The *PWFSLSmoke* R package provides functions to download, parse, and plot air monitoring data (Callahan et al., 2019) and provides the back-end software necessary to generate plots for displaying on the front-end web application. The AirFire web application was developed as an extension to the PWFSLSmoke R package to assist ARAs with the ability to quickly and easily create reports without writing or running R scripts or code. The application provides a data dashboard for viewing historical data with interactive plots with the ability to create custom data reports based on user selections. A similar model in which an R-package is used for accessing and processing sensor data would save users time and would allow the development of custom functions for different approaches to QC and more complex analysis, which are gaps we see in the current offerings. Additionally, the R-package could provide the back-end software to support a front-end web application to display historical air monitoring data to provide communities with more useful analysis and visualizations. This web application would allow community members to answer their questions about their local environment, which are not readily answered with the current offerings of real-time maps and limited historical data analysis.

In 2016, South Coast Air Quality Management District (South Coast AQMD) was awarded a U.S. EPA Science to Achieve Results (STAR) grant, titled "Engage, Educate and Empower California Communities on the Use and Applications of 'Low-cost' Air Monitoring Sensors" under Assistance Agreement No. R836184. The main objective of this STAR grant was to provide communities with the necessary knowledge to appropriately select, use, and maintain low-cost sensors and to correctly interpret the data collected by air sensor networks. South Coast AQMD has engaged 14 California communities through a series of workshops to introduce the STAR grant project, provide technical guidance on sensor technology and deployment (siting, installation, configuration, and registration) of air quality sensors, review deployment progress and examine community data sets, and provide software tools and resources for community scientists to engage with collected data sets and create informative data visualizations. Roughly 400 PM sensors (i.e., PurpleAir PA-II, Draper, UT USA) were distributed to community members under the STAR grant.

The objectives of the software development associated with this project were to build an FOSS R package and data viewer web application that would address the challenges identified with the data management and visualization of low-cost air quality sensors deployed within the U.S. EPA STAR grant project. This paper summarizes the development of an R package and web application designed to address the environmental data science challenges created by deploying 400+ air quality sensors in 14 different communities. We wanted an open source R package that would allow users to download sensor data, add spatial metadata, perform data fusion with other relevant data sets, and

create maps and plots for viewing data collected by air monitoring sensors. We also wanted the package designed with functions so that minimal coding would be required to complete tasks. Understanding that many would prefer to interact with an online GUI application, we wanted to build a web application that would provide an interactive data experience allowing users to make selections and explore the community air monitoring data sets by generating pre-defined data visuals based on their user input selections. The South Coast AQMD collaborated with Mazama Science to develop the R package *AirSensor* and web application *AirSensor DataViewer* (*DataViewer*) to meet these software development aims.

4.2   Methods - Software Design and Characteristics

4.2.1   Community Engagement

The on-going engagement with the STAR grant communities has provided the motivation to develop software tools to enhance the community members' ability to interact with historical data and extract meaningful information about their local environment. After displaying a static time of day bar chart showing the diurnal $PM_{2.5}$ trends during a community workshop, one community group leader asked, "How do I generate that plot on a regular basis and share with my community members?" In one STAR grant community, a sensor host wanted to know the best time to walk her dog to reduce her exposure to particulate pollution. Additionally, multiple participants from different communities shared their difficulty downloading and analyzing the publicly accessible PA-II data especially with regards to the time/date reformatting required for plotting in Microsoft Excel. These discussions with community members on the data science challenges provided the motivation to build additional software tools to address the difficulty and

challenges posed by analyzing these large community air monitoring data sets. Increasing the number of data-sharing events with effective data visualizations should provide participants with a better understanding of the principles of air quality, their local air pollution, and the proper use and application of low-cost air quality sensors (Sandhaus et al., 2019). Table S4.1 in the SI provides a summary of the environmental data science challenges that are addressed in this project.

4.2.2   Software Tools (R environment, RStudio, R Packages, and Shiny)

The R environment is an integrated suite of software facilities that is designed on a simple yet effective computer programming language, R. The R environment provides tools and functions for data processing, storage, calculation, and graphical display. Since R is designed essentially on a computer programming language, users are able to add further functionality to existing packages by defining new functions and developing packages of functions (The R environment 2019). RStudio, a public benefit corporation, provides a FOSS version of their Integrated Development Environment (IDE) for R which supports code execution, debugging, and workspace management (RStudio 2019; Allaire 2020). Instructions for installing R and RStudio can be found on the web and in the literature (Kadiyala and Kumar 2017b). The fundamental unit of shareable code in R is a package. Packages bundle together R code, data, documentation, and tests. Packages are sharable on the Comprehensive R Archive Network (CRAN), which is the public clearing house for R packages. CRAN hosts a wide variety of FOSS packages that allow researchers to collaborate and build upon already developed R code. The development of *AirSensor* leveraged R packages available on CRAN; most notably *MazamaSpatialUtils, openair*,

128

PWFSLSmoke, and worldmet. AirSensor is designed to be used with R version ≥ 3.3. This paper describes version 0.5 of the *AirSensor* package which is available on GitHub. The latest or master branch of *AirSensor* is also available on GitHub. The *AirSensor* package can be installed using the *devtools* package within R using the following code:

```
devtools::install_github("MazamaScience/AirSensor@version-0.5")
devtools::install_github("MazamaScience/AirSensor",    ref    =
"master")
```

Shiny is a FOSS R package that provides a framework for building interactive web applications. Shiny allows the user to turn R derived analysis and plots into interactive web applications without requiring HTML, CSS, or JavaScript programming. Shiny allows for the development of an online GUI for viewing and sharing R data analytics. Since not all users would be comfortable using the R environment which does require coding, R Shiny was leveraged to develop the *DataViewer* web application to provide an interactive data experience for community members that would prefer to interact with the sensor data in a web application rather than in the R programming environment.

4.2.3   AirSensor - R Package

Rather than describing each individual function in *AirSensor*, the following examples will showcase the three primary data objects available through the package, how to apply quality control measures on the imported data, and how to generate plots for each of the data objects. A complete guide to *AirSensor* functions and operations can be found within the R-environment after the package has been loaded. Helpful R vignettes are also available within the package to provide the user with code examples for using the *AirSensor* functions and working with the sensor data.

4.2.4   Data access, extraction, and data objects overview

   AirSensor currently accesses data generated by PurpleAir sensors. *AirSensor* accesses real-time data from www.purpleair.com/json and historical data from PurpleAir through a ThingSpeak Representational State Transfer (REST) API. Extracted data is enhanced with spatial metadata and transformed into efficient data objects for downstream analytics. Within the *AirSensor* package, the three primary data objects are the Purple Air Synoptic (PAS), Purple Air Timeseries (PAT), and AirSensor (*sensor*) data object. Functions exist for creating or loading these data objects as well as manipulating and visualizing them. An overview of the *AirSensor* R package data access, data objects, and functions is provided in Figure 4.1. After installing or loading the package, a data archive repository can be set to access archived data. These data directories allow access to archived data from a specific network of sensors (i.e. STAR grant sensors) or for a specific geographic area (i.e. Southern California) so that the R user can access and load historical data more efficiently from a data archive rather than the ThingSpeak REST API. The data archives are kept current with cron jobs that are scheduled to run every hour to pull and add the most recent data to the archive. Loading data into R from an existing data archive is more efficient than creating new data objects from the ThingSpeak API. For the U.S. STAR grant sensors deployed by the South Coast AQMD, the specific data archive can be accessed at `"http://smoke.mazamascience.com/data/PurpleAir"` or `"http://"aqmd.com"/data/PurpleAir"`. The archives allows STAR grant community group members access to historical sensor data starting from 10/01/2017. Within *AirSensor*, a base archive can be set by the following code:

```
setArchiveBaseUrl("http://smoke.mazamascience.com/data/PurpleAir"
) setArchiveBaseUrl("http://"aqmd.com"/data/PurpleAir")
```
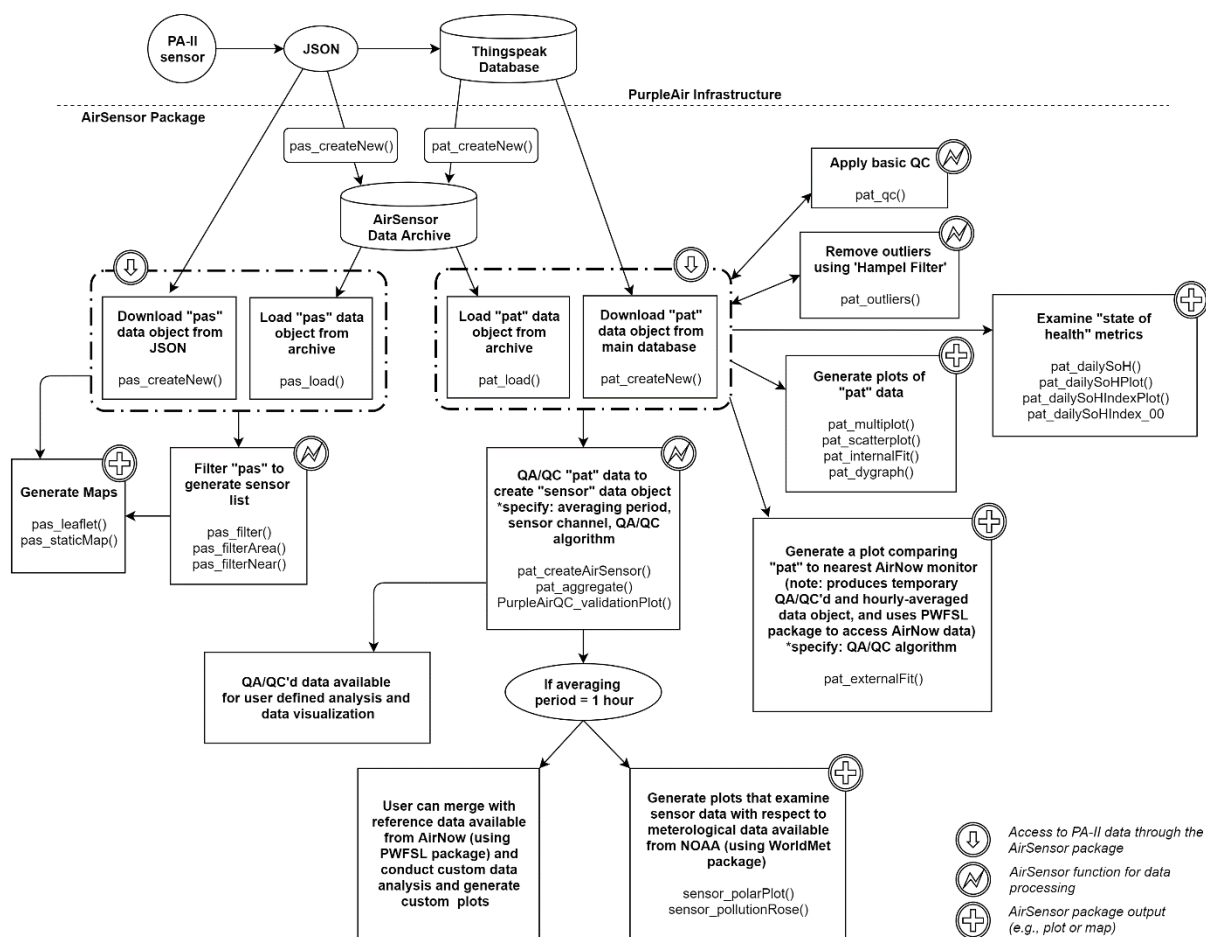

Figure 4.1 Flow Chart for data flow and functionality of the *AirSensor* R package.

4.2.5   Purple Air Synoptic - Data Object

The Purple Air Synoptic (PAS) data object provides an instantaneous view of the measured values from a network of sensors. A PAS can be created from the JSON data available at www.purpleair.com/json or loaded by accessing a data archive (Figure 4.1). At the time of this writing, the time resolution of the PA-II sensors is 120 seconds and

therefore a new PAS data object would be available roughly every 120 seconds. The available functions for manipulating PAS data object include pas_filter(), pas_filterArea(), and pas_filterNear(). The PAS data can be plotted on a map to display the instantaneous data collected by the sensor network with the pas_leaflet() and pas_staticMap() functions. Figure 4.2 shows a PAS data object displayed on an interactive map using the pas_leaflet() function which maps sensor locations and colors the locations according to Air Quality Index (AQI). The map is interactive in that the user can select an individual sensor and view the values recorded at that location for the time the PAS object was created. If a user is interested in loading specific states or air districts, the user can apply filters when generating the PAS data object. The leaflet map can be modified with options for map tiles, parameter displayed, and what type of sensors to display (i.e. inside or outside sensors). Note that the current data archives only contain PAS data for the U.S. To create a PAS for an alternative country, the user will need to use the pas_createNew function and specify which country or countries by their ISO 3166 alpha-2 country code. Figure 4.2 was produced by the following two lines of code:

```
pas_example <- pas_load()        # Load synoptic PurpleAir Data for U.S.
pas_leaflet(pas_example)         # Create an interactive map of synoptic data for U.S.
```
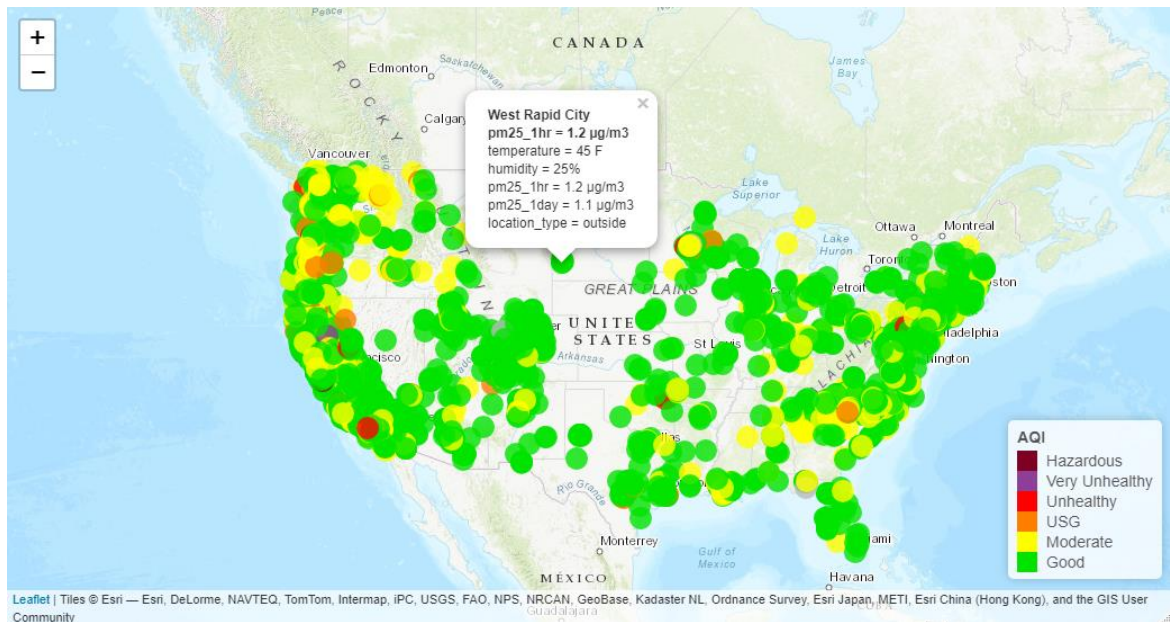
Figure 4.2 Interactive leaflet map created from a PAS data object.

4.2.6   Data Fusion Enhancements

Data fusion with other relevant data sources provides benefits for custom analytics, for applying data quality checks, and for providing information on local weather conditions. Data fusion provides the ability to tell a more complete story about local air pollution by fusing collected sensor data with other publicly available data sets. *AirSensor* has been integrated with the *PWFSLSmoke* R package for access to regulatory air monitoring data via the AirNow API and integrated to the *worldmet* R package for access to the U.S. National Oceanic and Atmospheric Administration (NOAA) Integrated Surface Database for meteorological data (Callahan et al., 2019; Carslaw 2019). These data fusion enhancements provide the ability to generate comparison plots between a low-cost sensor and the nearest regulatory-grade instrument and allow for sensor data to be joined with nearest meteorological data so that wind roses, pollution roses, and bivariate polar plots

133

can be generated to provide insights into local air pollution trends. Data fusion enhancements are performed on both the PAT and *sensor* data objects.

4.2.7   Purple Air Timeseries (PAT) - Data Object and Quality Control functions

The PAT timeseries data object provides timeseries data on a per-sensor basis. Data manipulation functions for the PAT data object include filtering, sampling, and joining. A PAT can be loaded from a data archive using the pat_load() function or can be created from the PurpleAir ThingSpeak API with the pat_createNew() function. To load a PAT data object, the user will need to specify the sensor label (name) and a start and end date. The code example below loads a PAT data object for a sensor in Seal Beach, CA that was deployed as part of the STAR grant community deployments. The PAT data object includes data from January 01 to December 31, 2018. Subsequent example code and plots displaying the *AirSensor* functions will be performed on this PAT data object or a filtered PAT data object created from the SCSB_20 sensor located in Seal Beach, CA. The PAT data object can be loaded into the R environment and filtered by date with the following code:

```
pat_example <- pat_load(
  label = "SCSB_20",
  startdate = 20180101,
  enddate = 20181231,
  timezone = "America/Los_Angeles",
)
# Create a PAT filtered for June/July 2018
pat_JuneJuly <- pat_filterDate(
  pat_example,
  startdate = "20180627",
  enddate = "20180708"
)
```

Time series data can be processed for time averaging, QC algorithms, and outlier detection and removal or replacement. The user can create their own framework for

applying QC functions depending on their project requirements. The pat_aggregate() function returns a data frame with aggregate statistics for a PAT data object. The returned dataframe includes the mean, median, standard deviation, minimum, maxima, and count for the aggregate time period chosen. Note that the PA-II sensor has two identical sensors (model PMS 5003, Plantower, China) that report the same types and amounts of data and for reference purposes are labeled as channel A and channel B, respectively. For the paired channel A and B PM$_{2.5}$ data columns, the function also returns the t-test statistic (based on an unpaired, two-sample student's t-test), p-value, and degrees of freedom. Several built-in QC algorithms exist and are labeled as pat_qc, hourly_AB_01, and hourly_AB_02. The pat_qc function allows the user to perform a first-level QC check for values that are considered "out-of-spec" with regards to the manufacturer defined specifications for the acceptable ranges for PM$_{2.5}$, temperature, and humidity. The PurpleAirQC_hourly_AB_00() function allows the user to perform an hourly average of the A and B sensor channels when sufficient sub-hourly data exists for both channels within each hour. The default min-count for sub-hourly data is set to 20 data points; requiring a data recovery for A and B channels > 66% for the current time-resolution at 120-seconds. No further QC is applied with this function. Note that the PA-II's time resolution has changed with firmware updates over time. As firmware updates have not been performed across the board simultaneously for all sensors in the PurpleAir network, the following dates are estimates for firmware releases and data resolution. Time resolution for data prior to February 2017 is 20 seconds, from February 2017 to March 2017 is 40 seconds, from March 2017 to May 2017 is 70 seconds, from May 2017 to May 2019 is 80 seconds, and

data recorded after May 2019 is 120 seconds. The function PurpleAirQC_hourly_AB_01 allows the user to perform an hourly average of the A and B sensor when sufficient sub-hourly data exists and when data is considered statistically similar. Data is invalidated when (1) minimum count < 20 values, (2) when both the means of channels A and B are not statistically the same (two-sample t-test p-value < $1e^{-4}$) and the mean difference between channels A and B is greater than 10 $\mu g/m^3$, and (3) when the mean difference between A and B is greater than 20 $\mu g/m^3$ for $PM_{2.5}$ values less than 100 $\mu g/m^3$. These conditions assume that the air entering the channel A and B sensors is the same and therefore the means of the two channel measurements should be statistically similar. When measurements from these sensor channels agree, the user can have higher confidence in the low-cost air quality measurements and the subsequent data averaging of the two sensors into one value. The two-sample t-test is a statistical technique to determine whether the difference between two means is significant. The default settings of these QC checks can be modified to adjust the QC check to individual project requirements. Additionally, new QC functions can be created or adapted from these available functions and *AirSensor* users are encouraged to create their own custom QC functions and submit these functions to be added to the *AirSensor* package through GitHub. These QC procedures can be visualized with the PurpleAirQC_validationPlot() function which creates a series of timeseries plots for channel A and B, the difference between channel A and B, t-test p-value, min count, and the hourly averaged final output (Figure 4.3).
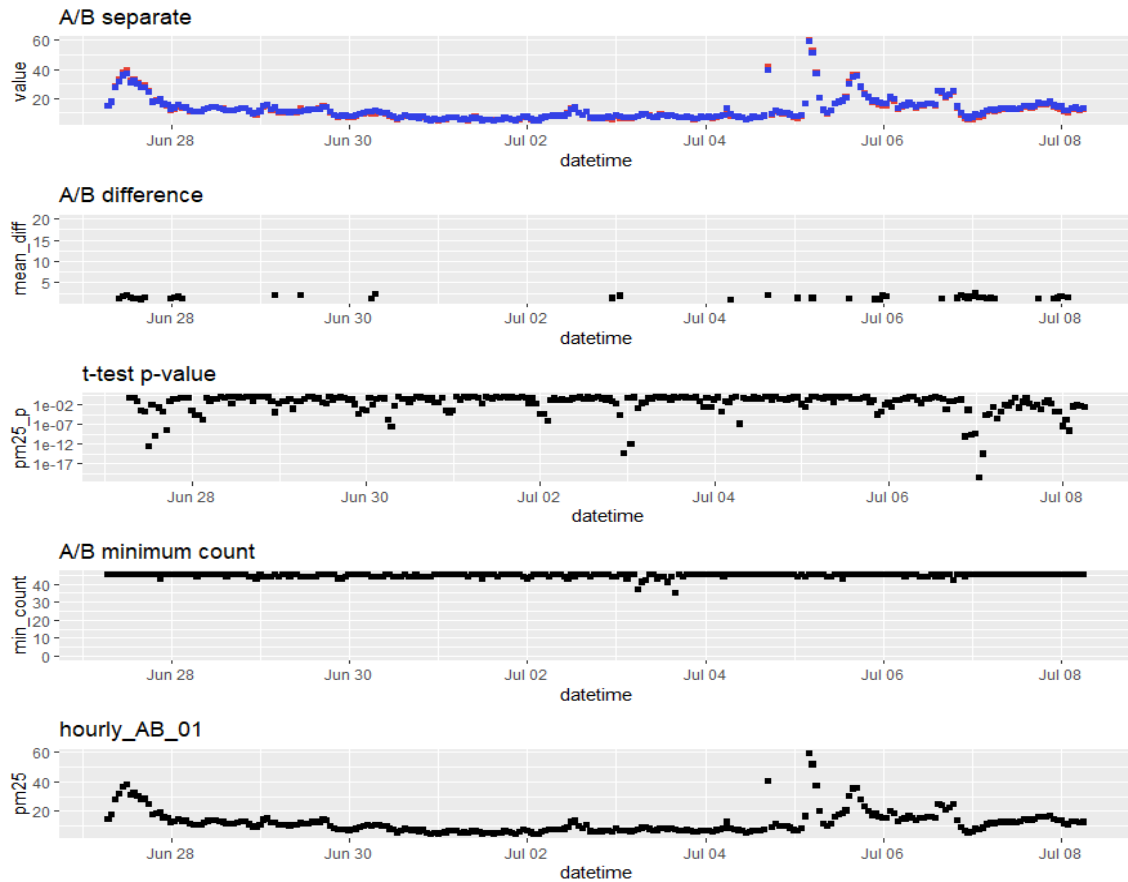
Figure 4.3 Plot generated to visualize the QC_01 algorithm for SCSB_20 located in Seal Beach, CA.

The *AirSensor* pat_outlier() function provides an outlier detection function that allows the user to apply a rolling Hampel filter to identify points that may be outliers, and if desired, replace those identified outliers with a rolling median value. The Hampel Filter is an outlier detection technique that uses the Median Absolute Deviation (MAD). For each data point, a median and standard deviation are calculated using neighborhood values within a sample window size. If the MAD of a single data point is a specified number of standard deviations (threshold minimum) from the median value for the sample window, then the data point is flagged as an outlier. Default values for the pat_outlier() function

137

include sample window = 23 and a threshold minimum = 8. These default values can be altered by the end-user to meet the specific QC requirements of their monitoring project and data analysis. Adjusting the parameters on the function for identifying outliers would adjust the number of points detected as outliers. Figure 4.4 provides an example of the pat_outlier function with potential outliers identified as red asterisks.
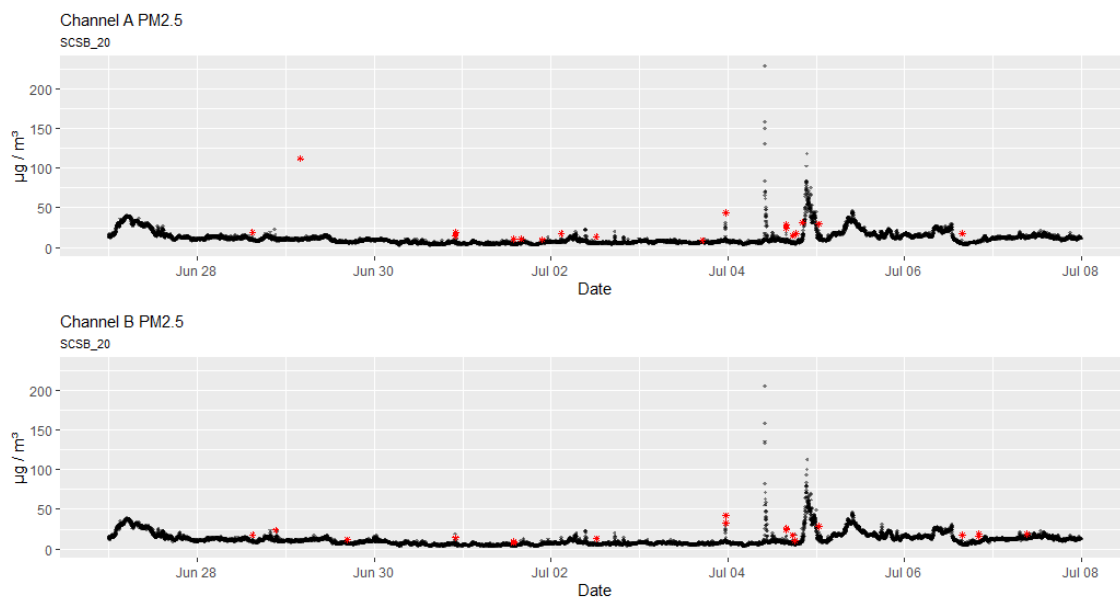
Figure 4.4 Plot generated with the rolling Hampel filter identifying potential outliers in red asterisks for SCSB_20 from June 27 to July 8, 2018.

In this example, a date filter was applied to the pat_example previously generated to only include the June 27 to July 8, 2018 time period that would be impacted by a special event: 4th of July fireworks. The default window size was left at 23 allowing for an estimated 30-min rolling time window with the 80-second time-resolved data. The outlier detection function appears to identify many of the one-off high values as outliers but does not considered the elevated $PM_{2.5}$ concentrations due to the fireworks to be outliers. This

function allows *AirSensor* data users to quickly implement sophisticated outlier detection and visualize the results of their outlier detection functions. Figure 4.4 was produced by the following R-code:

```
pat_outliers(pat = pat_JuneJuly)      # generate the outlier plot
```

Most of the plotting functions within *AirSensor* are performed on the PAT timeseries data objects. Data visualization functions for the PAT include plotting raw data time series, interactive time series, multiplot time series (A, B, Temp, RH), scatter plot for a channel A vs. B comparison, and scatter plot with regards to the nearest reference monitor. The channel A and B PM$_{2.5}$ concentrations generated by the PA-II can be compared using the pat_interalFit() function as shown in Figure 4.5.
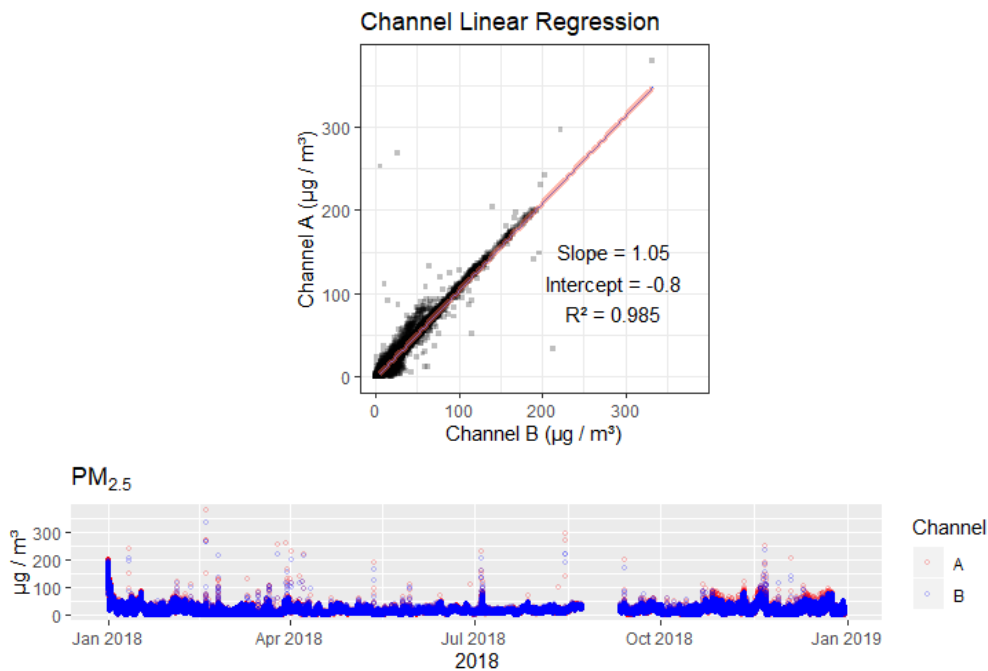

Figure 4.5 Scatter plot and timeseries rendered using the pat_internalFit function to compare channel A and B within a single PA-II sensor, SCSB_20, for 2018.

139

In this example for SCSB_20 for 2018, the A and B sensors agree with each other with an $R^2 > 0.98$, slope of 1.05 and an intercept of -0.8. Since the two sensors perform similarly for 2018-time frame, the blue points representing the B sensor are plotted over top of the red points representing the A sensor. The code to generate the Figure 4.5 plot is:

```
pat_internalFit(pat_example) #Create A/B Channel comparison plots
```

A sensor can also be compared to the nearest reference station with the pat_externalFit() function (Figure 4.6). In this example, the sensor is 3.1 km away from the regulatory monitoring station equipped with a Met One Beta Attenuation Monitor (BAM), which is a U.S. EPA designated Class III FEM (EQPM-0308-170) for $PM_{2.5}$. As the time resolution of the reference data is hourly, the QC procedures previously described are applied to hourly aggregate the sensor data in the *pat* data object in this function. Additionally, the pat_externalFit() function allows the user to specify which QC algorithm to apply. This external fit plot shown in Figure 4.6 indicates that while the sensor follows the typical daily $PM_{2.5}$ trends of the nearby regulatory-grade monitor for $PM_{2.5}$ with $R^2 >$ 0.73, the sensor tends to estimate higher concentrations in comparison to the nearby regulatory-grade instrument. This slope/intercept offset could be due to a local emission source impacting this particular sensor location or could be due to sensor measurement bias error that has been identified in prior publications (Feenstra et al., 2019; Magi et al., 2019). For the time-series in Figure 4.6, the purple colored points represent the 1-hr PurpleAir sensor data and the black colored points represent the 1-hr regulatory-grade instrument data. If the two agree closely within an hour, the black point would be plotted on top of the purple point for that hour. The plot in Figure 4.6 is created with the following:

```
pat_externalFit(pat_example)
```
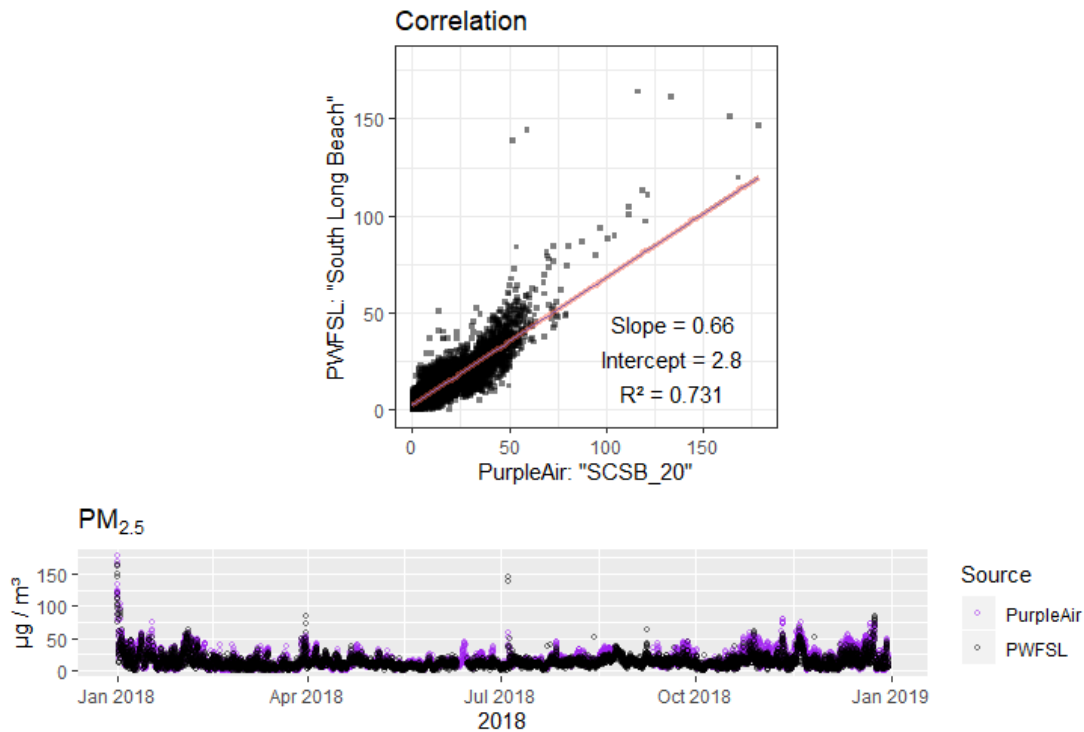

Figure 4.6 Scatter plot and timeseries plot rendered using the pat_externalFit() function which compares the PA-II sensor, SCSB_20, in Seal Beach, CA to a nearby regulatory-grade PM$_{2.5}$ instrument in Long Beach, CA.

The pat_scatterplot function provides a multi-panel scatterplot for variables in the PAT data object with an example of the plot shown in Figure 4.7. This plot allows the researcher to determine if there is a lack of correlation between the A and B sensor channels or if there are higher than expected correlations between PM$_{2.5}$ concentrations and weather conditions (temperature and humidity). This plot also provides the timeseries and distribution of data points for PM, temperature and humidity. In Figure 4.7, the distribution plots for the A and B sensor channels indicate PM$_{2.5}$ concentrations for this sensor are

141

typically less than 25 µg/m³. The datetime column provides an indication of periods of

downtime with a noticeable downtime seen in August and September of 2018.
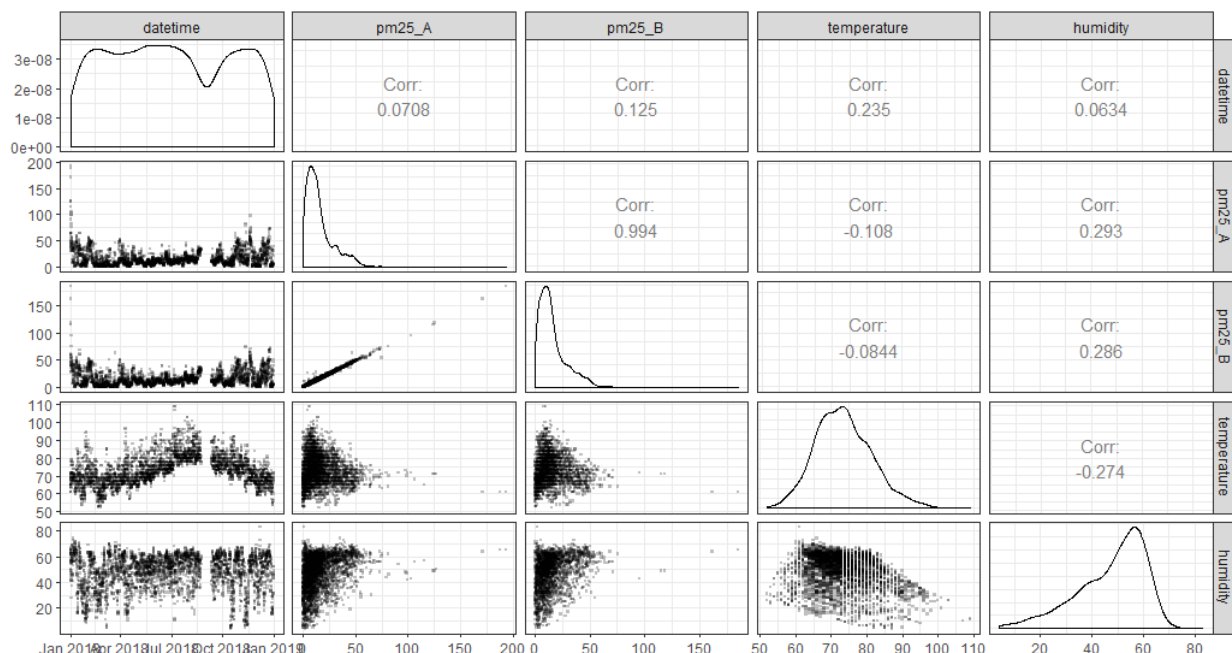
Figure 4.7 Figure generated using the pat_scatterplot function to graphically view the distribution variables in the PAT timeseries data object

The pat_dygraph function provides a useful exploratory plot that provides an

interactive time-series plot for both channel A and B allowing the user to zoom in/out and

investigate date/times when PM$_{2.5}$ concentrations may be higher than normal (Figure 4.8).

Using the interactive time-slider located below the plot allows the user to quickly zoom in

to dates and times with high particle pollution events to further investigate these events,

which may be due to special circumstances (i.e. Jan 1st or July 4th fireworks or wildfire

smoke event). With a small amount of code, the dygraph provides a versatile, interactive

plot, where the user can explore a large amount of data at customizable levels with the time

slider and zoom in/out features. Figure 4.8 is created with the following:

```
pat_dygraph(pat_example)
```
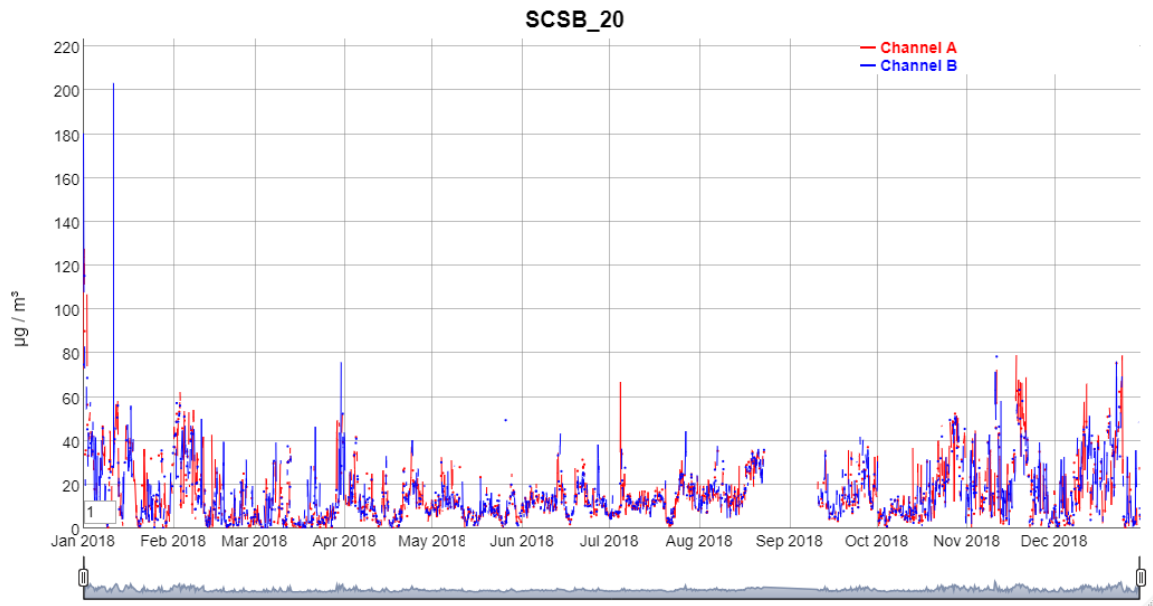

Figure 4.8 Dygraph plot with interactive time-slider generated by the pat_dygraph function

4.2.8 Hourly QC data object (*sensor*)

The *sensor* data object is generated from a PAT data object with the pat_createAirSensor() function which creates a data object on a per sensor basis. The user will need to specify a PAT data object, time averaging period, parameter, channel, QC algorithm, and min count. The QC algorithms applied in creating the *sensor* data object are described earlier in Section 4.2.7 with regards to the QC functions that can be applied to a PAT timeseries data object. The functions with *AirSensor* that can be performed on a *sensor* data object begin with "sensor_". An example creating a *sensor* data object is shown in the code below:

```
AirSensor_example <- pat_createAirSensor(
    pat=pat_JuneJuly,
    period = "1 hour",
    parameter = "pm25",
    channel = "ab",
    qc_algorithm = "hourly_AB_01",
    min_count = 20
)
```

Plots available for the *sensor* data object within the *AirSensor* package include a bivariate polar plot and pollution rose, which wrap functions from the openair R package. Meteorological data is retrieved from the NOAA *worldmet* R package. The nearest meteorological monitoring station is coupled with the *sensor* data object to build the bivariate polar plot and pollution rose, which are shown in Figure 4.9 and Figure 4.10. These two plots provide the user with the ability to couple wind direction and wind speed with $PM_{2.5}$ pollutant data to determine whether pollution events can be attributed to specific meteorological conditions and potentially identify pollution sources. A more in-depth analysis of these plots and their application in analyzing air monitoring datasets is accessible within the published literature on the 'open-air' R package development (Carslaw and Ropkins 2012) and use of bivariate polar plots (Carslaw and Beevers 2013; Grange et al., 2016). The code to create the pollution rose and polar plot is as follows:

```
sensor_pollutionRose(AirSensor_example) # Code for Pollution Rose
sensor_polarPlot(AirSensor_example)      # Code for Polar plot
```
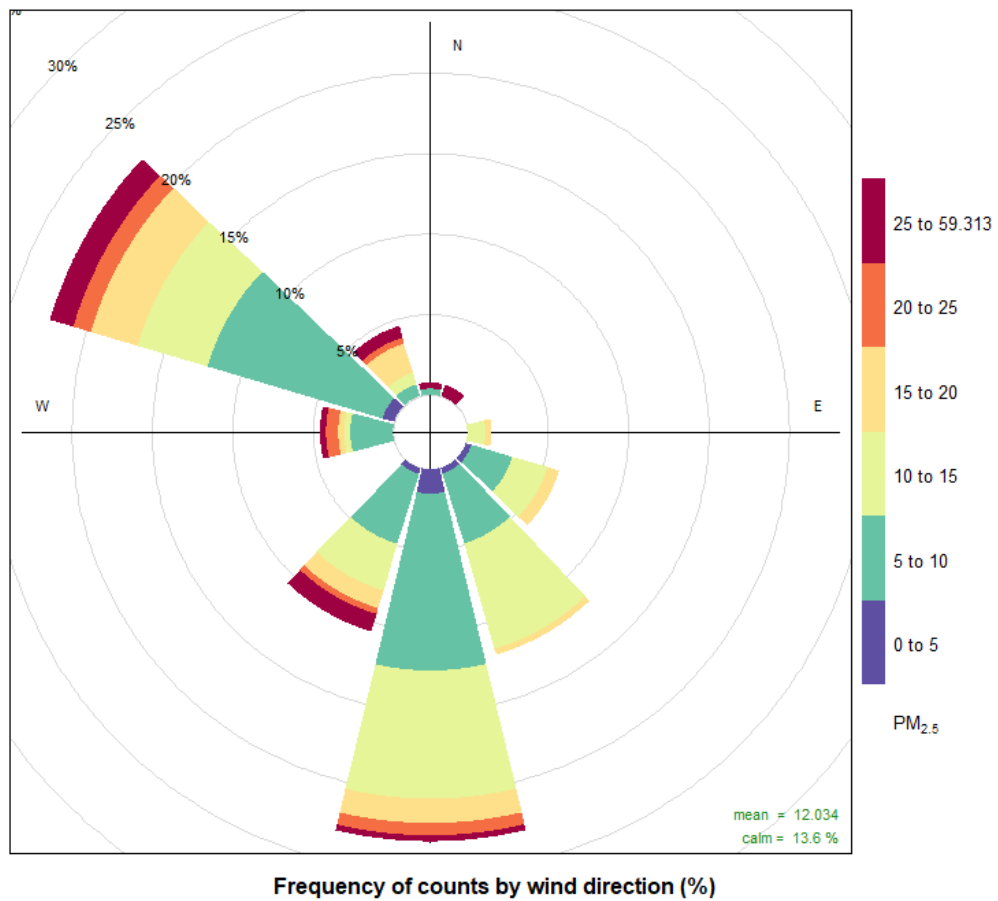
Figure 4.9 PM$_{2.5}$ Pollution Rose generated by the sensorpollutionRose() function for SCSB_20 located in Seal Beach, CA for June 27 to July 8, 2018.
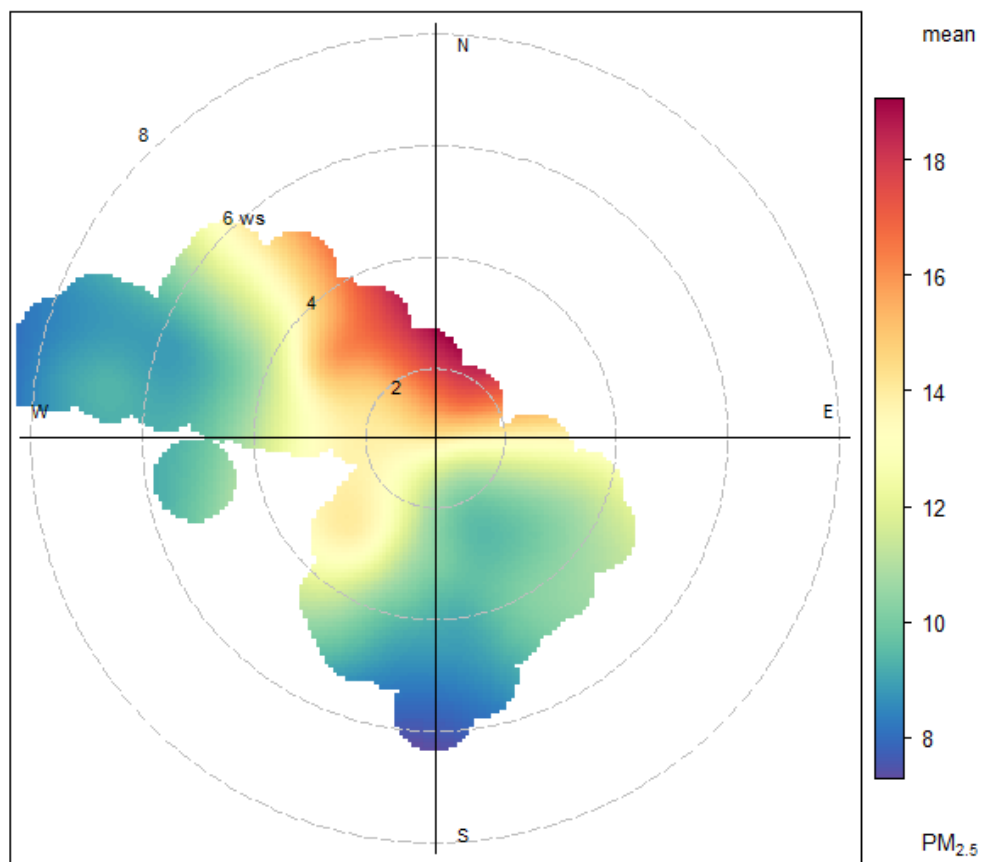
Figure 4.10 PM$_{2.5}$ Bivariate Polar Plot generated by the sensorpolarPlot() function for SCSB_20 located in Seal Beach, CA for June 27 to July 8, 2018.

4.2.9   Timestamp and Time Averaging for AirSensor Data Objects and Functions

AirSensor and *AirSensor* functions have been designed to appropriately handle timestamps and various time zones of potential users. Users should understand how time stamps are stored and visualized within *AirSensor* and take appropriate steps when creating and visualizing *AirSensor* data objects; especially if using plotting functions outside of the *AirSensor* package to visualize data. The PurpleAir API provides access to data stored in Coordinated Universal Time (UTC). The *AirSensor* data objects (PAS, PAT, and sensor) all store data with a UTC timestamp. When creating or loading either a PAT or a *sensor* data objects, the user can specify the local time zone of the sensor selected. If a time zone is not specified when creating a data object for a single day, the date/time parameters will be passed as UTC, which for a sensor located in the Pacific Time Zone (+8h UTC) would return a data object with data from 08:00 AM to 08:00 AM local time of the following day. In *AirSensor,* time stamps are labeled and time averages are coded as "time beginning". For example, a 1-hr time average with a timestamp of 14:00 would be an average of the data collected between 14:00 and 14:59. This holds true even with the 2-min time-matched channel A and B sensor data available in *AirSensor*. The PurpleAir PA-II channel A and B sensors report at different times within a 120-sec time interval. In *AirSensor*, the seconds are dropped and data from the A and B sensor are assigned to a 2-min time beginning time stamp for matching purposes between the two raw sensors within a PA-II sensor. Since data is stored as UTC, the plotting functions within *AirSensor are* coded to appropriately apply time shifts based on the sensor's location (time zone) so that data will be plotted and displayed in the local time.

147

4.2.10 AirSensor DataViewer Web Application Overview

The *DataViewer* application was developed to provide an online interactive data experience for the community air monitoring networks deployed under the U.S. EPA STAR grant. These communities and sensor names are listed in SI Table S4.2. This interactive online user experience provides access to the functionality of the *AirSensor* R package for users that would not be able to download R and run code or scripts to access, process, and visualize community data. While the infrastructure to generate the types of plots that had resonated with community group members during the workshops was developed in the *AirSensor* package, the ability for community group members to use that infrastructure and generate visualizations in an interactive web accessible user-friendly online GUI without writing a single piece of code is provided in the *DataViewer* application. Plots that generated the most interest with community group members, including calendar plots, concentration maps, community time-lapse videos, and sensor performance plots between the A and B internal sensors and between the sensor and nearest reference $PM_{2.5}$ monitor, were prioritized for incorporation in the *DataViewer*. The following sections will provide an overview of the back-end infrastructure required for the *DataViewer* application and the methodology for the *DataViewer* color scale and timelapse videos. The front-end of the *DataViewer*, which is the online GUI and the primary point of interaction for community members, will be highlighted in the results section. Examples will be provided using data from sensors in the community of Seal Beach, California.

4.2.11 Cloud Computing Resources

Cloud computing provides computing services over the internet using a pay-as-you-go pricing model. Computing services typically include computing power, storage, networking, and analytics. Cloud computing can provide benefits by allowing programmers to focus on building new and innovative applications rather than acquiring and maintaining the infrastructure required for their computational needs. The cloud can provide benefits with cost reductions for IT infrastructure and can increase the scalability, elasticity, reliability, and security of computational services in comparison to computation services provisioned locally or on-premise. Azure, which is Microsoft's public cloud computing platform, was used to support the computational requirements of the *DataViewer* application. The application could also be run on another public cloud platform or on premise if desired. The computation services required include running scheduled tasks (cron jobs) for creating data objects, storing data in structured data directories, and hosting the *DataViewer* application. The data archive consists of a set of flat files defined by a simple directory and naming protocol with the data ingest scripts written in the R programming language. A virtual machine (VM) was configured on Azure with the structured directories for the data directories along with required software (i.e., Git, Apache, Docker, and R). A second VM was configured to host the *DataViewer* application. Figure 4.11 provides a simplified system architecture for the *DataViewer* application.
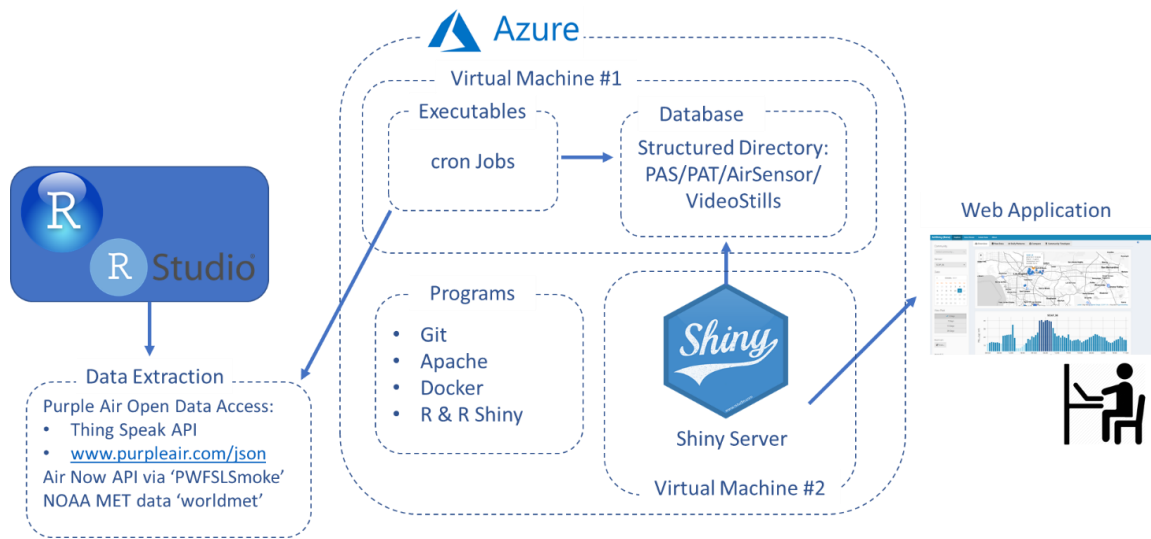
Figure 4.11 System Architecture for the *DataViewer* Application

4.2.12 DataViewer Color Scale

Determining an appropriate color scale for pollutant concentrations generated by low-cost sensors is challenging. Historically, air quality has been colored according to the Air Quality Index (AQI) with values ranging from 0 to 500 with six distinct color categories; good (green), moderate (yellow), unhealthy for sensitive groups (orange), unhealthy (red), very unhealthy (purple), and hazardous (maroon). Historically AQI has been calculated at 24-hour averages due to the scientific information about air pollution exposure and public health. In 2013, the U.S. EPA released a new AQI calculation method (NowCast Reff method) for $PM_{2.5}$ that calculates AQI hourly based on the previous 12 hours with the most recent hourly pollutant concentrations given larger weighting when air quality is changing rapidly (Mintz et al., 2013). The NowCast method is more responsive to real-time changes in air quality and responds faster to air quality events like smoke from wildfires. The U.S. EPA in the Air Sensor Toolbox suggested a new pilot version color/concentration scale that could be used for 1-min high time resolution data from low-cost air quality sensors

(U.S. Environmental Protection Agency 2019). This scale uses four shades of blue for low, medium, high, and very high PM$_{2.5}$ concentrations and is shown in SI Figure S4.2. The scale from the AirSensor Toolbox was created for 1-min sensor data in contrast to this work in which low-cost sensor data is processed with QC algorithms and time-averaged to 1-hr concentrations prior to being displayed in the *DataViewer* application. Furthermore, the authors wanted to provide users with a clearer differentiation among the higher pollutant levels sometimes indicated by the sensors. Hence, a new color scheme was developed for the *DataViewer* that includes 5 concentration categories represented by two colors (blue and purple) with variations in the hue and luminance as shown in Table 4.1.

Color Hex # (RGB)	PM$_{2.5}$ Concentration ($\mu g/m^3$)
#ABE3F4 (171,227,244)	PM$_{2.5} \leq 12$
#118CBA (17,140,186)	$12 < $ PM$_{2.5} \leq 35$
#286096 (40,96,150)	$35 < $ PM$_{2.5} \leq 55$
#8659A5 (134,89,165)	$55 < $ PM$_{2.5} \leq 75$
#6A367A (106,54,122)	PM$_{2.5} > 75$

Table 4.1 DataViewer color/concentration scale for 1-Hr PM$_{2.5}$ concentrations

4.2.13 FFmpeg and digital stills and video stills creation.

One of the desires of the community groups was to view historical time-lapse concentration maps to view past air quality events in their communities. To accomplish this task, time cron jobs run hourly to create video still images for each of the 14 STAR grant communities. These community time-lapse images are stored in the structured data directory in sequence and converted into mp4 video files using FFmpeg, which is a FOSS (Dawes 2019; FFmpeg 2019).

4.3 Results

4.3.1 Leveraging the AirSensor package

The *AirSensor* R package meets the community needs for those desiring to work with the data programmatically in the R environment. Through the *AirSensor* package, real-time and historical data from the STAR grant communities (listed in SI Table S4.2) can be accessed, loaded into R, and visualized used pre-built plotting functions. These plotting functions allow the user to create useful and interactive plots that can be shared within a community group and deliver actionable information for the community members to answer questions like "When is particle pollution highest in my community?" and "What time of day or day of week would be best to plan an outdoor activity (i.e. walk dog or golf game) to reduce my particle pollution exposure?" *AirSensor* creates a data flow for the end-user to create data objects for synoptic data, time-series data, and QC hourly $PM_{2.5}$ data. With the functions of this R package highlighted in the methods section, the user can easily create informative plots for community members to understand their local environment with minimal coding required. The *AirSensor* R package and associated functions provide

the necessary back-end software analysis and plotting functions to create the front-end *DataViewer* web application, which is usable and useful to a much broader segment of the public. The *DataViewer* application is the front-end interface that is the primary point of interaction for community members in this project to gain insights into their local air quality conditions. This solution provides an example of how these types of tools and solutions can enhance public engagement with data from low-cost sensor networks.

4.3.2   DataViewer Application

The *DataViewer* application, version 0.9.7, has a hierarchical page and tab structure with 4 top-level pages: Explore, View Data, Latest Data, and About. The View Data page is for viewing tabled data and provides the ability to download data in 3 to 30-day intervals on a per sensor basis. For sensors deployed within the STAR grant, historical data can be accessed back to the start of the U.S. EPA STAR grant sensor deployments: 10/01/2017. The View Data page includes high resolution (2-min) time-matched PA-II PM$_{2.5}$ data from the A and B sensor channels, temperature (°F), and relative humidity (%). This data output provides the user with a clean time-matched data set for the A and B sensor. Creating a similar data set outside of the *AirSensor* R package or *DataViewer* application would likely be time consuming and difficult; especially if the user were not proficient with Microsoft Excel or data science environments. Attempting to create a similar dataset in Excel would require downloading two separate data files (A and B), modifying date/time column appropriately to work in Excel, and merging the two files based on the time stamp. The Latest Data page provides visual access to the latest non-QC data on a per sensor basis with timeseries plots provided for sensor channel A, channel B, humidity, and temperature. The

"About" page provides an overview of the *DataViewer*, its intended purpose, QC procedures, and a disclaimer message.

The Explore page has the most functionality for exploring and analyzing community air monitoring data and includes six tabs: Overview, Calendar, Raw Data, Daily Patterns, Compare, and Timelapse. In the Overview tab, the user can select a community, a single sensor (sensor name), a date (end date), and view past data with options for viewing the prior 3, 7, 15, or 30 days to the selected end date. The Overview tab (Figure 4.12) provides a map that displays the average $PM_{2.5}$ for all sensors within the selected community for the time period selected (3, 7, 15, or 30-day average) and a bar chart that displays hourly $PM_{2.5}$ concentrations for the selected sensor.
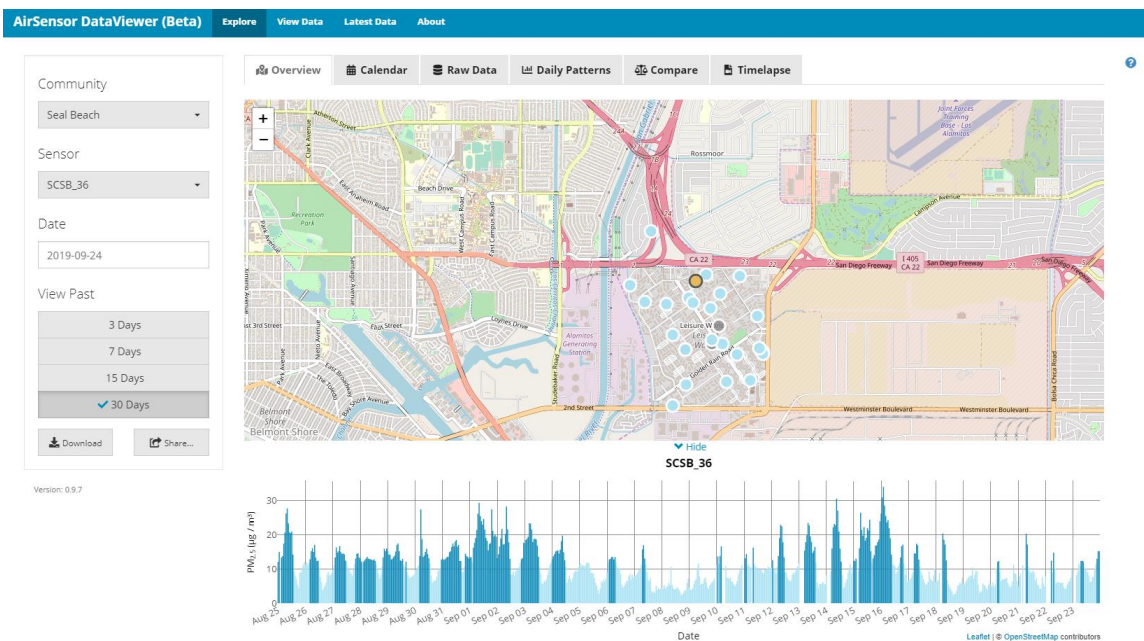

Figure 4.12 Overview tab in the *DataViewer* application showing $PM_{2.5}$ concentrations and sensor locations for Seal Beach, CA.

This overview tab provides the user with access to historical pollutant concentrations for the user-selected timeframe for their community and individual sensor. By changing the date, the user can quickly identify spatial differences between locations since the map indicates an average $PM_{2.5}$ concentration for the entire timeframe chosen (3-30 days). Additionally, the user can examine the bar chart below the map to view the recorded $PM_{2.5}$ concentrations for a single selected sensor.

In the Calendar tab, a 1-year calendar plot is rendered for a single selected sensor. The user selects a community, sensor, and date with a calendar plot being generated for the entire calendar year of the date selected (Figure 4.13). The calendar plot is interactive and when the user hovers over a date, the 24-Hr averaged $PM_{2.5}$ concentration is displayed. The calendar plot is easily understood by community members and provides an intuitive view of a complete year of $PM_{2.5}$ data for a single sensor. The calendar tab is great place to start when exploring a community data set in order to find dates with atypical 24-hr $PM_{2.5}$ concentrations. The user can then further examine these atypical pollution events at higher time resolution with other tabs available within the Explore page. The calendar plot especially resonated with the community members and sensor hosts; and therefore, was a priority for inclusion in the *DataViewer* application. Calculating and rendering the calendar plot is computationally expensive and may take a few moments to display when interacting with the *DataViewer* application, but the result is well worth the wait to provide this informative plot. Throughout the workshops, we received the most feedback and discussion from community members when showing the calendar plot. Additionally, we did not

receive any negative feedback or confusion from community members on how to interpret

calendar plots.
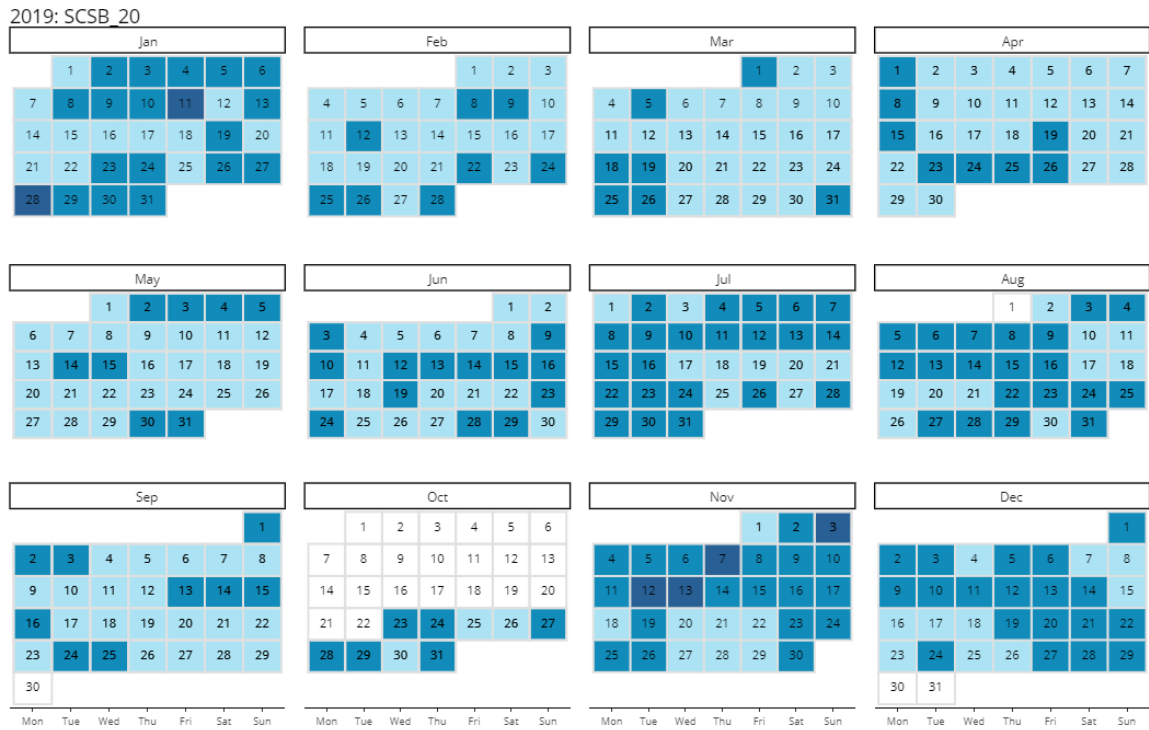
Figure 4.13 Calendar Plot generated using the AirSensor DataViewer Application. The darker shades indicate higher levels of pollution as set forth in the color scale provided in Table 4.1.

The Raw Data tab (Figure 4.14) provides the raw time-series data for channels A

and B, humidity, and temperature. Below the time series plots, the Raw Data tab provides

a comparison between the channel A and B sensors. This comparison provides both a time-

series and a scatterplot that indicates the regression statistics between the channel A and B.

This functionality is leveraged from the pat_internalfit() function in the *AirSensor* R

package. These comparison plots provide the user with the ability to check on the

performance of an individual sensor by viewing how well the two internal raw sensors

within the PA-II agree for the selected time period. If a user is concerned with the performance of an individual sensor, this tab can be used to determine if both the raw sensors are responding to changes in particle concentrations similarly. Low correlation and/or a large slope/intercept offset are indicative of a sensor performance issue and that one or both sensors may be experiencing a malfunction.
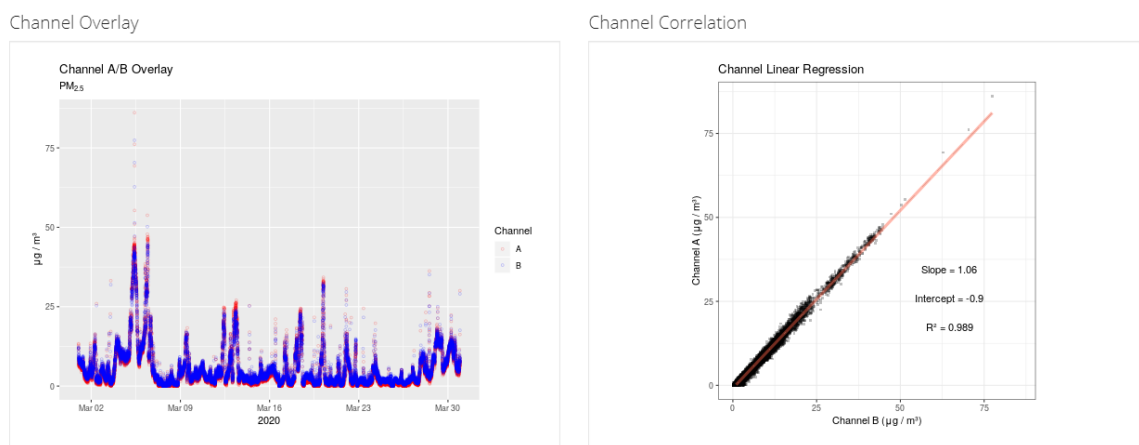
Figure 4.14 Example of Raw Data tab in the DataViewer application

The Daily Patterns tab (Figure 4.15) provides a bar chart illustrating the diurnal trend for PM$_{2.5}$, a pollution rose, and a summary table for the NOAA weather data for the time period selected. The daily patterns bar chart provides the average concentration by hour of day for the time period selected. With this tab, the *DataViewer* user can determine on average what hour of the day has the highest and lowest particle pollution. This plot helps to inform users as to when the best time of day would be for scheduling physical activity to reduce particle pollution exposure. The pollution rose allows the user to determine if pollution can be attributed to specific meteorological conditions. For the example in Figure 4.15, the plot indicates that higher concentrations are consistently

157

coming from the east of the sensing location; potentially indicating that a source of particle

pollution may be present east of the sensing location.
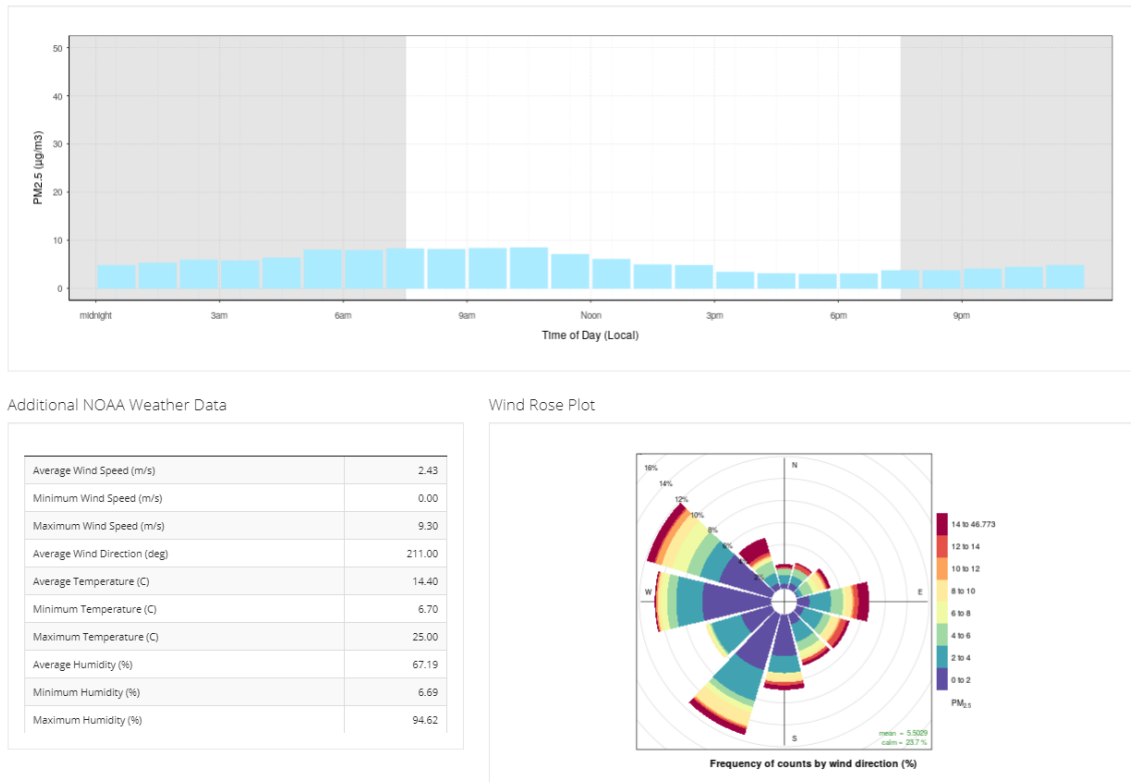
Figure 4.15 Snapshot of the Daily Patterns tab in the DataViewer application

The Compare tab provides a comparison between the sensor data and the nearest

continuous regulatory $PM_{2.5}$ monitoring site. The Compare tab provides a map indicating

the location of the sensor and nearest monitoring site along with a timeseries and scatter

plot comparison for the two data sources, allowing the user to determine if the selected

sensor follows the typical trends for $PM_{2.5}$ recorded at the nearby reference station for the

time period selected. The *DataViewer* application is leveraging the *AirSensor*

pat_externalfit() plotting function which was shown prior in Figure 4.6. While the distance

between the regulatory monitor and the low-cost sensor is provided on the Sensor-Monitor

Comparison timeseries plot, the map provided in the *DataViewer* on this tab allows the user the opportunity to visualize the distance between and spatial context of the two monitoring locations. Understanding the siting of the low-cost air quality sensor and the air monitoring station is crucial to understanding the information provided by the comparison plot. If either the sensor or regulatory monitor is installed in a near-source environment (i.e. near-road), the user should not expect the two measurements to agree.

The final tab in the Explore page is the Timelapse tab. This tab provides the user with the ability to generate a 6-day timelapse PM$_{2.5}$ concentration video on a per community basis and is shown in Figure 4.16. Right-clicking on the video allows the user to save a MP4 video to their computer and share if desired. This timelapse concentration map allows the user to view pollution events that may have taken place within a community during a selected time frame and visualize the flow of pollutants in/out of a community.
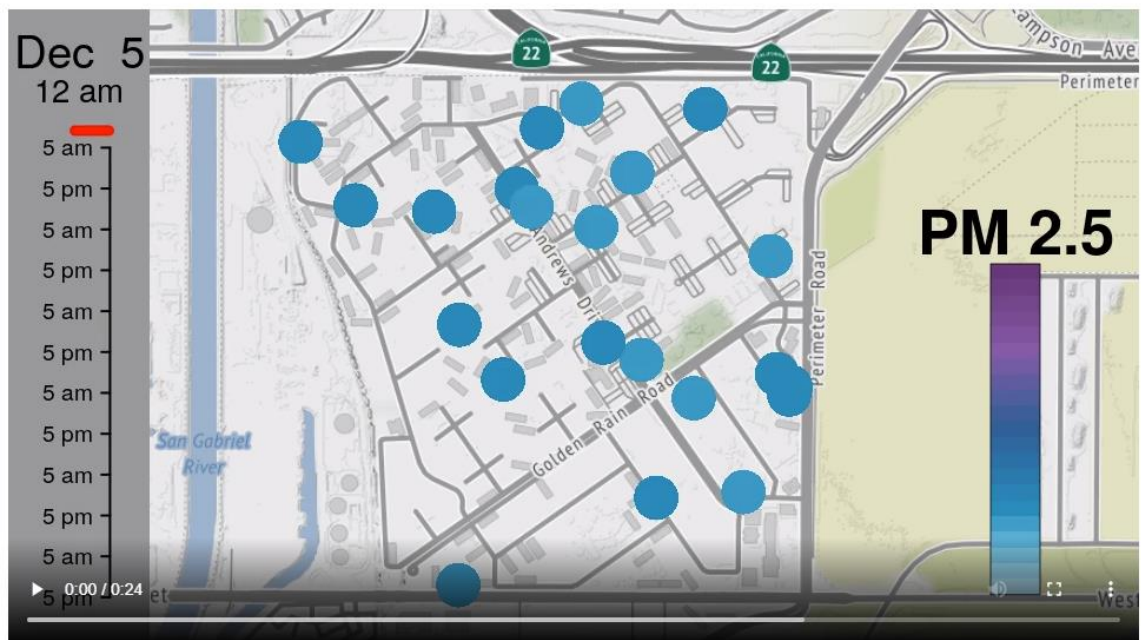

Figure 4.16 Community timelapse video tab

An informative approach to using this timelapse video is to first use the calendar plot feature to identify dates with elevated $PM_{2.5}$ mass concentrations ($\mu g/m^3$). After identifying those dates, the user can then choose an inclusive time period to view the community timelapse to better understand the pollution event with the hourly time-resolved data provided by the timelapse video.

4.4   Discussion

While online systems exist to view real-time and recently recorded measurements, FOSS tools for accessing, processing, and analyzing historical air monitoring data collected by low-cost sensors are less available to the public. Developing FOSS tools for archiving, interpreting, and communicating data from sensors has been identified as a concrete next step towards building a system for filling the air quality data gap (Pinder et al., 2019). This work provides a FOSS R package and a web application designed to fill that air quality data gap by providing the software tools to view both real-time and historical hyper-local air quality information generated by networks of air monitoring sensors. Access to hyper-local air quality information is expected to spawn an increased desire to interact with air quality information and allow community members to take appropriate actions based on results generated from their community monitoring networks. The *AirSensor* R package and *DataViewer* application provide a framework and data flow for communities to transform their community monitoring data sets into insightful information through interactive data experiences and data explorations. When meaningful results and observations are formulated, community members can take appropriate actions to reduce their exposure to air pollutants. These actions could include planning transportation (e.g.,

walk, bike, motor vehicle) routes to reduce air pollution exposure and scheduling physical activity events (e.g., golf game, sporting practice, sporting event) during hours of the day or day of the week that have been identified to have lower $PM_{2.5}$ mass concentrations based on historical data analysis. Using these local measurements and access to historical data for pollution trend analysis for time of day, community members can make a judgement on what hours of the day would likely provide lower particle pollutant conditions for activities like walking their dog. Our experience with sharing the *DataViewer* with the community leaders and members participating in the STAR grant has been positive with users enjoying the interactive data experience provided within the *DataViewer*. These community members have shared how this *DataVeiwer* provides them with the analysis capabilities to better understand their local air quality conditions. Plots that previously seemed out of reach due to required technical data analysis skills and coding experience are now readily available and generated with only a few selections and mouse clicks within the *DataViewer* application.

FOSS software developments provide efficiency by building a community of proactive data users around shared tools and allowing for multiple parties (i.e. agencies, entities, individuals) to contribute to software development and enhancing software functionalities. This benefit has already been realized as with the USFS AirFire group is funding a development to *AirSensor* for functions to calculate state-of-health metrics designed to access sensor performance to create a list of sensors that appear to be functioning properly. This information will be used in the context of wildfire air quality response. FOSS allows for researchers to collaborate and build upon the foundation established in this

development. FOSS developments can also provide a high level of transparency in terms of data analysis and integrity as the end-user is able to select which post-processing steps are appropriate for their data analysis. With FOSS tools and publicly available data sets, researchers can reproduce data analysis techniques and develop additional functions with the interoperability associated with FOSS development.

4.5 Conclusions

This novel work brings these software systems to the end-users or community members in a FOSS format with all the advantages of open software developments. Not only is the end-user able to access, process, and analyze historical sensor data, but the user also has access to the source code and functions with the option to create their own custom functions for QC, filters, and advanced analytics. Allowing the community to build upon this existing work provides benefits to the sensing community as a whole. Developing this software in the R-environment also provides for data fusion enrichment by coupling the collected air monitoring sensor data with meteorological data and regulatory air monitoring data through other open-source packages in the R environment. The *AirSensor* package has established a foundation upon which further enhancements and refinements can be developed. Both *AirSensor* and *DataViewer* source codes are available on Github with links provided in the SI. Collaboration and input to help shape the *AirSensor* open source project is encouraged to best meet the needs of the air sensing community.

The *AirSensor* R package is sensor specific, working with any publicly registered Purple Air PA-II sensors. The *DataViewer* solution is both sensor- and project-specific and therefore limited to the PA-II sensors deployed by South Coast AQMD under the STAR

grant. The authors believe that the data flow works well for air monitoring sensor data with the data objects going from synoptic data to time-series data and then to hourly QC sensor data. The blueprint developed to make the *DataViewer* operational could be applied to other projects and communities to visualize data collected by their PA-II sensor networks. The work discussed in this paper focused on the initial data handling and analysis capabilities required for a community air monitoring network of $PM_{2.5}$ sensors. Planned future work will focus on several improvements to the AirSensor R package, the data archive database design, and the *DataViewer* application. The AirSensor R package and archive will be improved by adding functionality to handle unique timeseries identifiers and incorporating PM_1 and PM_{10} data. Additional plotting functionality will include enhancements to create multi-sensor comparison plots and visualize sensor state-of-health metrics for both individual sensors and sensor networks. The *DataViewer* will be enhanced by improving the appearance, usability, data handling, and performance of the application.

References

Ahangar, F. E., F. R. Freedman and A. Venkatram (2019). "Using Low-Cost Air Quality Sensor Networks to Improve the Spatial and Temporal Resolution of Concentration Maps." International Journal of Environmental Research and Public Health **16**(7): 17.

Air Fire Tools. (2020). "WFAQRP-AirFire Tools Information."   Viewed 02/05/2020, from https://tools.airfire.org.

Air Quality Egg. (2020). "Air Quality Egg Portal."   Viewed 02/05/2020, from https://airqualityegg.com/portal/.

Air Watch. (2020). "Air Watch Bay Area."   Viewed 02/05/2020, from https://www.airwatchbayarea.org/.

AirNow. (2020). "AirNow Developer Tools." AirNow API. Viewed 02/04/2020, from https://docs.airnowapi.org/.

Allaire, J. (2020). "RStudio, PBC." https://blog.rstudio.com/2020/01/29/rstudio-pbc/ 2020.

Bailey, E. (2015). "raqdm: Access data from EPA's Air Quality Data Mart in R." R package version 0.1. Viewed 12/26/19, from https://github.com/ebailey78/raqdm.

Breathe London. (2020). "Breathe London Map."   Viewed 02/05/2020, from https://www.breathelondon.org/.

BreezoMeter. (2020). "Air Quality Map."   Viewed 02/04/2020, from https://breezometer.com/air-quality-map.

Callahan, J., R. Aras, Z. Dingels, J. Hagg, J. Kim, H. Martin, H. Miller, S. Pease, R. Thompson and A. Yang. (2019). "PWFSLSmoke: Utilities for Working with Air Quality Monitoring Data." R package version 1.2.103. from https://github.com/MazamaScience/PWFSLSmoke.

Carslaw, D. (2019). "worldmet: Import Surface Meteorological Data from NOAA Integrated Surface Database (ISD)." R package version 0.8.7. Viewed 12/26/19, from http://github.com/davidcarslaw/worldmet.

Carslaw, D. C. and S. D. Beevers (2013). "Characterising and understanding emission sources using bivariate polar plots and k-means clustering." Environmental Modelling & Software **40**: 325-329.

Carslaw, D. C. and K. Ropkins (2012). "openair - An R package for air quality data analysis." Environmental Modelling & Software **27-28**: 52-61.

Conway, D. (2013). "The Data Science Venn Diagram." Viewed 05/31/19, from http://drewconway.com/zia/2013/3/26/the-data-science-venn-diagram.

Dawes, B. (2019). "Using FFmpeg To Convert Image Sequences To Video." Analogue + Digital Viewed 12/27/19, from http://brendandawes.com/blog/ffmpeg-images-to-video.

Feenstra, B., V. Papapostolou, S. Hasheminassab, H. Zhang, B. D. Boghossian, D. Cocker and A. Polidori (2019). "Performance evaluation of twelve low-cost PM2.5 sensors at an ambient air monitoring site." Atmospheric Environment **216**: 116946.

FFmpeg. (2019). "FFmpeg."   Viewed 12/27/19, from https://www.ffmpeg.org/about.html.

Gibert, K., J. S. Horsburgh, I. N. Athanasiadis and G. Holmes (2018). "Environmental Data Science." Environmental Modelling & Software **106**: 4-12.

Grange, S. K., A. C. Lewis and D. C. Carslaw (2016). "Source apportionment advances using polar plots of bivariate correlation and regression statistics." Atmospheric Environment **145**: 128-134.

HabitatMap. (2020). "AirCasting Map."   Viewed 02/05/2020, from http://aircasting.habitatmap.org/mobile_map.

Hagan, D. (2017). "py-openaq: python wrapper for the Open AQ API."   Viewed 12/26/19, from https://github.com/dhhagan/py-openaq.

Hagler, G. S. W., R. Williams, V. Papapostolou and A. Polidori (2018). "Air Quality Sensors and Data Adjustment Algorithms: When Is It No Longer a Measurement?" Environmental Science & Technology **52**(10): 5530-5531.

Hasenkopf, C., Adukpo, D., Brauer, M., Dewitt, H.L., Guttikunda, S., Ibrahim, A.I., Lodoisamba, D., Mutanyi, N., Olivares, G., Pant, P., Salmon, M., Sereeter, L. (2016). "To combat air inequality, governments and researchers must open their data." Clean Air Journal **26**(2): 8–10.

IQAir. (2020). "AirVisual Map." Viewed 02/05/20, from https://www.airvisual.com/air-quality-map.

IVAN Imperial. (2020). "Map of Monitors."   Viewed 02/05/2020, from https://ivan-imperial.org/air/map.

Kadiyala, A. and A. Kumar (2017a). "Applications of Python to evaluate environmental data science problems." Environmental Progress & Sustainable Energy **36**(6): 1580-1586.

Kadiyala, A. and A. Kumar (2017b). "Applications of R to Evaluate Environmental Data Science Problems." Environmental Progress & Sustainable Energy **36**(5): 1358-1364.

Luftdaten. (2020). "Measuring Air Data with Citizen Science."   Viewed 02/05/2020, from https://luftdaten.info/en/home-en/.

Magi, B. I., C. Cupini, J. Francis, M. Green and C. Hauser (2019). "Evaluation of PM2.5 measured in an urban setting using a low-cost optical particle counter and a Federal Equivalent Method Beta Attenuation Monitor." Aerosol Science and Technology: 13.

Martin, R. V., M. Brauer, A. van Donkelaar, G. Shaddick, U. Narain and S. Dey (2019). "No one knows which city has the highest concentration of fine particulate matter." Atmospheric Environment: X **3**: 100040.

Mintz, D., S. Stone, P. Dickerson and A. Davis. (2013). "Transitioning to a new NowCast Method."   Viewed 11/21/19, from https://www3.epa.gov/airnow/ani/pm25_aqi_reporting_nowcast_overview.pdf.

OK Lab Stuttgart. (2020). "Open Data Stuttgart."   Viewed 02/05/2020, from www.github.com/opendata-stuttgart.

OpenAQ. (2020). "Open Data: Countries."   Viewed 01/24/2020, from https://openaq.org/#/countries.

Pinder, R. W., J. M. Klopp, G. Kleiman, G. S. W. Hagler, Y. Awe and S. Terry (2019). "Opportunities and challenges for filling the air quality data gap in low- and middle-income countries." Atmospheric Environment **215**: 116794.

Plume Labs. (2020). "Air Quality Map."   Viewed 02/04/2020, from https://air.plumelabs.com/air-quality-map.

PurpleAir. (2020). "PurpleAir Map."   Viewed 02/05/2020, from https://www.purpleair.com/map.

RStudio. (2019). "R Studio."   Viewed 11/08/2019, from https://rstudio.com/.

Salmon, M. (2019). "ropenaq: Accesses Air Quality Data from the Open Data Platform OpenAQ." R package version 0.2.7. from https://CRAN.R-project.org/package=ropenaq.

Sandhaus, S., D. Kaufmann and M. Ramirez-Andreotta (2019). "Public participation, trust and data sharing: gardens as hubs for citizen science and environmental health

literacy efforts." <u>International Journal of Science Education Part B-Communication and Public Engagement</u> **9**(1): 54-71.

Smart Citizen Kit. (2020). "Smart Citizen Kit Map." Viewed 02/05/2020, from https://smartcitizen.me/kits/.

Snyder, E. G., T. H. Watkins, P. A. Solomon, E. D. Thoma, R. W. Williams, G. S. W. Hagler, D. Shelow, D. A. Hindin, V. J. Kilaru and P. W. Preuss (2013). "The Changing Paradigm of Air Pollution Monitoring." <u>Environmental Science & Technology</u> **47**(20): 11369-11377.

The R environment. (2019). "The R environment."   Viewed 11/08/2019, 2019, from https://www.r-project.org/about.html.

U.S. Environmental Protection Agency. (2019). "Air Sensor Toolbox: What Do My Sensor Readings Mean? Sensor Scale Pilot Project."   Viewed 11/21/2019, from https://www.epa.gov/air-sensor-toolbox/what-do-my-sensor-readings-mean-sensor-scale-pilot-project.

U.S. Environmental Protection Agency. (2020a). "Air Data." <u>Air Quality System (AQS) API</u> Viewed 02/04/2020, from https://aqs.epa.gov/aqsweb/documents/data_api.html.

U.S. Environmental Protection Agency. (2020b). "Real Time Geospatial Data Viewer (RETIGO)."   Viewed 02/05/2020, from https://www.epa.gov/hesc/real-time-geospatial-data-viewer-retigo.

uRADMonitor. (2020). "Global Environmental Monitoring Network."   Viewed 02/05/2020, from https://www.uradmonitor.com/.

World Air Quality Index Project. (2020). "World's Air Pollution: Real-time Air Quality Index."   Viewed 01/24/2020, 2020, from https://waqi.info/.

Supplemental Information - Chapter 4

1. Figure S4.1 OpenAQ color scale
2. Table S4.1 Challenges to Address with Software Development
3. Table S4.2. Communities Sensor Networks included in the DataViewer application
4. Figure S4.2. EPA Pilot version color/concentration scale for PM$_{2.5}$
5. Table S4.3. Helpful Resources and Links
6. R-script that generated all visuals

1. OpenAQ color scale
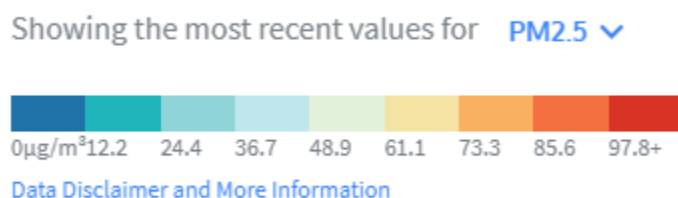
Figure S4.1 OpenAQ color scale for PM$_{2.5}$
Source: https://openaq.org/#/map; accessed 12/31/19

2. Table S4.1 Challenges to Address with Software Development

The discussions with community members that took place during the STAR grant workshops helped South Coast AQMD become aware of the need for additional tools. These tools could be used by the community members to address the difficulties with and challenges posed by analyzing large community air pollution data sets. These discussions along with knowledge of common environmental data science challenges resulted in a list of challenges to address that are provided in the table below.

#	Challenge	Addressed (AirSensor)	Addressed (DataViewer)	Future improvement
1	Access both real-time and historical data	Y	Y	Add import functions for additional PM fractions
2	Transform UTC times to local time stamps	Y	Y	
3	Store, process, and work with large data sets	Y	Y	
4	Work with other relevant datasets for advanced analysis	Y	Y	Enhance spatial metadata with additional fields
5	Build meaningful, easy-to-interpret plots	Y	Y	
6	Apply quality control measures on data	Y	Y	Create additional QC functions and sensor state of health metrics
7	Create timeseries plots and pollution maps	Y	Y	
8	Build animations of past data	N	Y	Provided in *DataViewer* application. Future *AirSensor* releases may provide for animations.
9	Create updated plots (calendar plot, time of day bar chart, etc.) to share with community members	Y	Y	
10	Share and reproduce analysis	Y	Y	
11	Create visualizations with no data science experience or experience with Microsoft Excel	N	Y	
12	Merge community geographic information (i.e. potential sources of concern, sensitive locations, demographics, etc.) with the collected community air monitoring sensor network data to better understand our local environment with the goal of improving public health	N	N	The ability to do this in the R-environment does exist, but the user would need to develop their own custom functions. Future *AirSensor* releases may provide additional data fusion enhancements with other publicly available data sets.

Table S4.1 Environmental Data Science Challenges with Low-cost Air Sensor Networks

3. Table S4.2. Communities Sensor Networks included in the DataViewer application

Community	Sensor List (Distributed)	# of Sensors (Distributed)
Oakland	SCAH_01 to SCAH_30	30
Richmond	SCAN_01 to SCAN_30	30
Alhambra / Monterey Park	SCAP_01 to SCAP_50	50
Big Bear Lake	SCBB_01 to SCBB_02	2
El Monte	SCEM_01 to SCEM_07	7
Sycamore Canyon	SCSH_01 to SCSH_30	30
Imperial Valley	SCIV_01 to SCIV_25	25
Nipomo	SCNP_01 to SCNP_25	25
Paso Robles	SCPR_01 to SCPR_25	25
Seal Beach	SCSB_01 to SCSB_33	33
South Gate	SCSG_01 to SCSG_29	29
Temescal Canyon	SCTV_01 to SCTV_55	55
West Los Angeles	SCUV_01 to SCUV_30	30

Table S4.2 Communities Sensor Networks included in the DataViewer application

4. EPA Pilot version color/concentration scale for PM$_{2.5}$

Pilot version	
1-minute particle pollution (PM$_{2.5}$) readings	
Not for regulatory purposes	
Low **0-29 µg/m3**	Enjoy your outdoor activities.
Medium **30-69 µg/m3**	If medium readings continue (for an hour or more), use the Air Quality Index to plan outdoor activities.
High **70 - 499 µg/m3**	You may be near a source of particle pollution like dust, smoke or exhaust. Check the Air Quality Index to plan outdoor activities.
Very High **≥500 µg/m3**	You may be near a source of particle pollution like dust, smoke or exhaust. Check the Air Quality Index to find out if you should adjust outdoor activities. Very high readings may mean the sensor is not working properly.
🔧	Sensor may be offline. Check the Air Quality Index.

Figure S4.2 EPA Pilot version color/concentration scale for PM$_{2.5}$

Source: https://www.epa.gov/air-sensor-toolbox/what-do-my-sensor-readings-mean-sensor-scale-pilot-project; accessed 12/07/19

5. Helpful Resources and Links

Resource	Link
AirSensor R package ver. 0.5 (GitHub Repository)	https://github.com/MazamaScience/AirSensor/tree/version-0.5
AirSensor R package (GitHub Repository)	https://github.com/MazamaScience/AirSensor
AirSensor DataViewer (GitHub Repository)	https://github.com/MazamaScience/AirSensorShiny
DataViewer access link (SCAQMD)	http://asdvdev.aqmd.gov/airsensor-test/app/
DataViewer access link (Mazama)	http://tools.mazamascience.com/airsensor-test/app/
Data Repository (Mazama)	http://smoke.mazamascience.com/data/PurpleAir
Data Repository (South Coast AQMD)	http://"aqmd.com"/data/PurpleAir

Table S4.3 List of AirSensor open access code repositories and data archives

6. R-Script for generating all plots and visuals in this paper.

```
# ----- Installation -----

# Install prerequisite libraries
install.packages('MazamaCoreUtils')
install.packages('MazamaSpatialUtils')

# Additional spatial dataset required for spatial analysis
library(MazamaSpatialUtils)

dir.create('~/Data/Spatial', recursive = TRUE)
setSpatialDataDir('~/Data/Spatial')
installSpatialData()

# Install AirSensor version 0.5 from Github
devtools::install_github("MazamaScience/AirSensor@version-0.5")

# Install latest version of AirSensor from GitHub
# devtools::install_github("MazamaScience/AirSensor", ref = "master")

# Load AirSensor library
library(AirSensor)

# Set archive base url location
setArchiveBaseUrl("http://smoke.mazamascience.com/data/PurpleAir")
#setArchiveBaseUrl("http://aqmd.com/data/PurpleAir")




# ----- PAS Data Object -----

pas_example <- pas_load()      # Load current PAS for US
pas_leaflet(pas_example)       # Create an interactive map of PAS

# ----- PAT Data Object -----

# Load PAT for 2018 from Archive for sensor in Seal Beach, CA USA.
# If sensor is not part of STAR grant or a data archive,
# use pat_createNew() function

pat_example <- pat_load(
  label = "SCSB_20",
  startdate = 20180101,
  enddate = 20181231,
  timezone = "America/Los_Angeles",
)
```

```
# Filter pat by date for June July 2018
pat_JuneJuly <- pat_filterDate(
  pat_example,
  startdate = "20180627",
  enddate = "20180708"
)

# Quality Control for PAT Data object
Table_1 <- pat_aggregate(pat_example) # returns data frame with
aggregate statistics

pat_exampleQC <- pat_qc(pat_example)  # apply quality control on PAT
data

PurpleAirQC_validationPlot(
  pat_JuneJuly,
  period = "1 hour",
  qc_algorithm = "hourly_AB_01",
  min_count = 20
)

# PAT outliers

# Plot indicating outliers as red asterisk
pat_outliers(
  pat = pat_JuneJuly
)


# PAT Plots
pat_internalFit(pat_JuneJuly)
pat_externalFit(pat_JuneJuly)
pat_scatterplot(pat_JuneJuly)
pat_dygraph(pat_example)


# ----- AirSensor Data Object -----

# Create an AirSensor data object
AirSensor_example <- pat_createAirSensor(
  pat = pat_JuneJuly,
  period = "1 hour",
  parameter = "pm25",
  channel = "ab",
  qc_algorithm = "hourly_AB_01",
  min_count = 20
)

# Plots for Sensor Data object
sensor_pollutionRose(AirSensor_example)      # Code for Pollution Rose
sensor_polarPlot(AirSensor_example)          # Code for Polar Plot
```

Chapter 5: Conclusions

5.1 Summary

The main objective of this research was to provide clarity and vision on the appropriate use and applications of low-cost air quality sensors for ambient air monitoring. Designing, developing, implementing, and deploying low-cost air quality sensors for ambient air monitoring applications comes with many challenges. These challenges include quantifying the performance of commercially available low-cost sensors, developing defensible methods for deploying sensor networks for ambient air monitoring applications, and communicating sensor data to the public in an understandable and meaningful way. The ultimate goal of this research was to address these challenges by systematically evaluating the performance of sensors according to a documented protocol, deploying sensors with scientifically defensible methodology for a specific application, and developing methodologies and tools to disseminate community air monitoring data as information to the public.

To systematically investigate the performance of low-cost air quality sensors, it was necessary to perform sensor performance evaluations according to a documented protocol. The protocol standardizes the performance evaluation process and provides for similarities across evaluations in terms of location, number of sensors evaluated, type of regulatory-grade instrument used for comparison, length of evaluation, time-resolution, and performance metrics used. The performance evaluation of 12 low cost $PM_{2.5}$ sensors provides guidance and clarity on the evolving market of low-cost PM sensors and significantly adds to the available literature on sensor performance evaluations due to the large number of sensors evaluated and that evaluations were performed according to a

176

standard protocol. This work provides guidance on appropriate performance metrics by which to evaluate sensor performance against regulatory-grade instrumentation and investigates the impact of environmental conditions on sensor performance. These performance evaluation results can be used globally to assist and aid researchers and community members in selecting sensors to best fit their ambient air monitoring needs. Additionally, these results provide clarity on how to interpret low-cost sensor data and how to reduce confusion when data between low-cost sensors and regulatory-grade instrumentation do not agree. The degree to which some sensors follow the trend of regulatory-grade instrumentation indicates that low-cost $PM_{2.5}$ sensors can provide meaningful data, while the measurement error between sensors and regulatory instrumentation indicates improvement to hardware and/or software for sensors is still needed to reduce these measurement errors. This work also pointed to the increasing bias error between sensor and regulatory-grade instrumentation as RH increased, indicating the need for manufacturers to develop sensors that correct for the impact of RH on $PM_{2.5}$ sensors. Applying such corrections would increase the usefulness and usability of these low-cost tools, especially for the general public and community groups looking to deploy sensor networks.

In the next stage of this research, an Internet of Things (IoT) air quality sensor node was developed and deployed to perform parallel monitoring to evaluate three potential relocation sites for a regulatory ambient air monitoring site measuring ozone. The requirement of an accurate sensor node guided the sensor selection, deployment methodology, and performance metrics used to quantify the measurement error of the

177

sensor network. The deployment methodology included an initial calibration, pre-deployment co-location calibration, and a post-deployment co-location verification. This methodology allowed for the quantification of the measurement error of the sensor network with post-deployment co-location results indicating the Mean Absolute Error (MAE) to be less than 2 ppb. Properly quantifying the measurement error through the deployment methodology provided defensible data and established high confidence in the cross-site comparison analysis to select an appropriate relocation site. This research was a significant development both in terms of hardware design and methodology. This systematic approach can be used in other ambient air monitoring applications with sensors that require quantification of the measurement error. The development of the sensor node can also be duplicated in part or in whole for interested researchers desiring to build a sensor node that can be deployed remotely, transmit data wirelessly, and measure ozone or another air pollutant. This research is significant in that it provides a concrete example of developing and deploying sensors for a specific ambient air monitoring application: parallel monitoring. This framework, which includes choosing the right sensor for the application and applying a methodology for sensor calibration and verification, should be used when utilizing air quality sensors for ambient air monitoring applications.

The last stage of this research involved how to communicate and disseminate community monitoring data as interpretable information to the public. Data communication and dissemination is key to engaging, educating, and empowering the community when performing air monitoring studies in a community. Developing tools to process, analyze, and view local air monitoring data allows the community to take

appropriate actions and/or make decisions to reduce exposure to harmful air pollutants. This work sets a framework for how to engage community members with varied interest in and knowledge of air quality and atmospheric sciences through an online application that provides both meaningful and understandable information. The development of the AirSensor R package addresses the challenges with the data management of large community monitoring data sets. The DataViewer web application was developed to provide an interactive data experience allowing users to make selections and explore the community air monitoring data sets by generating pre-defined data visuals based on their user selected inputs. Informative and interactive plots rendered on the DataViewer application provide the local community members with the information needed to better understand their local environment and determine when air pollution is typically higher within their community. The AirSensor R package and DataViewer application provide a framework and data flow for communities to transform their community monitoring data sets into insightful information through interactive data experiences and data explorations. This novel work brings these software systems to the end-users or community members in a FOSS format with all the advantages of open software developments. Not only is the end-user able to access, process, and analyze historical sensor data, but the user also has access to the source code and functions with the option to create their own custom functions for QC, filters, and advanced analytics. Allowing the community to build upon the framework established provides benefits to the sensing community as a whole. The novel FOSS development sets the path forward and several entities (U.S. EPA and U.S. Forrest Service)

have already started considering these tools and their expansion for use in their applications.

5.2 Limitations and Future Directions

The use and application of low-cost air quality sensors for ambient air monitoring is increasing and evolving rapidly. Since the low-cost air quality sensor market is an emerging market with new devices becoming commercially available each quarter, continuing and advancing the sensor performance evaluation work is important. The sensor performance evaluation work will be continued and sustained through the AQ-SPEC program, which provides the much-needed information to the public on sensor performance. The evaluations performed in this work were limited to 30-60 days which may not identify potential drift or offset issues that may arise for long term deployments greater than 60 days. The evaluations are also limited in that they occurred at one location with specific particle properties and environmental conditions that may not be transferable to other regions. As the performance of low-cost sensors will improve with future technology advances and their use and applications become adopted more broadly, opportunity exists to create sensor performance verification and/or certification programs. Such standardization programs would develop more rigorous field testing and laboratory testing protocols to provide a more complete understanding of sensor performance under various ambient conditions. A verification or certification process would test sensors at multiple ambient air monitoring locations and include multiple seasons to ensure that the sensor performs across the potential conditions found in a specific region, state, or country. An approach for such a standardization program could be implemented either as a tiered

system or a single application system. In California with the recent passage of Assembly Bill (AB) 617, air monitoring agencies are monitoring and implementing measures to reduce air pollutants in communities. Creating a certification or standardization program for sensors to be used specifically for AB 617 community monitoring would provide guidance to both communities and local agencies on which sensors are appropriate for developing community monitoring networks under AB 617 funding. Since these sensors are deployed in sensor networks, the performance of the network can be verified with scientifically valid deployment methodologies. If such a standardization system was in place for community monitoring networks, the certification program may even exam the performance of the network of sensors rather than looking at individual sensor performance. Since many AB 617 monitoring communities do have regulatory air monitoring stations installed within their community boundaries, the sensor network deployments can be deployed and evaluated based on their performance within the monitored community. By narrowing the number of sensors that meet specifications and standards, researchers would be able to collaborate and focus on specific data quality control measures and data communication applications for the sensors which meet the performance requirements for AB 617 community sensor networks. This would allow for tools and applications to be developed and shared across communities within the state and maximize use of state funding. Long term performance over time should also be examined under various conditions to determine how sensors will perform when deployed in real world ambient conditions for extended periods of time. Since many potential applications do exist for the use of sensors in ambient air monitoring, a standardization program could

take a tiered approach based on application grouping. This approach would work well for implementing broader standards at a federal level with tiered performance requirements dependent on application (regulatory, fence-line, research, epidemiology, citizen science, community monitoring, and science education). Additionally, laboratory evaluations under controlled conditions would allow for the investigation of sensor performance under conditions that may not be attainable in ambient (uncontrolled) conditions. Laboratory experiments can be designed to evaluate performance of sensors under various combinations of concentrations, temperature, relative humidity, and controlled interferent. Chamber experiments will provide information on the sensor's specificity and sensitivity to targeted pollutant, interferent pollutant, and environmental conditions. Sophisticated chamber equipment and experiments could examine sensor performance with regards to the impact of vibration, wind effects, and altitude changes, which will provide insights into the utility of sensors for both mobile and stationary sensing applications.

With regards to the evaluation of the spatial and temporal ozone trends in the San Bernardino mountains, this study is limited due to the specific application of the project to locate an appropriate relocation site. This study was performed in a relatively tight geographical area and over a 2-month period during the high ozone season. A more comprehensive study to investigate spatial and temporal trends in the region could be designed and would include additional sites (urban/rural) and be performed for a longer duration to include multiple seasons. The sensor node cost is relatively high at $6,500 USD when equipped with the solar option. Much of this cost is actual ozone sensor itself which may be a limiting factor for use in community monitoring projects. Ideally, advancements

in technology may lead to less expensive sensors that are highly accurate and can be incorporated into integrated sensor solutions with less overall cost.

The AirSensor R package version 0.5 is limited in that the package is sensor specific for working with Purple Air PA-II sensors that are registered as public. The DataViewer solution is both sensor- and project-specific and therefore limited to the sensors deployed by South Coast AQMD under the STAR grant project. The current AirSensor R-package, DataViewer, and data repositories are currently focused on $PM_{2.5}$ data only. The blueprint developed to make the DataViewer operational could be applied to other projects and communities to visualize data collected by other networks of PA-II sensors. The initial development as presented in this work is the foundation of a suite of FOSS tools which are currently being expanded as this thesis is written. Additional developments for the AirSensor R package will include adding the $PM_{1.0}$ and PM_{10} size fractions from the PA-II sensor, improving data processing R scripts, new data access functions, and the development of sensor state-of-health metrics. These upgrades to the AirSensor R package should be completed Summer 2020 with the software being released on the Comprehensive R Archive Network (CRAN), which is the public clearing house for R packages. Publishing on CRAN will allow for a wider audience to use and contribute to the AirSensor project due to the ease of installing the R package. Future work should identify scientifically relevant correction techniques for PA-II data using the data access functions to both sensor and regulatory-grade data in AirSensor along with already CRAN published R libraries for machine learning and modelling. If the data can be improved programmatically for a region or state, the data will become more relevant and provide end users with more accurate

measurements of their local air quality conditions. With regards to the DataViewer application, future work will look to improve the usability of the application through continuing the feedback loop between community members using the application and the development team. This will ensure the both community leaders and members are provided the needed data visualization tools to understand their local historical air quality trends. Future work can create similar type DataViewer environments for specific applications like wildfire response or sensor state-of-health metrics. The latter would allow researchers to examine a regional deployment of sensors and quickly identify sensors that are not performing well and schedule maintenance, repair, or replacement of non-operational sensors. Removing or replacing poor performing sensors from the sensor network will provide a higher trust in the data collected knowing that the sensors displayed are exceeding pre-determined sensor state-of-health metrics. Further developments should look to refine existing and create new QC algorithms to process the data from the two raw sensors within a PA-II to create a single data point per sensors. This ongoing development and collaboration will continue through the AirSensor Project available on GitHub.

5.3   Closing Remarks

This body of research is significant in that it develops methodologies for the use and application of air quality sensors to enable community monitoring. This research provides clarity and guidance on the performance for $PM_{2.5}$ sensors, network applications for sensors, and data communication for community monitoring sensor networks. The sensor performance evaluations in Chapter 2 provide sensor performance metrics that are important in both sensor selection and in building out sensor networks. This research along

with research by others within the low-cost air quality sensing space has shown that this technology can provide an enhanced understanding of our local environment and has the potential to supplement the current regulatory monitoring networks for monitoring community air quality. The ability to collect hyper-local air quality information provides the data necessary for communities impacted by air pollution to take actions to reduce their exposure if data is appropriately communicated in an intuitive, user friendly, and understandable format. The DataViewer web application presented in Chapter 4 provides an example of how community air monitoring data from sensor networks can be visualized to allow the community to explore and understand their historical local air quality trends. The sensor network developed in Chapter 3 for parallel monitoring provides a sensor node design and deployment methodology to generate scientifically defensible sensor network data. As the technology and performance of air quality sensors improves, the potential ambient air monitoring applications for sensors will expand and provide additional opportunities to develop sensor networks that collect defensible data allowing for researchers to answer technical questions and discover   previously unknow air pollution phenomena. The future of air quality sensors is promising both in terms of technology advancement and ambient air monitoring applications. With developing scientifically sound methodologies and fostering by key stakeholders, the air quality sensing community will continue to thrive and discover more applications for the use and application of air quality sensors with the potential to help improve quality of live and public health in our communities.